Universidade de Lisboa

Faculdade de Farmácia

ANTIBACTERIAL ACTIVITY OF THE CHEMICAL CONSTITUENTS OF THE AFRICAN MEDICINAL PLANT *GREWIA HEXAMITA* AGAINST RESISTANT BACTERIA

Sara Filipa Santos do Jogo

Dissertation supervised by Professora Doutora Maria José Umbelino Ferreira
and co-supervised by Professora Doutora Noélia Maria da Silva Dias Duarte

Pharmaceutical and Medicinal Chemistry

2019

"Valeu a pena? Tudo vale a pena
Se a alma não é pequena.
Quem quer passar além do Bojador
Tem que passar além da dor.
Deus ao mar o perigo e o abismo deu,
Mas nele é que espelhou o céu."

Fernando Pessoa, *in* Mensagem.

To my parents, Carlitos and Nita.

Abstract

The main objective of this work was to contribute to the validation of the use of the medicinal plant *Grewia hexamita* (Malvaceae) in the treatment of infectious diseases, in the traditional medicine of Mozambique.

Bioassay-guided fractionation of the methanol extract of the roots of *Grewia hexamita* led to the isolation of four triterpenes, three pentacyclic, namely lupeol (**2.1**), betulin (**2.2**) and betulinic aldehyde (**2.3**) and a new tetracyclic triterpene named 3β-caffeoyl-cycloartane (**2.4**). Two steroids, β-sitosterol (**2.5**) and 7-oxo-β-sitosterol (**2.6**), two phenolic compounds, *p*-hydroxybenzaldehyde (**2.7**) and vanillin (**2.8**), as well as *S*-(+)-pantolactone (**2.9**), a γ-butyrolactone, were also isolated. Acylation of lupeol (**2.1**) and betulin (**2.2**), isolated in large amount, using acetic anhydride and benzoyl chloride, gave rise to four derivatives (**2.10**-**2.13**). The structures of the compounds were characterized by their spectroscopic data (IR, MS and one- and two-dimensional NMR).

The evaluation of the antibacterial activity was performed by the microdilution method in sensitive *Staphylococcus aureus* (ATCC 6538) and resistant strains (MRSA ATCC 43866 and VISA CIP 106760) and in a vancomycin-resistant *Enterococcus faecalis* strain (VRE FFHB H164). Gram-negative strains, namely *Salmonella typhymurium* (ATCC 13311), *Pseudomonas aeruginosa* (ATCC 9027) and *Escherichia coli* were also used.

The best results were found for the pentacyclic triterpenes lupeol (**2.1**) and betulin (**2.2**), which showed significant antibacterial activity against both sensitive *S. aureus* and MRSA strains (MIC = 30 and 15 $\mu g.mL^{-1}$, respectively) and against resistant VISA strains (MIC 62 $\mu g.mL^{-1}$). In turn, betulinic aldehyde (**2.3**) exhibited MIC = 30 $\mu g.mL^{-1}$ and 62 $\mu g.mL^{-1}$, against sensitive and MRSA strains, respectively, and no significant activity against VISA. No inhibitory activities of bacterial growth were observed in Gram-positive *E. faecalis* VRE FFHB H164 nor in Gram-negative bacteria.

Combination assays, by the checkerboard method, were also performed to evaluate the type of interaction between the compounds and reference antibiotics. It was intended to determine the existence of synergistic effect between them and thus their ability to reverse bacterial resistance. Betulinic aldehyde (**2.3**) restored synergistically the antibacterial activity of the two β-lactam antibiotics tested, amoxicillin from 62 to 3.8 $\mu g.mL^{-1}$, corresponding to a 16-fold reduction (FICI = 0.31) and oxacillin from 62 to 7.5 $\mu g.mL^{-1}$ (FICI = 0.37), corresponding to a 8-fold reduction. 7-Oxo-β-sitosterol (**2.6**) was also able to interact synergistically with amoxicillin, lowering the antibiotic MIC from 250 $\mu g.mL^{-1}$ to 30 $\mu g.mL^{-1}$ (FICI = 0.48), corresponding to a 8-fold reduction. Synergistic effects were also obtained against the VISA CIP 106760 strain, with β-sitosterol (**2.5**), vanillin (**2.8**) and pantolactone (**2.9**).

According to the results obtained, the most active compounds may be promising prototypes for the development of new antibiotics against resistant strains.

Keywords: *Grewia hexamita*, medicinal plant, antibacterial, *Staphylococcus aureus*, synergism.

Resumo

Esta dissertação teve como principal objetivo o isolamento e identificação de compostos antibacterianos a partir da planta medicinal africana *Grewia hexamita* (Malvaceae), de modo a validar cientificamente a sua utilização no tratamento de doenças infeciosas.

Para tal, procedeu-se ao estudo fitoquímico bioguiado do extracto metanólico das raízes, a parte da planta utilizada pelas populações, recorrendo a várias técnicas cromatográficas, nomeadamente cromatografia em coluna e cromatografia em camada fina. Das frações solúveis em acetato de etilo e *n*-hexano (as que exibiram melhores atividades antibacterianas) foram isolados e caracterizados nove compostos, nomeadamente, três triterpenos pentacíclicos, lupeol (**2.1**), betulina (**2.2**) e aldeído betulínico (**2.3**) e um novo triterpeno tetracíclico designado 3β-cafeoil-cicloartano (**2.4**), dois esteróides, β-sitosterol (**2.5**) e 7-Oxo-β-sitosterol (**2.6**), dois compostos fenólicos, p-hidroxibenzaldeído (**2.7**) e vanilina (**2.8**), e uma γ-butirolactona, a S-(+)-pantolactona (**2.9**). Adicionalmente, foram também preparados dois derivados do lupeol (**2.10** e **2.11**) e da betulina (**2.12** e **2.13**) através de reacções de esterificação com o anidrido acético e o cloreto de benzoílo.

As estruturas dos compostos foram estabelecidas com base nos seus dados espetroscópicos (IV, MS e RMN unidimensional - ^{1}H, ^{13}C e DEPT - e bidimensional - ^{1}H-^{1}H-COSY, HSQC e HMBC).

A avaliação da actividade antibacteriana foi efectuada pelo método da microdiluição em meio líquido em estirpes de *Staphylococcus aureus* sensíveis (ATCC 6538) e resistentes à meticilina e à vancomicina (MRSA ATCC 43866 e VISA CIP 106760, respetivamente) e numa estirpe de *Enterococcus faecalis* resistente à vancomicina (VRE FFHB H164). A actividade antibacteriana foi também avaliada em bactérias Gram-negativas, nomeadamente *Salmonella typhymurium* (ATCC 13311), *Pseudomonas aeruginosa* (ATCC 9027) e *Escherichia coli*.

Os triterpenos pentacíclicos lupeol (**2.1**) e betulina (**2.2**) foram os mais ativos, apresentando uma actividade antibacteriana significativa contra as estirpes de *S. aureus* sensíveis (CMI = 30 $\mu g.mL^{-1}$) e resistentes à meticilina e à vancomicina (CMI = 15 e 62 $\mu g.mL^{-1}$, respetivamente). O aldeído betulínico (**2.3**) exibiu igualmente actividade antibacteriana contra as estirpes de *S. aureus* sensíveis e MRSA resistentes (CMI de 30 $\mu g.mL^{-1}$ e 62 $\mu g.mL^{-1}$, respectivamente), mas não mostrou actividade significativa contra as estirpes resistentes à vancomicina. Nenhum dos compostos testados se mostrou ativo contra a estirpe de *E. faecalis* VRE FFHB H164 nem nas bactérias Gram-negativas.

Com o objectivo de avaliar o tipo de interacção entre os compostos testados e os antibióticos de referência, foram realizados ensaios de combinação recorrendo ao método de *checkerboard*. O aldeído betulínico (**2.3**) restaurou sinergicamente a atividade antibacteriana dos dois antibióticos β-lactâmicos testados, a amoxacilina (redução dos valores de CMI de 62 para 3,8 $\mu g.mL^{-1}$), correspondendo a uma redução de 16 vezes (FICI = 0,31) e da oxacilina (variação do valor de CMI de 62 para 7,5 $\mu g.\ mL^{-1}$) (FICI = 0,37), correspondendo a uma redução de 8 vezes. O 7-oxo-β-sitosterol (**2.6**) também exibiu sinergismo com a amoxicilina alterando o valor de CMI do antibiótico de 250 $\mu g.mL^{-1}$ para 30 $\mu g.mL^{-1}$ (FICI = 0.48), correspondendo a uma redução de 8 vezes. Foram também obtidos efeitos sinérgicos dos compostos β-sitosterol (**2.5**), vanilina (**2.8**) and pantolactona (**2.9**) contra a estirpe VISA CIP 106760.

De acordo com os resultados obtidos, os compostos mais ativos podem ser promissores para o desenvolvimento de novos antibióticos contra estirpes bacterianas resistentes.

Palavras-chave: *Grewia hexamita*, planta medicinal, antibacteriano, *Staphylococcus aureus*, sinergismo.

Acknowledgments

To Professor Maria José Umbelino, my supervisor, for the way she directed and thoroughly revised my work. In addition to your valuable suggestions, criticism and guidance, I am essentially grateful for the availability, perseverance and encouragement you have always conveyed to me.

To Professor Noélia Duarte, an example of competence and dedication, I thank you for your willingness to help me whenever I asked and guidance, which were crucial in never letting me go down, keeping me on the right track.

To Professor Aida Duarte for the availability of her laboratory where the biological tests were performed, always demonstrating availability and attention and to Professor Margarida Madureira who helped me in conducting the antibacterial assays, always being so calm, quick and practical.

To Dr. Silva Mulhovo of the Departamento de Ciências Agropecuárias da Universidade Pedagógica de Maputo for his support in collecting and sending the plant for this study.

To Pedro Russo and Inês Agostinho from the Students Office, you two are fairies in an human body, thanks for answering to my thousand questions and doubts always so patiently and kind.

To the NatProdChem working group, especially father David and mother Shirley, I thank you for all the support, friendship and patience you have provided over the past two years that have contributed to us becoming a small family. To the *kids* next door, His Royal Highness Jorge Grilo, Eliza little broccoli and Rita Gazela, thank you so much for helping me reach the little clover I became. Actually, Shirley my little piece of chocolate and Rita Gazelicious, this line is all yours because I don't know how to thank you for what you did for me.

To my homies, some from around the world, some living daily with me and others coming from many years ago. Goddamn, I boast your patience and thank you very much for your friendship and emotional support.

Last but certainly not least, to my family my biggest support. To my parents, the most important people in my life who raised me to be the determined, ambitious woman I am today, I will be forever grateful and I will make you very proud of me. To all my cousins, their parents and my grandmother, my forever Ohana thank you. To you Duarte Lopes, love of my life, my husband and best friend, words will never express how grateful I am to have you in my life.

Once again, and never enough, to all of you my most sincere **thank you**!

Abbreviations and Symbols

BAS	β-amyrin synthase
CAS	Cycloartenol synthase
CBC	Chair-boat-chair
CC	Column chromatography
CCC	Chair-chair-chair
CEMEC	Centro de Estudos Moçambicanos e Etnociências
cf.	from latin, *confer*/*conferatur*
$CHCl_3$	Chloroform
COSY	Correlation spectroscopy
CPQ	Curcubitiadienol synthase
d	doublet
dd	doublet of doublets
DCM	Dichloromethane
DEPT	Distortionless enhancement by polarization transfer
DMAPP	Dimethylallyl diphosphate
DNA	Deoxyribonucleic acid
DXP	Deoxyxylulose-5-phosphate
eq.	equivalent
ESI-MS	Electrospray ionisation mass spectrometry
et al.	from latin, *et alia*
EtOAc	Ethyl Acetate
FDP	Farnesyl diphosphate
FICI	Fractional inhibitory concentration index
FPS	Farnesyl pyrophosphate synthase
GDP	Geranyl diphosphate

GGDP	Geranyl geranyl diphosphate
HMBC	Heteronuclear multiple bond correlation
HSQC	Heteronuclear single quantum correlation
Hz	Hertz
H_2O	Water
H_2SO_4	Sulfuric acid
IPP	Isopentenyl diphosphate
IR	Infrared
J	Coupling constant
m	multiplet
MDR	Multidrug-resistance
MeOH	Methanol
MIC	Minimum inhibitory concentration
MRSA	Methicillin resistant *Staphylococcus aureus*
MSSA	Methicillin sensitive *Staphylococcus aureus*
m.p.	Melting point
m/z	Mass-to-charge ratio
NMR	Nuclear magnetic resonance
NPs	Natural products
PBPs	Penicillin binding proteins
PDR	Pandrug resistant
ppm	parts per million
QT	Triple quadrupole
s	singlet
SHC	Squalene-hopene cyclase
SQE	Squalene monoxidase or epoxidase

SQS	Squalene synthase
t	triplet
TB	Tuberculosis
td	triplet of doublets
TLC	Thin layer chromatography
UV	Ultraviolet
VRE	Vancomycin resistant *Enterococcus*
v/v	volume per volume
XDR	extensively drug resistance
δ_H	Chemical shift in the ^{1}H NMR spectrum
δ_C	Chemical shift in the ^{13}C NMR spectrum

Table of Contents

Figures Index

Schemes Index

Tables Index

CHAPTER 1

Introduction

1. Introduction

Throughout the history of mankind, humans have turned to Nature to meet their basic needs, including drugs to treat a wide range of diseases. In particular, plants, have being the support of traditional medicine systems (Cragg and Newman 2013). The oldest recorded text for the use of natural products, as therapeutic agents was written in Mesopotamia around 2600 BC (Bernardini *et al.* 2018). Nowadays, we can enjoy the benefits of herbal medicines thanks to our ancestors who, over thousands of years, discovered plants that had medicinal properties and identified toxic plants (Jamshidi-Kia, Lorigooini and Amini-Khoei 2018).

It is not by chance that natural products are always present in pharmacological research. They are inexhaustible sources of compounds with diverse biological activities, constituting prototypes for the development of several drugs currently used in therapeutics. These compounds, included in secondary metabolites, are molecules that plants produce to control their environment, survive and reproduce (Newman and Cragg 2016). Their contribution to drug development has been extensively documented since its structural diversity and biological activity make them the most valuable sources of drugs and drug leads (Li *et al.* 2019).

Some species of genus *Grewia* have been used as folk medicines for a long time in Asian countries and pharmacological studies corroborate these uses revealing that the extracts of this genus are highly bioactive. The knowledge of the extent and mode of inhibition of specific compounds, which are present in the plant extracts, may contribute to the successful application of such natural compounds for treatment of infection disorders like fungal and bacterial diseases (Ullah, Uddin and Siddiqui 2012).

In this dissertation important information is presented in the context of a bioassay-guided phytochemical study of one of the species representing traditional African medicine, *Grewia hexamita* (Malvaceae family) from Mozambique. The developed work plan had particular incidence in the isolation and identification of the bioactive constituents of this species, together with the evaluation of the antibacterial activity of the isolated compounds.

This dissertation is divided into four distinct parts. The first part, which is the following brief state of the art, seeks an appropriate contextualization to the problem addressed in the laboratory, such as the botanical, chemotaxonomic, phytochemical and

subfamily aspects to which the species under study belongs. Some characteristics of the groups of compounds isolated in the study are also mentioned, as well as their relevance in the bacterial resistance to antibiotics. In the second chapter will be presented and discussed the results obtained that allowed to establish the structures of the isolated and derivatized compounds, as well as the results obtained in the evaluation tests of antibacterial activity. In a third chapter all the experimental work involved is related to the isolation and characterization of all compounds, as well as the techniques used in the biological assays. The last part of this dissertation will present the main conclusions regarding this work.

1.1. The *Grewia* genus

The species studied in this dissertation, *Grewia hexamita*, corresponds to a species cataloged of the genus *Grewia* included in the subfamily Grewioideae and belongs to the family of Malvaceae, formely Tiliaceae (Boon and Pooley 2010).

The Malvaceae is a family of flowering plants estimated to contain 243 genera with more than 4225 species. Malvaceae family plant members are distributed worldwide and since ancient times have been used as a folk remedy for the treatment of skin diseases, as an antifertility agent, antiseptic, and carminative (Vadivel, Sriram and Brindha 2016).

The *Grewia* genus comprises approximately 150 species of small trees and shrubs, distributed in subtropical and tropical regions of the World and is the only genus in the family that yields edible fruits (Zia-Ul-Haq *et al.*, 2013). The name *Grewia* was given due to Nehemiah Grew, one of the founders of plant physiology science, while the specific name *hexamita* refers to six threads, but the meaning is obscure. *G. hexamita* (Glen 2005) is well-known for its nutritional and therapeutic attributes. Despite its diverse use, it has suffered notable disregard, as is evident from the lack of literature on this plant.

Grewia hexamita is a large, multi-stemmed shrub or small tree, 5 m high. It has a rough, dark grey bark. The branches are reddish brown, with conspicuous lenticels, and are covered in reddish hairs when young. The flowering time is September-December (Burrows *et al.* 2018).

Figure 1.1 Botanical aspects of the species *Grewia hexamita*. A – Leaves, bark, branch. B – Fruit and flower. C – Seeds.

Many species of this genus are used in folk medicine for the treatment of malaria, diarrhoea, dysentery, typhoid fever, small pox, cough, irritable condition of intestine and bladder, eczema and rheumatism (R.N. Chopra, Nayar, and I.C. Chopra 1956). Anti-bacterial (Grierson and Afolayan 1999), and anti-malarial (Ma *et al.*, 2006) activities have also been reported from this genus.

1.2. Secondary metabolites: differentiation compounds conferring adaptive roles

The sum of all the biochemical reactions executed by an organism can be defined as metabolism where metabolites are the intermediates and the originated products are usually small molecules. A. Kossel in 1891 introduced the term “secondary” implying that while primary metabolites are present in every living cell capable of dividing, secondary metabolites are present only incidentally and are not primordial purport for organism’s life. Contrary to primary, if secondary metabolites are absent the life of an organism will not curtail although its survival is impaired to a larger extent (Tiwari and Rana 2015, Thirumurugan *et al.* 2018).

For those reasons, secondary metabolites or natural products can be defined as a varied group of natural metabolic products that are insignificant for vegetative growth of the producing organisms, but they are considered differentiation compounds conferring adaptive roles, for example, by functioning as defense compounds or signaling molecules in ecological interactions, symbiosis, metal transport, competition, and so on (Demain and Fang 2000).

The multitude of secondary metabolite secretions is harvested by human kind to improve their health (antibiotics, immunomodulators, enzyme inhibitors, antitumor

agents, and growth promoters of animals and plants), extending the pyramid of healthy nutrition (nutraceuticals and pigments), increasing agricultural productivity (pesticides, insecticides, pheromones and effectors of ecological competition and symbiosis) and hence impacting our society economics in a certain positive way (Thirumurugan *et al.* 2018).

1.3. Terpenoid biosynthesis

Secondary metabolism has three main starting materials which are shikimic acid, aminoacids and acetate being that the first two are, respectively, the precursors of many aromatic compounds and alkaloids. On the other hand, acetate is either the precursor of prostaglandins, polyacetylenes, and macrocyclic antibiotics *via* the stepwise addition of C_2 units, and isoprenoids (terpenoids) *via* the mevalonate pathway and the mevalonate-independent pathway (Mann, 1987; Lange *et al*, 2000).

Terpenoids (also named isoprenoids) are a large and diverse class of naturally occurring compounds derived from five-carbon isoprene units assembled and modified in multiple ways. Most are polycyclic structures that differ from one another in their basic carbon skeletons as well as in functional groups.

The terpenoid biosynthesis has two major steps, the first one includes the synthesis of the main intermediates: isopentenyl diphosphate (IPP) and dimethylallyl diphosphate (DMAPP) generated by the mevalonate pathway (A) and the deoxyxylulose-5-phosphate pathway (DXP) (B) (Scheme 1.1) (Lange *et al* 2000). The second step, which is depicted in Scheme 1.2, includes the prenyltransferase-catalyzed condensation of these two C_5 units to geranyl diphosphate (GDP) and the subsequent 1',4-additions of isopentenyl diphosphate to generate farnesyl (FDP) and geranyl geranyl diphosphate (GGDP). These prenyl diphosphates go through a series of cyclizations based on variations of the same mechanistic motif (head-to-tail) to produce the parent skeletons of each class, thereby GDP (C_{10}) origins monoterpenes, FDP (C_{15}) to sesquiterpenes and GGDP (C_{20}) to diterpenes (Bohlmann *et al*, 1998). On the other hand, the isoprenoid units may be attached in an irregular way, as in the triterpene squalene (C_{30}), which is a product of two molecules of farnesyl diphosphate coupled tail-to-tail (Thomas 2004). The terpenoid synthases (cyclases) are responsible for these cyclizations and may be preceded by a

range of redox modifications on the present skeletal type to produce other terpenoid metabolites (Bohlmann *et al* 1998; Duarte 2008), (Scheme 1.2).

Terpenoids can be classified according to the number of isoprene units as hemiterpenes (C5), monoterpenes (C10), sesquiterpenes (C15), diterpenes (C20), sesterterpenes (C25), triterpenes (C30), and tetraterpenes (C40). In particular, triterpenes are one of the largest classes of terpenoids with more than 20,000 different compounds reported to date. Triterpenes and steroids possess the same precursor squalene (Scheme 1.2). However, a distinction is made between steroids and triterpenes based on the way in which these molecules are synthesized. In steroids biosynthesis, 2,3-oxidosqualene is cyclized to lanosterol (in fungi and animals) or cycloartenol (in plants) via the chair-boat-chair (CBC) conformation. In triterpene biosynthesis, in contrast, this substrate is folded into a different conformation – the chair-chair-chair conformation (CCC) – prior to cyclization into a huge array of triterpenes of diverse skeletal types, of which just one (β-amyrin) is shown as an example in Scheme 1.2 (Thimmappa *et al.* 2014).

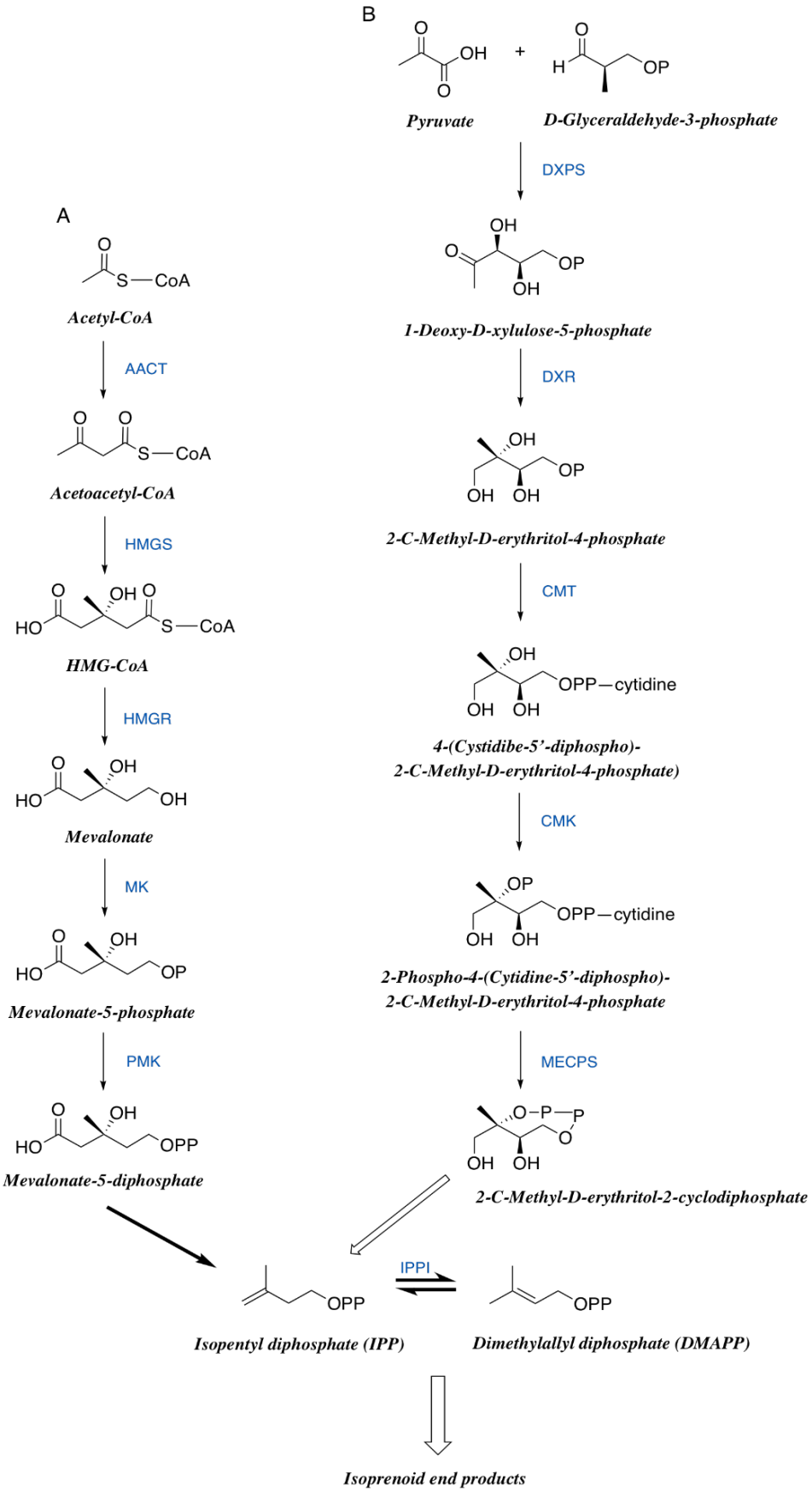

Scheme 1.1 Biosynthesis of isopentenyl diphosphate (IPP) and dimethylallyl diphosphate (DMAPP) by the mevalonate pathway (A) and the DXP pathway (B) (Lange *et al.* 2000 and Duarte 2008).

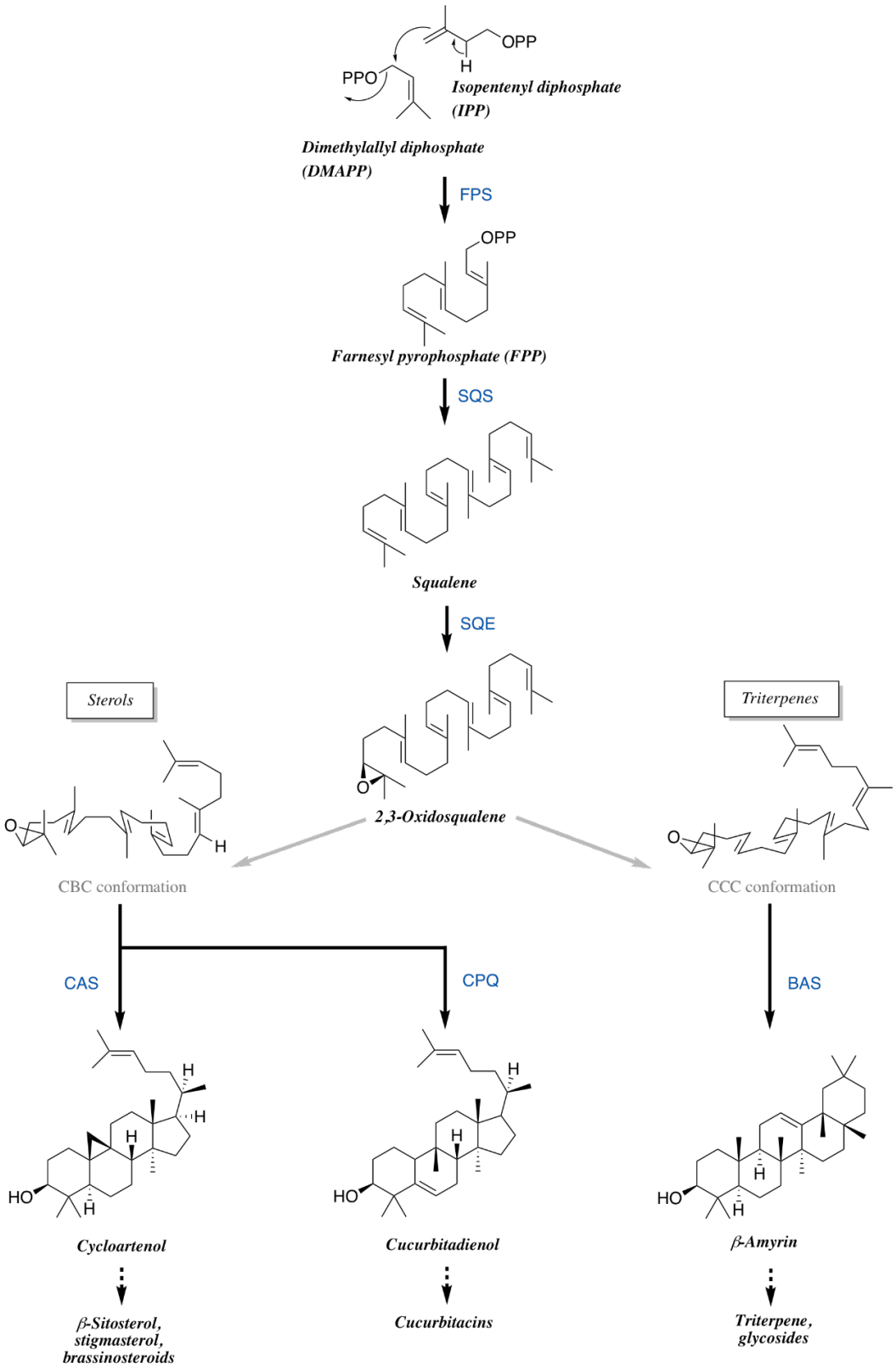

Scheme 1.2 The biosynthetic route to steroids and triterpenes. The enzymes that catalyze the various steps are indicated in boxes. Enzyme abbreviations: FPS, farnesyl pyrophosphate synthase; SQS, squalene synthase; SQE, squalene monooxygenase or epoxidase; SHC, squalene-hopene cyclase; CAS, cycloartenol synthase; CPQ, cucurbitadienol synthase; BAS, β-amyrin synthase. Other abbreviations: CBC, chair-boat-chair; CCC, chair-chair-chair (Thimmappa *et al.* 2014).

Thus, steroids are considered to be modified triterpenes containing the tetracyclic ring system of lanosterol and cycloartenol but lacking three methyl groups (Mann, 1987; Dewick 2009). Steroids are important structural components of membranes and also have roles in signaling (as steroidal hormones). On the contrary, triterpenes are not considered as fundamental for development and normal growth, and while they do exist in plants in simple unmodified form, they often build up as conjugates with carbohydrates and other macromolecules, especially as triterpene glycosides. Triterpene glycosides have important ecological and agronomic functions and also have a wide range of commercial applications in the food, pharmaceutical, cosmetics and industrial biotechnology departments (Kemmen *et al.* 2014).

1.4. Literature review

In this chapter, a bibliographical review of new compounds isolated over the last years is presented for the *Grewia* genus. Some general characteristics, including biosynthetic aspects, of each of the major classes of secondary metabolites of this genus are also presented. Some of the classes of metabolites recovered were triterpenes, sterols, flavones, lactones and alkaloids.

This bibliographic review was carried out by consulting the "ScienceDirect" database and the "ISI Web of Knowledge" research platform, in the period between January 2010 and July 2019, and were used as the key words *Grewia spp.*, *Grewia hexamita*, natural products, triterpenes, antibacterial activity.

1.5. Major families of secondary metabolites of the *Grewia* genus

To the best of our knowledge, the first phytochemical investigation on *Grewia* genus can be traced back to 1965. Friedelin was the first pentacyclic triterpenoid reported from *G. tiliaefolia* (Anjaneyulu *et al.* 1965) and its presence in *G. biloba* was also confirmed (Khadeer Ahamed *et al.* 2010). Since then, plenty of studies regarding chemical and biological aspects of plants within the genus *Grewia* have been reported.

Until now, several alkaloids, including harman, 6-methoxyharman and 6-hydroxyharman (Jaspers *et al.* 1986), flavone C-glycosides, including vitexin and isovitexin (Jayasinghea *et al.* 2004), lignans like grewin, nitidanin, bilagrewin (Ma *et al.* 2006), gulonic acid γ-lactone; 3,21,24 trimethyl-5,7-dihydroxyhentriacontanoic acid δ-lactone (Khadeer Ahamed, Krishna and Dandin. 2010) and triterpenoids (Ahamed, Krishna and Malleshappa 2009; Anjaneyulu *et al.* 1965; Ma *et al.* 2006) have been reported.

1.5.1. Triterpenes and steroids

As referred above, friedelin (**1.1**) was the first pentacyclic triterpenoid reported from *G. tiliaefolia* (Anjaneyulu *et al.* 1965). It was also reported from *G. biloba* along with *epi*-friedelan-3-ol (**1.2**) (Ahamed, Krishna, and Malleshappa 2009). Ursene-3,19,28-triol (**1.3**), α-amyrin (**1.4**), and ursolic acid (**1.5**) were isolated from the roots of *G. villosa* (Bashir, Turner and Rose 1982). Anti-malarial bioassay-directed fractionation of the methanolic extract prepared from a sample of the combined leaves, twigs, and stems of *G. bilamellata* led to the isolation of compounds, including two triterpenes 3α,20-lupandiol (**1.6**) and 2α,3β-dihydroxy-olean-12-en-28-oic acid (**1.7**) (Ma *et al.* 2006). Lupeol (**1.8**) and betulin (**1.9**) were reported from *G. bicolour*, *G. tiliaefolia*, and *G. damine* (Jaspers *et al.* 1986; Badami *et al.* 2004). Lupenone (**1.10**), β-Amyrin (**1.11**) and lanost-9(11)-en-12-one (**1.12**) were isolated from *G. asiatica* (Abou and Sleem 2005). These compounds are summarized in **Table 1.1**.

Table 1.1 Triterpenes isolated and described in literature from *Grewia spp*.

S. No.	Compounds	Species	Reference
1.1	Friedelin	*G. tiliaefolia, G. biloba* *G. asiatica*	Anjaneyulu *et al.* 1965, Abou and Sleem 2005
1.2	Epi-friedelan-3-ol	*G. biloba*	Anjaneyulu *et al.* 1965
1.3	Ursene-3,19,28-triol	*G. villosa*	Bashir, Turner and Rose 1982
1.4	*α*-Amyrin	*G. villosa* *G. asiatica*	Bashir, Turner and Rose 1982, Abou and Sleem 2005
1.5	Ursolic acid	*G. villosa*	Bashir, Turner and Rose 1982

Continuation Table 1.1

1.6	3*a*-20-Lupandiol	*G. bilamellata*	Ma *et al.* 2006
1.7	2*a*,3 β -dihydroxyolean-12-en-28-oic acid	*G. bilamellata*	
1.8	Lupeol	*G. bicolour, G. tiliaefolia, G. damine*	Badami *et al.* 2004, Jaspers *et al.* 1986, Abou and Sleem 2005
1.9	Betulin	*G. bicolour, G. tiliaefolia, G. damine*	
1.10	Lupenone	*G. asiatica*	Abou and Sleem 2005

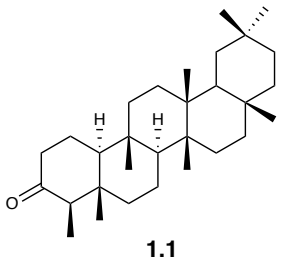

1.1

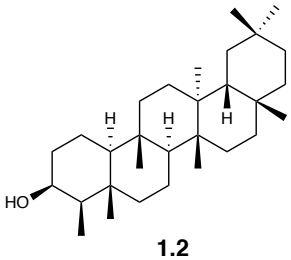

1.2

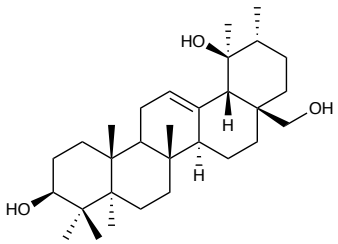

1.3

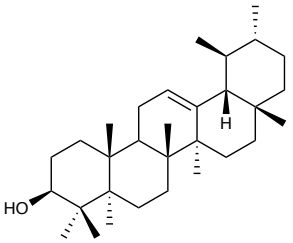

1.4

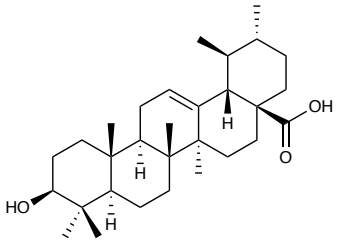

1.5

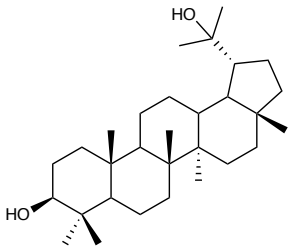

1.6

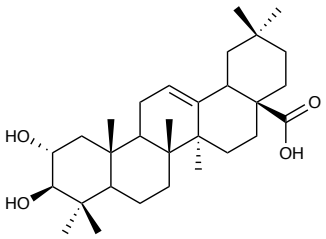

1.7

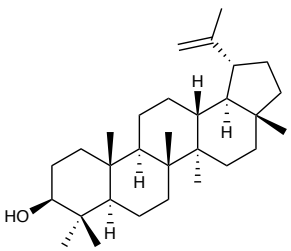

1.8

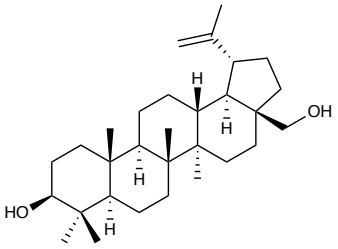

1.9

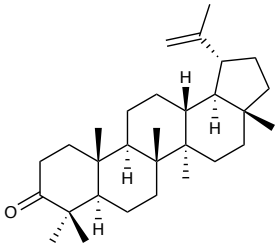

1.10

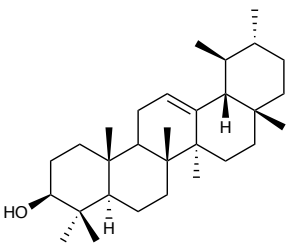

1.11

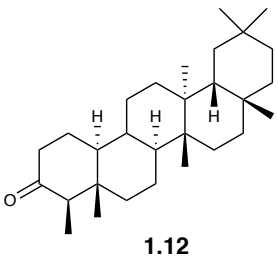

1.12

In Table 1.2 are summarized the five steroids (**1.13**-**1.17**), including β-sitosterol (**1.13**) and daucosterol (**1.14**), reported from different species of this genus (Ma *et al.* 2006, Jaspers *et al.* 1986; Ahamed, Krishna, and Malleshappa 2009).

Table 1.2 Steroids isolated and described in literature from *Grewia spp.*

S. No.	Compounds	Species	Reference
1.13	β-Sitosterol	*G. bicolour, G. biloba, G. asiatica*	Jaspers *et al.* 1986, Ahamed, Krishna and Malleshappa 2009, Abou and Sleem 2005
1.14	Daucosterol	*G. bilamellata*	Ma *et al.* 2006
1.15	Stigmast-7-en-3-ol	*G. asiatica*	Gupta, Sharma and Verma 2012
1.16	Stigmasterol		
1.17	Campesterol		

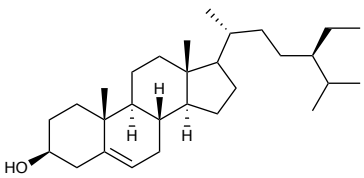

1.13

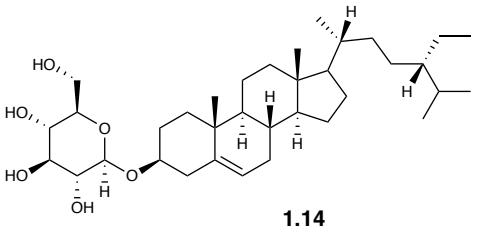

1.14

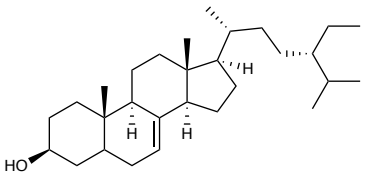

1.15

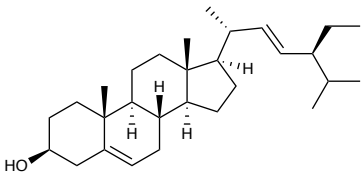

1.16

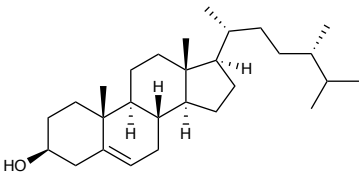

1.17

1.5.2. Alkaloids

Three alkaloids (Table 1.3), harman (**1.18**), 6-methoxyharman (**1.19**) and 6-hydroxyharman (**1.20**) were isolated from the methanolic extract of *G. asiatica,* which showed anti-bacterial properties (Jaspers *et al.* 1986).

Table 1.3 Alkaloids isolated and described in literature from *Grewia spp.*

S. No.	Compounds	Species	Reference
1.18	Harman	*G. bicolour*	Jaspers *et al.* 1986
1.19	6-Methoxyharman		
1.20	6-Hydroxyharman		

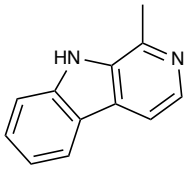

1.18

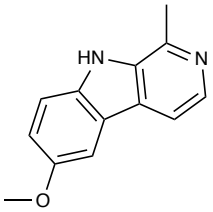

1.19

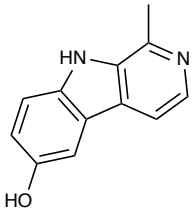

1.20

1.5.3. Flavones

Two flavone C-glycosides, vitexin and isovitexin, have been isolated from *n*-butanol fraction of the methanolic extract of leaves of *G. damine* (Jayasinghe *et al.* 2004).

Fruits and flowers of *G. asiatica* contain narigenin (**1.23**), quercetin (**1.24**) and catechin (**1.25**) (Table 1.4) (Chattopadhyay and Pakrashi 1975).

Table 1.4 Flavones isolated and described in literature from *Grewia spp.*

S. No.	Compounds	Species	Reference
1.21	Vitexin	*G. damine*	Jayasinghe *et al.* 2004
1.22	Isovitexin		
1.23	Narigenin	*G. asiatica*	Chattopadhyay and Pakrashi 1975
1.24	Quercetin		
1.25	Catechin		

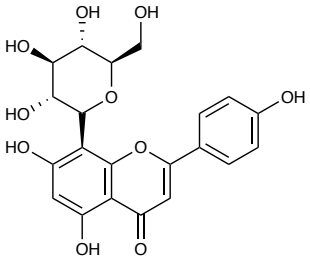

1.21

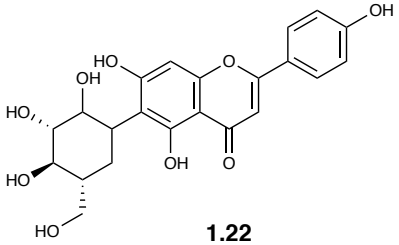

1.22

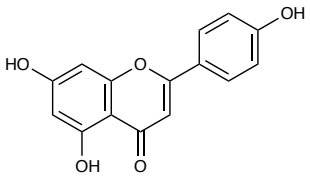

1.23

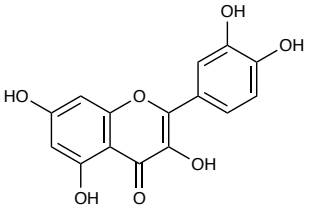

1.24

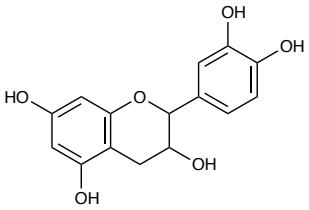

1.25

1.5.4. Anthocyanines

Fruits of *G. asiatica* contain three anthocyanines such as pelargonidin 3,5-diglucoside (**1.26**), cyanidin-3-glucoside (**1.27**) (Chattopadhyay and Pakrashi 1975) and cyanidin 3-galactoside (**1.28**) (Table 1.5) (Nair *et al.* 2005).

Table 1.5 Anthocyanines isolated and described in literature from *Grewia spp*.

S. No.	Compounds	Species	Reference
1.26	Pelagornidin 3,5-diglucoside	*G. asiatica*	Chattopadhyay and Pakrashi 1975
1.27	Cyanidin 3-glucoside		
1.28	Cyanidin 3-galactoside		Nair *et al.* 2005

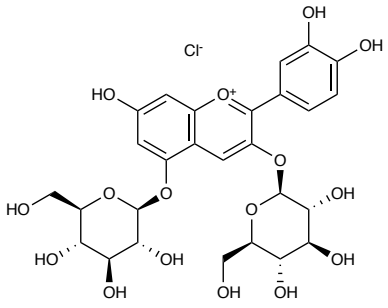

1.26

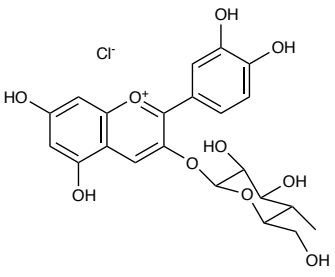

1.27

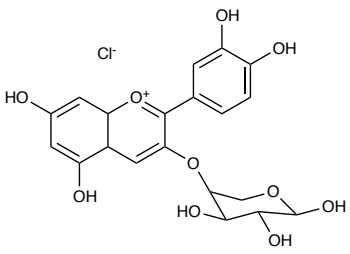

1.28

1.5.5. Lignans: Coumarinolignans and Neolignans

Lignans isolated from the plants of the genus *Grewia* (Table 1.6) covered coumarinolignans and neolignans. Three coumarinolignans, grewin (**1.29**), nitidanin (**1.30**), and cleomiscosin D (**1.31**), were isolated from *G. bilamellata* and three neolignans have also been reported. They were isolated and characterized from chloroform fraction of *G. bilamellata* as 8-*O*-40' neolignans, guaiacylglycerol- β-coniferyl ether isomers (*threo* (**1.32**) and *erythron* (**1.33**)) and bilagrewin (**1.34**) (Ma *et al.* 2006)..

Table 1.6 Lignans isolated and described in literature from *Grewia spp.*

S. No.	Compounds	Species	Reference
1.29	Grewin	*G. bilamellata*	Ma *et al.* 2006
1.30	Nitidanin		
1.31	Cleomiscosin D		
1.32	Guaiacylglycerol- β-coniferyl ether (*threo*)		
1.33	Guaiacylglycerol- β-coniferyl ether (*erythron*)		
1.34	Bilagrewin		

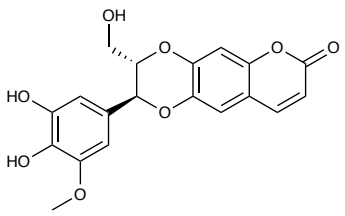

1.29

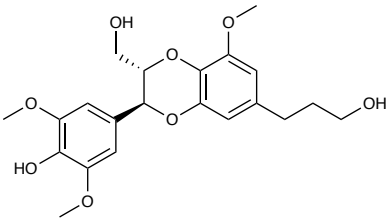

1.30

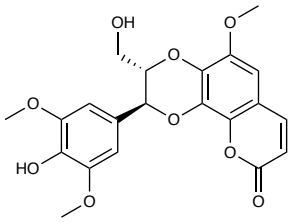

1.31

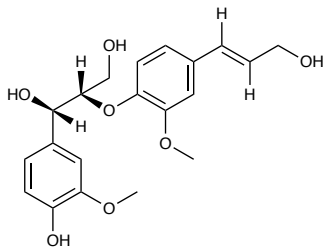

1.32

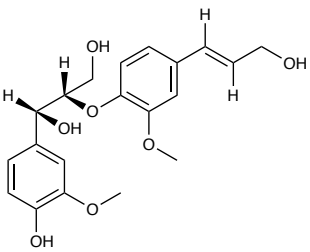

1.33

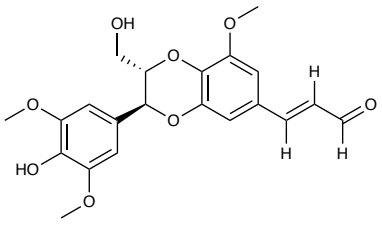

1.34

1.5.6. Other compounds

Three lactones, gulonic acid γ-lactone (**1.35**), 3,21,24-trimethyl-5,7-dihydroxyhentriacontanoic acid δ-lactone (**1.36**) and D-erythro-2-hexenoic acid γ-lactone (**1.37**) are reported from *G. tiliaefolia* and *G. asiatica* (Khadeer Ahamed, Krishna and Dandin. 2010).

The presence of vitamins A (**1.38**) and C (**1.39**) has also been reported from *G. asiatica* (Yadav 1999). Heneicosanoic acid (**1.40**), an organic acid, was reported from *G. biloba* (Ahamed, Khrisna and Malleshappa 2009).

Propyl palmitate (**1.41**), grewinol (**1.42**) and 2,6-dimethoxy-1-acetonylquinol (**1.43)** are reported from *G. biloba*, *G. bilamellata*, and *G. asiatica*, respectively (Lakshmi and Chauhan 1976; Ma *et al.* 2006; Ahamed, Khrisna and Malleshappa 2009).

Finally, 9,12-octadecadienoic acid methyl ester (**1.44**), α-methyl-l-sorboside (**1.45**), citric acid trimethyl ester (**1.46**), nonacosanol (**1.47**) and docosanol (**1.48**) were the main compounds identified in *G. asiatica* pomace extract (Gupta, Sharma and Verma 2012; Zia-Ul-Haq et al. 2013).

All of the previous compounds are summarized in Table 1.7.

Table 1.7 Other compounds isolated and described in literature from *Grewia spp*.

S. No.	Compounds	Species	Reference
1.35	Gulconic acid γ-lactone	*G.tiliafolia*	Ahamed, Krishna and Dandin *et al.* 2010
1.36	3,21,24-trimethyl-5,7-dihydroxyhentriacontanoic acid δ-lactone		
1.37	D-erythro-2-hexenoic acid γ-lactone		
1.38	Vitamin A	*G. asiatica*	Yadav 1999
1.39	Vitamin C		
1.40	Heneicosanoic acid	*G. biloba*	Ahamed, Khrisna and Malleshappa 2009
1.41	Propyl palmitate		

Continuation Table 1.7

1.42	Grewinol	*G. asiatica*	Lakshmi and Chauhan 1976
1.43	2,6-dimethoxy-1-acetonylquinol		Ma *et al.* 2006
1.44	9,12-octadecadienoic acid methyl ester		Gupta, Sharma and Verma 2012
1.45	α-methyl-1-sorboside		
1.46	Citric acid trimethyl ester		
1.47	Nonacosanol		Zia-Ul-Haq et al. 2013
1.48	Docosanol		

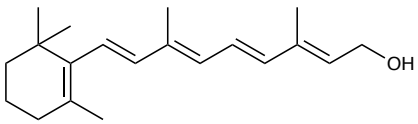

1.38

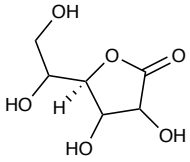

1.39

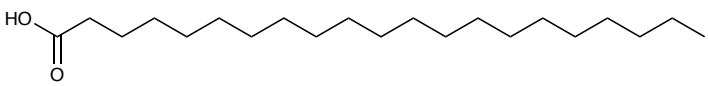

1.40

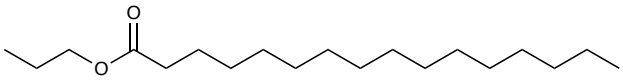

1.41

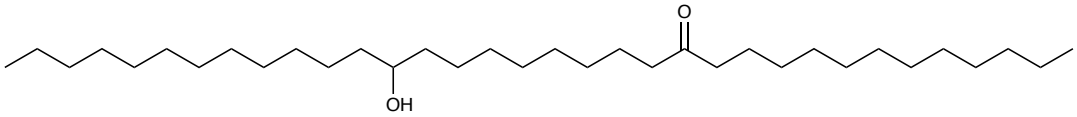

1.42

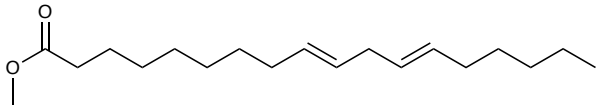

1.44

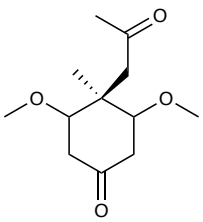

1.43

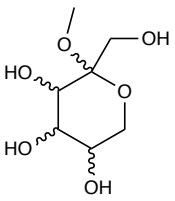

1.45

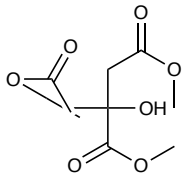

1.46

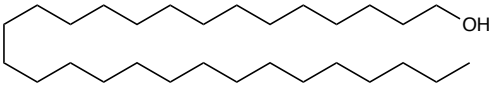

1.47

1.48

1.6. The threat of antibiotic resistance

1.6.1. Impact of resistant bacteria on public health

In 1928, casually spores from a filamentous fungus contaminated a petri dish with bacterial cultures in Alexander Fleming's laboratory at St Mary's Hospital in London, leading to the discovery of a bactericidal substance later designated and identified as penicillin. The introduction of this compound into therapy took about 12 years, curing patients with bacterial infections that would otherwise have succumbed (Tan and Tatsumura 2015). New antibiotics were discovered and revolutionized healthcare, becoming the foundation of many of the greatest medical advances of the twentieth century. Common but often fatal diseases such as pneumonia and tuberculosis (TB) have been effectively treated (Fair and Tor 2014)

However, bacteria and other pathogens have evolved to resist the new drugs used to combat them (Figure 1.2). This resistance has become a growing public health problem in recent years due to the misuse and overuse of antibiotics in both human and veterinary use (Figure 1.3). Ultimately, resistant microorganisms could evolve to multidrug-resistant forms (MDR) that are defined as the acquired nonsusceptibility to at least one agent in three or more antibiotic categories (Magiorakos *et al.* 2012). Moreover, extensively drug

resistant (XDR) and pandrug resistant (PDR) microorganisms have also became major concerns in clinical because these organisms can be resistant to all currently available antibiotics or remain susceptible only to potentially more toxic agents, leading to limited options for treatment (Magiorakos *et al.* 2012).

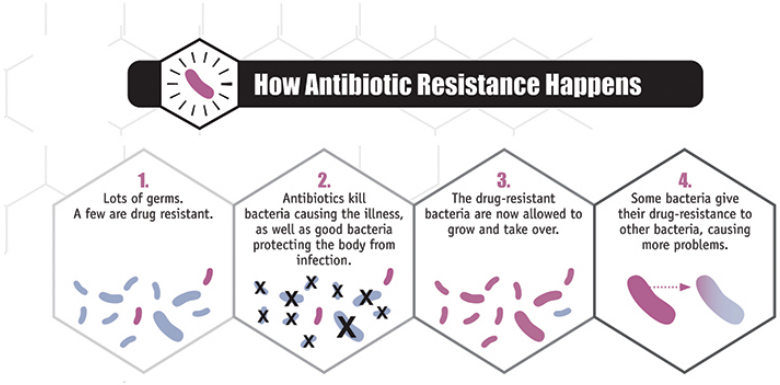

Figure 1.2 Antibiotic resistance. How some bacteria resist antibiotics, remain in the body and transmit their resistance. Adapted from CDC, 2013.

Examples of MDR bacteria are methicillin resistant *Staphylococcus aureus* (MRSA) and vancomycin resistant *Enterococcus* (VRE), fluoroquinolone resistant *Pseudomonas aeruginosa*, ceftazidime resistant *Klebsiella pneumoniae* and many other bacteria. The options for treating these bacteria are increasingly limited resulting in the resurgence of pathologies considered classically treatable. (Hansra and Shinkai 2011; Barnes and Sampson 2011).

Results from various surveillance programs indicate that there is a high percentage of nosocomial infections caused by MDR bacterial strains such as MRSA and VRE (Fig. 1.3). Joint analysis of data from 15 European countries revealed that over 10% of blood infections are caused by MRSA strains, and several of these countries have MDR strain prevalence rates close to 50% (European Center for Disease Prevention and Control, 2018). The threat stems not only from the high prevalence of resistance among bacteria but also from the rapidly increasing levels of resistance.

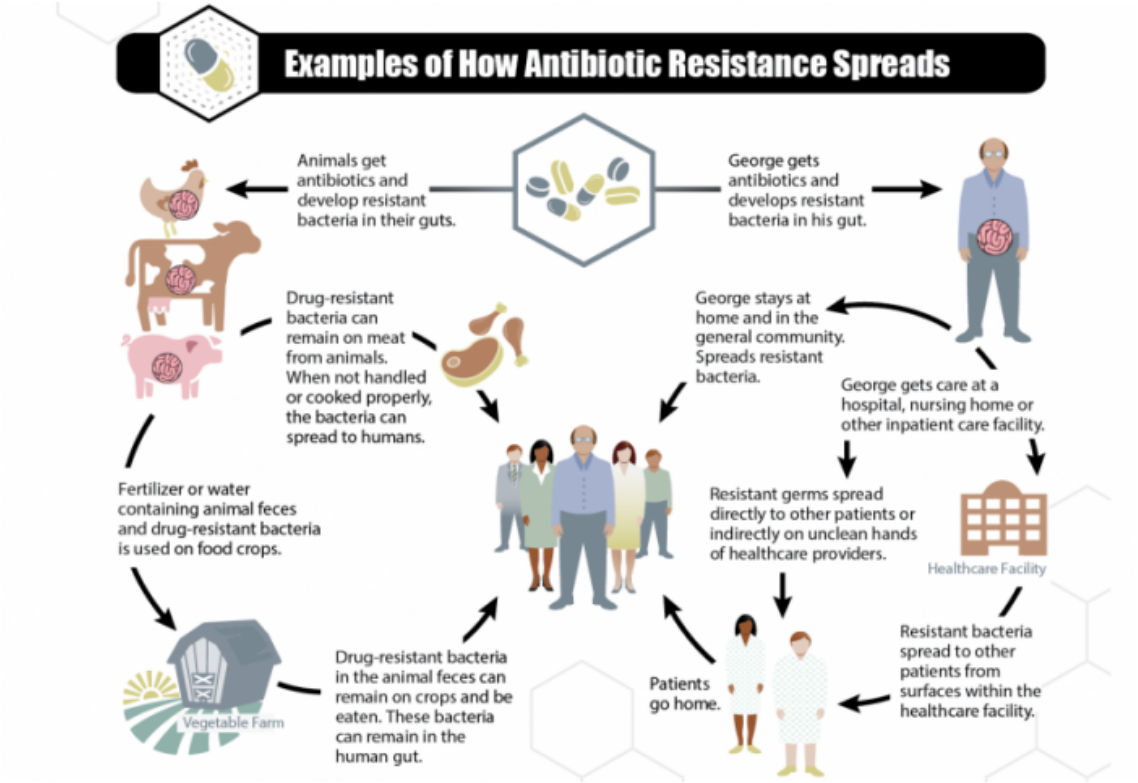

Figure 1.3 Ways in which antibiotic-resistant bacteria can proliferate. Adapted from CDC, 2013.

Antibiotic resistance is a worldwide problem. New forms of antibiotic resistance can cross international borders and spread across continents with ease. Many forms of resistance have spread with remarkable speed and world health leaders have described antibiotic resistant microorganisms as "nightmare bacteria" that pose a catastrophic threat to people in every country of the world (CDC, 2013). At the same time the pace of discovery of new antibiotics has slowed dramatically, (O'Neill 2014). One of the reasons for this decline is the challenges in identifying new chemicals that are both effective and non-toxic (Kalan e Wright, 2011).

1.6.2. Natural Products importance in the development of new drugs

Nowadays the economics of antibacterial research and development is considered "broken" and is commonly quoted as the principal cause for the lack of new therapies but the truth is that discover new antibacterial drugs is exceedingly difficult and science is not yet well advanced to allow the discovery of effective, efficient and non-toxic drugs. This has led to fears of a 'post-antibiotic era' (Jackson Czaplewski and Piddock, 2018). Therefore, there is an urgent need to find new approaches to antibiotic discovery.

A new approach is the concept of the 'magic bullet' – that is, a small-molecule drug which is both selectively lethal to bacteria and able to be administered to humans and animals (Czaplewski *et al.* 2016).

Although assuming the small-molecule approach, how will it be possible to go forward to identify new drugs? The answer is in Natural Products (NPs). Over the past century NPs have supplied a crucial start-point in drug discovery and antibacterial therapies (Brown, Lister and May-Dracka 2014), and as they appear to have a number of undiscovered chemical properties, this strategy offers great chances for exploitation in drug development (Mugumbate and Overington 2015). This realization has led to a renaissance of interest in natural products with antibiotic activity for the identification of new molecules, and their application in antibacterial drug discovery (Johnston and Magarvey 2015).

Currently, existing antibiotics are mostly from natural products whose purpose is to target the bacterial cell wall, DNA or ribosomes. With rare exceptions, these compounds generally have more than one molecular target and exert complex effects on the bacterial cell (Brown and Wright 2016). Taking the example of penicillin, a type of β-lactam antibiotic, covalently alter various target enzymes known as penicillin binding proteins (PBPs) which, in turn, are responsible for the synthesis and remodeling of the bacterial cell wall for growth and division. Some antibiotics target the ribosome by inhibiting protein synthesis, others target some topoisomerase enzymes to block DNA synthesis. It is important to emphasize that, this effect on manifold cellular targets creates a limitation in the frequency of natural resistance that can emerge from mutation in the target gene. Inhibition of the molecular targets of antibiotics usually outcome in complex downstream effects that exceed those of simple enzyme inhibition. Evidence-based, β-lactam antibiotics disarray the bacterial cell-wall synthesis machinery activity in a way far more complex than simple inhibition (Cho, Uehara and Bernhardt 2014).

Systems-biology approaches proposed that reactive oxygen species have been neglected as contributors to cell death (Dwyer, Collins and Walker 2015). Even though this hypothesis remains controversial, there is an enhanced appreciation that bacterial cell death is complex and likely demands the involvement of several cellular pathways. Numerous natural-product antibiotics are the product of selection for these complex traits over millions of years of evolution. For that reason, it is possibly expected that modern methods of drug discovery have yet to hand compounds with efficacy comparable to that

of the first generation of natural antibiotics and their semisynthetic derivatives (Brown and Wright 2016).

This experimental work was intended to contribute to the scientific validation of the therapeutic application of *G. hexamita* in traditional African medicine as an antibacterial agent by isolating some of its bioactive constituents.

CHAPTER 2

Results and Discussion

2. Results and Discussion

2.1. *Grewia hexamita* phytochemical study

Bioassay-guided fractionation of *Grewia hexamita* allowed the isolation and identification of four triterpenes, three with a pentacyclic scaffold, lupeol (**2.1**), betulin (**2.2**), and betulinic aldehyde (**2.3**) and a new tetracyclic triterpene named 3β-caffeoyl-cycloartane (**2.4**). In addition to these compounds, two steroids, β-sitosterol (**2.5**) and 7-oxo-β-sitosterol (**2.6**), two phenolic compounds, *p*-hydroxybenzaldehyde (**2.7**) and vanillin (**2.8**), as well as pantolactone (**2.9**), an γ-butyrolactone, have also been isolated (Figure 2.1). Their structures were characterized by spectroscopic methods mainly 1D-(^{1}H, ^{13}C) and 2D-NMR (DEPT, COSY, HMBC and HMQC) experiments and by comparisons with literature data. Furthermore, acylation of lupeol (**2.1**) and betulin (**2.2**), isolated in large amount, yielded four derivatives (**2.10**-**2.13**).

2.1.1. Triterpenes

2.1.1.1. Lupeol (**2.1**) and betulin (**2.2**)

Compound **2.1** was isolated as white crystals of m.p. 214-216 ºC and identified as lupeol based on the comparison of its physical and spectroscopic data to those described on the literature (Sai Prakash and Prakash 2012).

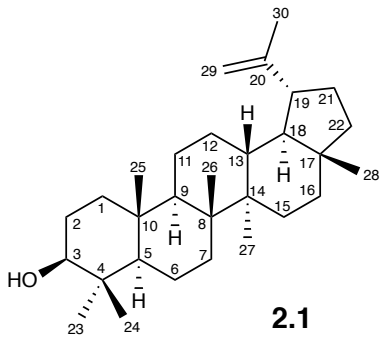

2.1

The ESI-MS with a protonated molecular ion at m/z 427 and the ^{13}C NMR spectrum were consistent with the molecular formula $C_{30}H_{50}O$. The six degrees of unsaturation are in agreement with the presence of five rings and a double bond.

The presence of a hydroxyl group was supported by the ^{1}H NMR spectrum by the existence of an oxymethine signal at δ_H 3.19 ppm, which was displayed as a double doublet (J = 11.0 and 5.3 Hz) indicative of its axial orientation (Table 2.1). The existence of an exocyclic double bond was suggested by a doublet of doublets at δ_H 4.57 (J = 2.4 and 1.3 Hz) and a doublet at δ_H 4.69 ppm (J = 2.4 Hz) that were assigned to the methylene protons. The presence of an isopropenyl group was indicated by the vinylic methyl signal at δ_H 1.68 ppm. Moreover, the ^{1}H NMR spectrum also displayed signals for six tertiary methyl groups at δ_H 0.76, 0.79, 0.83, 0.95, 0.97 and δ_H 1.03 ppm.

The ^{13}C and DEPT NMR spectra (Table 2.2) corroborated the data described above, showing thirty carbon resonances: six methyls, eleven methylenes (one sp^2 at δ_C 109.5 ppm), seven methines (one oxygenated at δ_C 79.2 ppm) and six quaternary carbons (one olefinic at δ_C 151.1 ppm).

All these data are in agreement with those reported in literature for lupeol [20(29)-lupen-3β-ol] and allowed the identification of compound **2.1** (Sai Prakash and Prakash 2012).

Table 2.1 ^{1}H NMR data of lupeol (**2.1**) and betulin (**2.2**), (300 MHz, $CDCl_3$; δ in ppm, J in Hz).

	2.1	**2.2**
Position	^{1}H	^{1}H
3	3.19 *dd* (11.0; 5.3)	3.19 *dd* (10.8; 5.3)
19	2.38 *td* (11.0; 5.6)	2.38 *td* (11.0; 5.6)
23	0.95 *s*	0.97 *s*
24	0.76 *s*	0.76 *s*
25	0.83 *s*	0.83 *s*
26	1.03 *s*	1.02 *s*
27	0.97 *s*	0.98 *s*
28	0.79 *s*	3.80 *dd* (10.8; 1.5) 3.33 *d* (10.8)
29	4.57 *dd* (2.4; 1.3) 4.69 *d* (2.4)	4.58 *dd* (2.3; 1.4) 4.68 *d* (2.2)
30	1.68 *s*	1.68 *s*

Table 2.2 ^{13}C and DEPT NMR data of lupeol (**2.1**) and betulin (**2.2**), (300 MHz, $CDCl_3$; δ in ppm, *J* in Hz).

	2.1		**2.2**			**2.1**		**2.2**	
Position	^{13}C	DEPT	^{13}C	DEPT	Position	^{13}C	DEPT	^{13}C	DEPT
1	38.9	CH_2	39.0	CH_2	16	35.8	CH_2	29.3	CH_2
2	27.6	CH_2	27.6	CH_2	17	43.12	C	47.9	CH
3	79.2	CH	79.1	CH	18	48.5	CH	47.9	CH
4	39.0	C	38.9	C	19	48.1	CH	48.9	CH
5	55.5	CH	55.6	CH	20	151.1	C	150.6	C
6	18.5	CH_2	18.5	CH_2	21	30.0	CH_2	29.9	CH_2
7	34.5	CH_2	34.4	CH_2	22	40.2	CH_2	34.1	CH_2
8	41.0	C	41.1	C	23	28.2	CH	28.1	CH
9	50.6	CH	50.6	CH	24	15.5	CH_3	15.5	CH_3
10	37.3	C	37.5	C	25	16.3	CH_3	16.3	CH_3
11	21.1	CH_2	20.9	CH_2	26	16.1	CH_3	16.1	CH_3
12	25.3	CH_2	25.4	CH_2	27	14.7	CH_3	14.9	CH_3
13	38.2	CH	37.3	CH	28	18.2	CH_3	60.7	CH_2
14	42.8	C	42.9	C	29	109.5	CH_2	109.8	CH_2
15	27.6	CH_2	27.2	CH_2	30	19.5	CH_3	19.2	CH_3

Compound **2.2** was isolated as white crystals of m.p. 248-251 ºC and identified as betulin based on the comparison of its physical and spectroscopic data to those described on the literature (Kwaji et al. 2018).

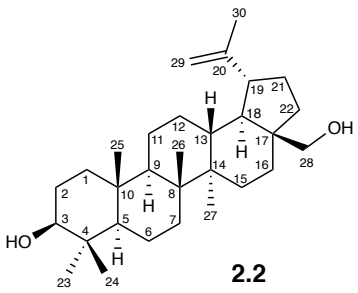

2.2

The ESI-MS, with a protonated molecular ion at m/z 443, and ^{13}C NMR spectrum were consistent with the molecular formula $C_{30}H_{50}O_2$. The six degrees of unsaturation are in agreement with the presence of five rings and a double bond.

In the ^{1}H NMR spectrum (Table 2.1), a doublet of doublets at δ_H 3.19 ppm (J = 10.8 and 5.3 Hz) indicated the presence of α-oriented hydrogen at C-3. Furthermore, two signals at δ_H 3.80 and 3.33 ppm, corresponding the diastereotopic methylene protons at C-28, and resonances at δ_H 4.58 and 4.68 ppm, assigned to the olefinic protons at C-29, together with a vinylic methyl group at δ_H 1.68 ppm could also be observed. The structure of compound **2.2** was further substantiated by the ^{13}C NMR and DEPT spectra that revealed thirty signals due to five quaternary carbons (one olefinic at δ_C 150.6 ppm), eight methines (two oxygenated, at δ_C 79.1 and 60.7 ppm), twelve methylenes (one sp^2 at δ_C 109.8 ppm) and five methyls (Table 2.2). The olefinic signals at δ_C 150.6 and 109.8 ppm corroborated the presence of the characteristic double bond at C-29 of lupane-type triterpenes.

Consequently, based on the comparison of the NMR data with literature, compound **2.2** was found to be lup-20(29)-ene-3,28-diol, commonly known as betulin (Kwaji et al. 2018), which differs from lupeol at C-28, having an hydroxyl group at this position.

2.1.1.1.1. Preparation of lupeol and betulin derivatives

Lupeol (**2.1**) and betulin (**2.2**), isolated in large amount, were acylated for increasing the number of compounds and further study their antibacterial activity.

2.1.1.1.2. Lupeol acetate (**2.10**) and lupeol benzoate (**2.12**)

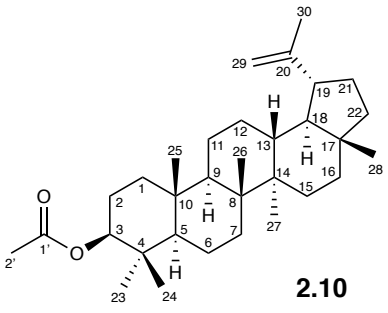

2.10

Acetylation of lupeol (Scheme 2.1) afforded compound **2.10.** This compound was obtained as colorless crystals of m.p. 220 ºC and identified as lupeol acetate based on the comparison of its physical and spectroscopic data with those described on the literature (Barla *et al.* 2006; da Silva *et al.* 2018).

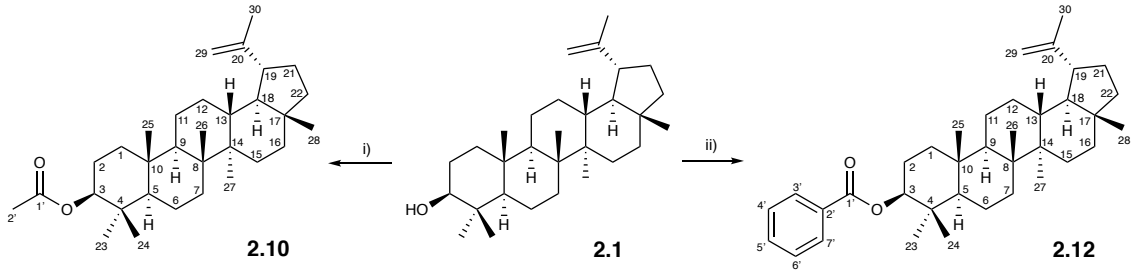

Scheme 2.1 Preparation of lupeol derivatives (**2.10** and **2.12**). [a]

[a] **Reagents and conditions:** (i) Pyridine (80 eq.) and Ac_2O (120 eq.), RT, O/N; ii) Pyridine (60 eq.) and benzoyl chloride (130 eq.), RT, O.N

The molecular formula, $C_{32}H_{52}O_2$, was substantiated by the ^{13}C NMR spectrum and ESI-MS, which exhibited a protonated molecule ion at m/z 469 $[M+H]^+$. The IR spectrum displayed an absorption band at 1735 cm^{-1} for ester carbonyl group.

The NMR data of compound **2.10** (Table 2.3) resembled those obtained for lupeol (**2.1**). As expected, in the ^1H NMR spectrum, the most remarkable differences were the presence of a new acetyl singlet at δ_H 2.05 ppm, and the downfield chemical shift of H-3 that appeared in compound **2.10** at δ_H 4.47 (*m*).

Table 2.3 ^1H NMR data of lupeol-3-acetate (**2.10**) and lupeol benzoate (**2.12**), (300 MHz, $CDCl_3$; δ in ppm, *J* in Hz).

Position	**2.10**	**2.12**
3	4.47 *m*	4.72 *m*
19	2.38 *td* (11.0; 5.6)	2.39 *td* (11.0; 5.6)
23	0.83 *s*	0.92 *s*
24	0.78 *s*	0.79 *s*
25	0.83 *s*	0.83 *s*
26	1.02 *s*	1.05 *s*
27	0.93 *s*	1.00 *s*
28	0.84 *s*	0.84 *s*
29	4.56 *dd* (2.8; 1.4) 4.69 *d* (2.5)	4.57 *dd* (2.6; 1.4) 4.69 *d* (2.6)
30	1.66 *s*	1.69 *s*
2’	2.05 *s*	–
3’	–	8.04[a] *m*
4’	–	7.44[b] *m*
5’	–	7.54 *m*
6’	–	7.44[b] *m*
7’	–	8.04[a] *m*

a, b Overlapped signals

In the ^{13}C NMR, the presence of the new signals at δ_C 171.2 and 21.5 ppm, together with the paramagnetic effect at C-3 (δ_C 81.8 ppm) were consistent with the introduction of a new acetyl group at this position (Table 2.4).

Table 2.4 ^{13}C and DEPT NMR data of lupeol-3-acetate (**2.10**) and lupeol benzoate (**2.13**), (300 MHz, CDCl3; δ in ppm, J in Hz).

	2.10		**2.12**			**2.10**		**2.12**	
Position	^{13}C	DEPT	^{13}C	DEPT	Position	^{13}C	DEPT	^{13}C	DEPT
1	38.1	CH_2	38.3	CH_2	20	151.1	C	151.1	C
2	23.8	CH_2	23.9	CH_2	21	29.9	CH_2	29.9	CH_2
3	81.8	CH	79.2	CH	22	40.1	CH_2	40.1	CH_2
4	38.5	C	38.5	CH_2	23	28.1	CH	28.3	CH
5	55.5	CH	55.5	CH	24	15.5	CH_3	16.1	CH_3
6	18.5	CH_2	18.4	CH_2	25	16.3	CH_3	16.9	CH_3
7	34.3	CH_2	34.3	CH_2	26	16.1	CH_3	16.4	CH_3
8	40.9	C	40.9	C	27	14.6	CH_3	14.6	CH_3
9	50.4	CH	50.5	CH	28	18.2	CH_3	18.2	CH_2
10	37.2	C	37.2	CH	29	109.5	CH_2	109.5	CH_2
11	21.1	CH_2	21.1	CH_2	30	19.4	CH_3	19.4	CH_3
12	25.2	CH_2	25.2	CH_2	1’	171.2	C	166.4	C
13	37.9	CH	38.1	C	2’	21.5	CH_3	131.1	C
14	42.9	C	42.9	C	3’	–	–	129.7	CH
15	27.5	CH_2	27.6	CH_2	4’	–	–	128.4	CH
16	35.7	CH_2	35.7	CH_2	5’	–	–	132.8	CH
17	43.1	C	43.1	CH	6’	–	–	128.4	CH
18	48.4	CH	47.9	CH	7’	–	–	129.7	CH
19	48.1	CH	48.4	CH					

Benzoylation of lupeol afforded compound **2.12** that was obtained as colorless crystals with m.p. 261 ºC. Its IR displayed an absorption band for the ester carbonyl group at 1718 cm^{-1}.

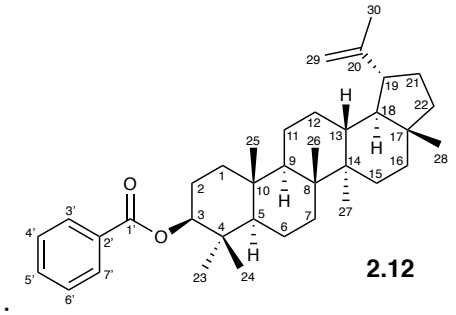

2.12

When comparing with lupeol (**2.1**) (Tables 2.3 and 2.4), the main differences in the ^{1}H NMR spectrum of compound **2.12**, were the presence of downfield signals corresponding to the aromatic protons at δ_H 8.04, 7.44 and 7.54 ppm. In turn, in the ^{13}C NMR, besides the extra signals for the benzene the ring and the carbonyl carbon (δ_C 166.4 ppm), the most significant changes were in the carbon signals of ring A (Table 2.4), namely at C-3 that was shifted downfield (δ_C 79.2 ppm).

All the physical and spectroscopic data were in agreement with those described in the literature for lupeol benzoate (Adotey *et al.* 2012)).

2.1.1.1.3. Betulin diacetate (**2.11**) and betulin dibenzoate (**2.13**)

Acetylation of betulin afforded compound **2.11** (Scheme 2.2.) isolated as colorless crystals of m.p. 219-221 ºC.

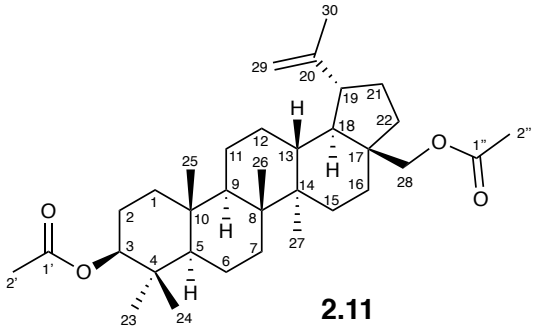

2.11

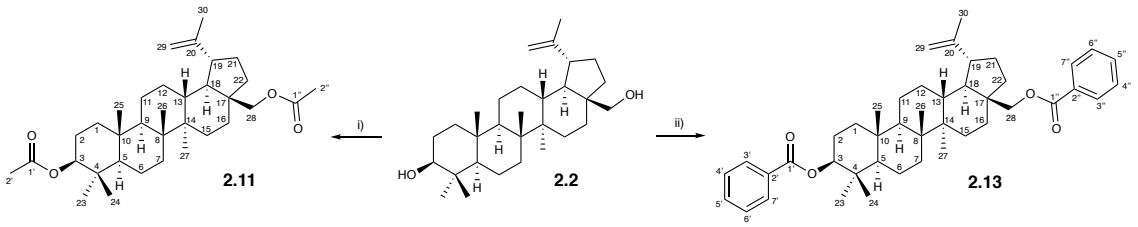

Scheme 2.2 Preparation of betulin (**2.2**) derivatives (**2.11** and **2.13**).[a]

[a] **Reagents and conditions:** i) Pyridine (110 eq.) and Ac_2O (90 eq.), RT, O/N; ii) Pyridine (110 eq.) and benzoyl chloride (40 eq.), RT, O.N.

The ESI-MS with a protonated molecular ion at m/z 527 $[M+H]^+$ and the ^{13}C NMR spectrum were consistent with the molecular formula $C_{34}H_{54}O_4$. The IR spectrum showed a strong absorption band at 1712 cm^{-1} corresponding to stretching vibrations of the carbonyl ester groups.

The NMR data of compound **2.11** (Table 2.5 and 2.6) resembled those found for betulin (**2.2**). Therefore, in the ^1H NMR spectrum, the most notable differences were the presence of two new acetyl singlets at δ_H 2.03 and 2.06 ppm, and the signals of H-3 and H-28 that were shifted downfield, appearing in compound **2.11** at δ_H 4.45 as a multiplet and two doublets of doublets at δ_H 3.83 (J = 11.0 and 1.2 Hz) and δ_H 4.23 (J = 11.0 and 1.9 Hz), respectively (Table 2.5). In the ^{13}C NMR, the resonances of two methyl groups at δ_C 21.2 and δ_C 21.5 ppm with the corresponding signals for each carbonyl at δ_C 171.2 and δ 171.8 ppm (Table 2.6), together with the downfield shifts of C-3 (δ_C 81.8 ppm) and C-28 (δ_C 62.9 ppm), were consistent with the introduction of the two new acetyl groups at this position (Table 2.4).

Compound **2.11** was identified as betulin diacetate based on the comparison of its physical and spectroscopic data to those described on the literature (Salah and Bakibaev 2017).

Table 2.5 ^{1}H NMR data of betulin diacetate (**2.11**) and betulin dibenzoate (**2.13**), (300 MHz, $CDCl_3$; δ in ppm, *J* in Hz).

Position	**2.11**	**2.13**
	^{1}H	^{1}H
3	4.45 *m*	4.70 *m*
19	2.43 *td*(10.9; 5.7)	2.54 *td* (10.8; 5.7)
23	0.83 *s*	1.00 *s*
24	0.83 *s*	0.92 *s*
25	0.82 *s*	0.91 *s*
26	1.01 *s*	1.09 *s*
27	0.95 *s*	1.02 *s*
28	3.83 *dd* (11.0; 1.2) 4.23 *dd* (11.0; 1.9)	4.10 *m* 4.54 *dd* (11.2; 1.8)
29	4.57 *dt* (2.7; 1.4) 4.67 *d* (2.3)	4.62 *dd* (2.3; 1.4) 4.73 *d* (2.3)
30	1.67 *s*	1.72 *s*
2’	2.06 *s*	–
3’	–	8.05[a] *m*
4’	–	7.44[b] *m*
5’	–	7.55[c] *m*
6’	–	7.44[b] *m*
7’	–	8.05[a] *m*
2’’	2.03 *s*	–
3’’	–	8.05[a] *m*
4’’	–	7.44[b] *m*
5’’	–	7.55[c] *m*
6’’	–	7.44[b] *m*
7’’	–	8.05[a] *m*

a, b, c Overlapped signals

Benzoylation of betulin afforded compound **2.13** (Scheme 2.2). This compound was obtained as colorless crystals with m.p. 142 ºC. Its IR displayed absorption bands for the ester carbonyl groups at 1716 cm^{-1}.

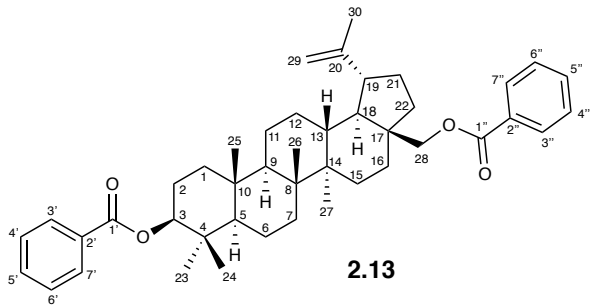

2.13

The ^{13}C NMR spectrum showed resonances for 44 carbon atoms, which agreed with the molecular formula $C_{44}H_{58}O_4$, and the ESI-MS exhibited a deprotonated molecule ion at m/z 649 $[M-H]^+$.

In the ^1H NMR spectrum of compound **2.13**, it is clear the presence of ten aromatic protons at δ_H 8.05, 7.44 and δ_H 7.55 (Table 2.5) and consequently the downfield chemical shift of H-3 and of the diastereotopic protons H-28 that appeared in compound **2.13** at δ_H 4.70 (*m*) and δ_H 4.10 (*m*) and 4.54 ppm (*dd*; *J* = 11.2 and 1.8 Hz), respectively. In the ^{13}C NMR, two ester resonances were spotted at δ_C 166.4 and δ_C 167.1 and the resonances of C-3 (δ_C 81.8 ppm) and C-28 (δ_C 63.4 ppm), where shifted downfield, confirming the introduction of the benzoyl moieties at these carbons (Table 2.6).

Table 2.6 ^{13}C and DEPT NMR data of betulin diacetate (**2.11**) and betulin dibenzoate (**2.13**), (300 MHz, $CDCl_3$; δ in ppm, *J* in Hz).

	2.11		**2.13**			**2.11**		**2.13**	
Position	^{13}C	DEPT	^{13}C	DEPT	Position	^{13}C	DEPT	^{13}C	DEPT
1	38.1	CH_2	38.3	C	23	28.1	CH	28.3	CH
2	23.8	CH_2	23.9	CH_2	24	15.5	CH_3	16.9	CH_3
3	81.8	CH	81.7	CH	25	16.3	CH_3	16.3	CH_3
4	38.5	C	38.3	CH_2	26	16.1	CH_3	16.2	CH_3
5	55.5	CH	55.6	CH	27	14.6	CH_3	14.6	CH_3
6	18.5	CH_2	18.3	CH_2	28	62.9	CH_2	63.4	CH_2
7	34.3	CH_2	34.3	CH_2	29	109.5	CH_2	110.1	CH_2
8	40.9	C	41.1	C	30	19.4	CH_3	19.3	CH_3
9	50.4	CH	50.4	CH	1’	171.2	C	166.4	C
10	37.2	C	37.2	CH	2’	21.5	CH_3	130.6	C
11	21.1	CH_2	21.0	CH_2	3’	–	–	129.7	CH
12	25.2	CH_2	25.3	CH_2	4’	–	–	128.4	CH
13	37.9	CH	37.8	C	5’	–	–	132.8	CH
14	42.9	C	42.2	C	6’	–	–	128.4	CH
15	27.5	CH_2	27.3	CH_2	7’	–	–	129.7	CH
16	35.7	CH_2	30.1	CH_2	1’’	171.8	C	167.1	C
17	43.1	C	46.8	CH	2’’	21.2	CH_3	131.1	C
18	48.4	CH	49.0	CH	3’’	–	–	129.7	CH
19	48.1	CH	48.0	CH	4’’	–	–	128.5	CH
20	151.1	C	150.3	C	5’’	–	–	133.0	CH
21	29.9	CH_2	29.8	CH_2	6’’	–	–	128.5	CH
22	40.1	CH_2	34.9	CH_2	7’’	–	–	129.7	CH

Compound **2.13** was identified as betulin dibenzoate based on the comparison of its physical and spectroscopic data to those described on the literature (Levdanskii, Levdanskii and Kuznetsov 2017).

2.1.1.2. Betulinic aldehyde (**2.3**)

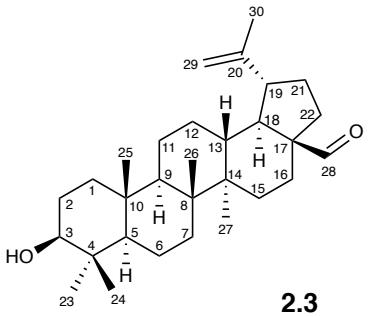

2.3

Compound **2.3** was isolated as an amorphous powder. The ESI-MS exhibited a protonated molecule ion at m/z 441 $[M+H]^+$, which, together with the ^{13}C NMR spectrum, substantiated the molecular formula $C_{30}H_{48}O_5$ (twelve degrees of unsaturation). The IR spectrum showed an absorption band at 1716 cm^{-1}, corresponding to a carbonyl group.

When comparing the NMR data of compound **2.3** with those of betulin (**2.2**), it was clear that these compounds have in common the same pentacyclic triterpenoid skeleton. In fact, from the analysis of Tables 2.1, 2.2, 2.7 and 2.8, it becomes evident that the only difference between these two compounds is at C-28 position. Thus, in the ^1H NMR spectrum of compound **2.3**, the singlet at δ_H 9.67 ppm indicated the presence of an aldehyde proton (Table 2.7) which was corroborated by the lack of the signals corresponding to diastereotopic methylene protons at C-28 (δ_H 3.80 and 3.33 ppm) (Table 2.1).

The presence of the aldehyde function was confirmed by the analysis of ^{13}C NMR spectrum where the signal at δ_C 60.7 ppm, found in betulin (**2.2**), was replaced by a signal at δ_C 206.9 ppm (Table 2.8), which was correlated in the HSQC spectrum with the singlet at δ_H 9.67 ppm.

Table 2.7 ^{1}H NMR data of betulinic aldehyde (**2.3**), (300 MHz, CDCl3; δ in ppm, J in Hz).

Position	^{1}H
3	3.18 *dd* (10.9; 5.1)
19	2.38 td (11.0; 5.6)
23	0.96 *s*
24	0.74 *s*
25	0.81 *s*
26	1.03 *s*
27	0.97 *s*
28	9.67 *br s*
29	4.62 dd (2.3; 1.4) 4.75 d (2.2)
30	1.68 *s*

Table 2.8 ^{13}C and DEPT NMR data of betulinic aldehyde (**2.3**), (300 MHz, $CDCl_3$; δ in ppm, J in Hz).

Position	^{13}C	DEPT	Position	^{13}C	DEPT
1	38.9	CH_2	16	28.6	CH_2
2	27.5	CH_2	17	59.5	C
3	79.0	CH	18	48.5	CH
4	39.0	C	19	47.6	CH
5	55.4	CH	20	149.9	C
6	18.4	CH_2	21	30.0	CH_2
7	34.4	CH_2	22	33.3	CH_2
8	40.9	C	23	28.2	CH
9	50.6	CH	24	15.5	CH_3
10	37.3	C	25	16.3	CH_3
11	20.9	CH_2	26	16.1	CH_3
12	25.6	CH_2	27	14.7	CH_3
13	38.8	CH	28	206.9	CH_3
14	42.7	C	29	109.5	CH_2
15	29.4	CH_2	30	19.5	CH_3

All these data were in agreement with those reported in literature for betulinic aldehyde and allowed the identification of compound **2.3** (Olennikov *et al.* 2017).

2.1.1.3. 3β-caffeoyl-cycloartane (**2.4**)

Cycloartanes are compounds also called 9,19-cyclolanostanes and are characterized by the presence of a cyclopropane ring in the molecule (Ali et al. 2007).

Compound **2.4**, a new compound isolated from fraction E9.1 of the EtOAc extract and from fraction HIJ4.2 of the *n*-hexane extract, was obtained as white crystals of m.p. 290 ºC and $[\alpha]_D^{25}$ + 39.3º.

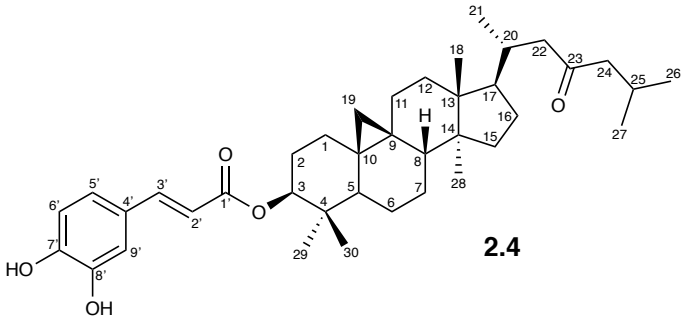

2.4

The ESI-MS showed the protonated molecule ion at m/z 605 $[M+H]^+$ and a ion at m/z 425 [M−caffeic acid + H]$^+$ (Scheme 2.3). These data, along with the ^{13}C NMR spectrum, were consistent with the molecular formula $C_{39}H_{56}O_5$. The twelve degrees of unsaturation are in agreement with the presence of six rings and six double bonds.

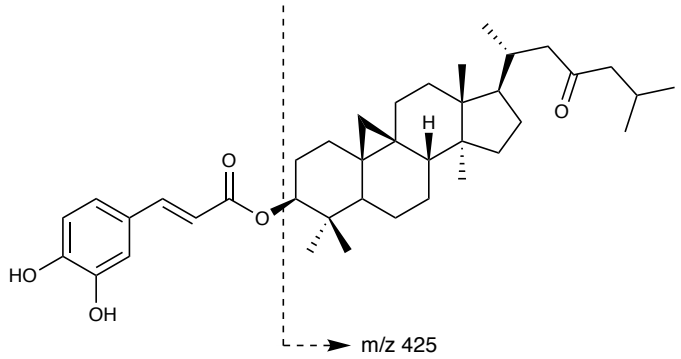

Scheme 2.3 Ion observed in the mass spectrum of compound **2.4**.

The IR spectrum exhibited a broad absorption band at 3288 cm^{-1} corresponding to the hydroxyl groups. It was also visible the presence of two strong bands at 1706 and 1716 cm^{-1}, corresponding to a carbonyl group and to an α, β-unsaturated ester group.

The ^1H NMR spectrum indicated the presence of protons characteristic of a cycloartane-type triterpene, namely the protons of the cyclopropane ring through two

very upfield signals at δ_H 0.36 (d, J = 4.2 Hz) and 0.60 (d, J = 4.2 Hz) ppm, attributable to H-19 (Table 2.9). The presence of three downfield signal for aromatic protons (δ_H 6.88 *d*, J = 8.4 Hz; 6.98, *dd,* J = 1.8 and 8.9 Hz ; and 7.13 ppm, *d* J = 1.8 Hz), assignable to a trisubstituted aromatic ring, along with two olefinic protons with a *trans* configuration at δ_H 6.26 (*d*, J = 15.9 Hz) and δ_H 7.56 (*d*, J = 15.6 Hz) ppm provided evidence for the presence of a caffeoyl ester moiety. Moreover, the ^{1}H NMR spectrum of **2.4** displayed signals due to seven methyl groups: four singlets corresponding to tertiary methyl groups (δ_H 1.00, 0.88, 0,88, 0.96) and two doublets of secondary methyls at δ_H 0.89 (d, J = Hz, 6 H) and 0.91 (d, J = 6.0 Hz) 0.92 (d, J = 6.3 Hz) and a signal at 4.68 (*dd,* J = 4.5 and 10.8 Hz*),* corresponding to H-3.

Table 2.9 ^{1}H NMR data of 3β-caffeoyl-cycloartane (**2.4**), (300 MHz, $CDCl_3$; δ in ppm, J in Hz).

Position	^{1}H
3	4.68 *dd* (4.5;10.8*)*
18	1.00 s
19	0.36 *d* (4.2) 0.60 *d* (4.2)
21	0.89 *d* (6.0)
22	2.15 *m* 2.46 *dd* (2.1; 15.9)
24	2.28 *d* (6.9)
26	0.92 *d* (6.3)
27	0.91*d* (6.0)
28	0.88 *s*
29	0.88 *s*
30	0.96 *s*
2’	6.26 *d* (15.9)
3’	7.56 *d* (15.9)
5’	6.98 *dd* (1.8; 8.9)
6’	6.88 *d* (8.4)
9’	7.13 *d* (1.8)

The ^{13}C NMR and DEPT spectrum indicated thirty-nine carbon resonances, namely seven methyl groups, eleven methylenes, eleven methines and ten quaternary carbons (Table 2.10). The carbonyl signal at δ_C 167.9 and the vinylic carbons at δ_C 145.0 and δ_C 116.1 were assigned to the carbonyl group and the double bond of the α,β-unsaturated ester group, respectively, while the signal at δ_C 212.8 ppm was assigned to the ketone function at C-23 of the side chain.

The 2D NMR spectra confirmed the structure of compound **2.4**, by the J_{H-H} correlations observed in the COSY spectrum and the long-range heterocorrelations observed in the HMBC spectrum (Scheme 2.4). In this way, ^{2}J correlations observed between C-23 and the diastereotopic methylene protons at C-22 and C-24 substantiated the location of ketone group in the side chain.

Table 2.10 ^{13}C and DEPT NMR data of 3β-caffeoyl-cycloartane (**2.4**), (300 MHz, $CDCl_3$; δ in ppm, *J* in Hz).

Position	^{13}C	DEPT	Position	^{13}C	DEPT
1	31.8	CH_2	21	25.5	CH_3
2	27.1	CH_2	22	50.9	CH_2
3	81.1	CH	23	212.8	C
4	39.8	C	24	52.8	CH_2
5	47.3	CH	25	25.6	CH
6	21.0	CH_2	26	22.9	CH_3
7	25.9	CH_2	27	22.7	CH_3
8	47.9	CH	28	19.4	CH_3
9	20.2	C	29	24.8	CH_3
10	26.1	C	30	15.5	CH_3
11	26.5	CH_2	1’	167.9	C
12	32.9	CH_2	2’	116.1	CH
13	45.5	C	3’	145.0	CH
14	49.1	C	4’	127.5	C
15	35.6	CH_2	5’	122.4	CH
16	28.5	CH_2	6’	115.5	CH
17	52.5	CH	7’	144.3	C
18	18.2	CH_3	8’	146.8	C
19	29.9	CH_2	9’	114.4	CH
20	33.1	CH			

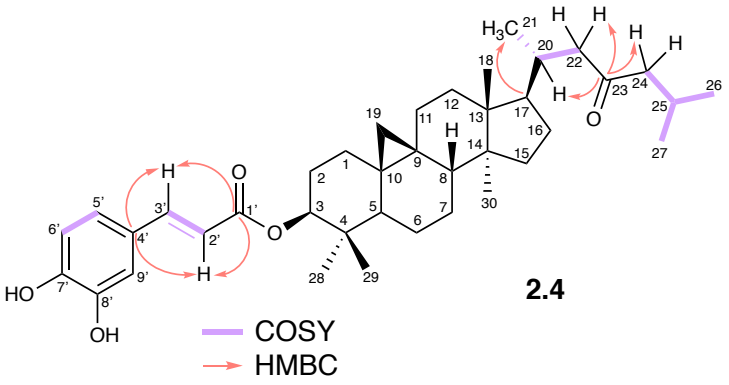

2.4

Scheme 2.4 Structural fragments established through the COSY experiment and the most relevant correlations observed in the HMBC spectrum of compound **2.4**.

2.1.2. Steroids

2.1.2.1. β-Sitosterol (**2.5**)

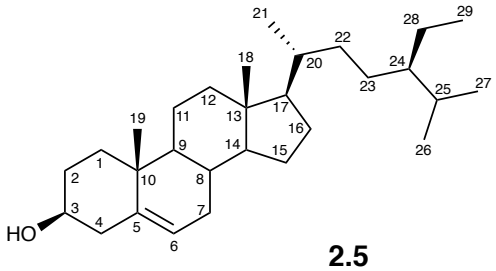

2.5

Compound **2.5** was isolated as white crystals of m.p. 141 ºC. The molecular formula ($C_{29}H_{50}O$) was concluded through the NMR spectra and confirmed by the ESI-MS which indicated a protonated molecular ion at *m/z* 414 $[M]^+$. The five degrees of unsaturation are in agreement with the presence of four rings and a double bond.

The ^1H NMR spectrum exhibited resonances at δ_H 3.52 and 5.35 ppm, both displayed as multiplets, corresponding to H-3α and to the vinylic proton H-6, respectively. Singlets at δ_H 0.68 and 1.01 ppm were assigned to H-18 and H-19 methyl groups, respectively (Table 2.11) and three doublets corresponding to the secondary methyls at δ_H 0.80 (J = 6.8 Hz), 0.83 (J = 6.5 Hz) and 0.92 (J = 6.5 Hz) ppm, and a triplet at δ_H 0.84 ppm assigned to H-29.

Table 2.11 ^{1}H NMR data of β-sitosterol (**2.5**) and stigmast-5-en-3β-ol-7-one (**2.6**), (300 MHz, $CDCl_3$; δ in ppm, *J* in Hz).

Position	**2.5**	**2.6**
	^{1}H	^{1}H
3	3.52 *m*	3.67 m
6	5.35 *dd* (4.8; 2.5)	5.69 *d* (1.7)
18	0.68 *s*	0.68 s
19	1.01 *s*	1.19 s
21	0.92 *d* (6.5)	0.92 *d* (6.6)
26	0.83 *d* (6.5)	0.82 *d* (6.5)
27	0.80 *d* (6.8)	0.84 *d* (6.8)
29	0.84 *t* (6.6)	0.80 *t* (6.6)

The ^{13}C NMR and DEPT spectra indicated twenty-nine carbon resonances, namely six methyl groups, eleven methylenes, nine methines (one *sp*2 at δ_C 121.8 ppm and one oxymethine at δ_C 71.9 ppm) and three quaternary carbons. The signal at δ_C 140.8 and 121.8 ppm were assigned to the olefinic carbons C-5 and C-6, respectively.

Table 2.12 ^{13}C and DEPT NMR data of β-sitosterol (**2.5**) and stigmast-5-en-3β-ol-7-one (**2.6**), (300 MHz, CDCl3; δ in ppm).

	2.5		**2.6**			**2.5**		**2.6**	
Position	^{13}C	DEPT	^{13}C	DEPT	Position	^{13}C	DEPT	^{13}C	DEPT
1	37.4	CH_2	36.5	CH_2	16	28.4	CH_2	28.7	CH_2
2	31.8	CH_2	31.3	CH_2	17	56.2	CH	54.8	CH
3	71.9	CH	70.7	CH	18	12.0	CH_3	12.1	CH_3
4	42.4	C	41.9	C	19	19.6	CH_3	17.5	CH_3
5	140.9	C	165.3	C	20	36.3	CH	36.2	CH
6	121.9	CH	126.2	CH	21	18.9	CH_3	19.1	CH_3
7	32.1	CH_2	202.5	C	22	34.1	CH_2	34.1	CH_2
8	32.1	CH	45.6	CH	23	26.3	CH_2	26.3	CH_2
9	50.3	CH	50.1	CH	24	46.0	CH	45.9	CH
10	36.7	C	38.4	C	25	29.3	CH	29.3	CH
11	21.2	CH_2	21.4	CH_2	26	19.9	CH_3	19.9	CH_3
12	39.9	CH_2	38.9	CH_2	27	19.5	CH_3	19.2	CH_3
13	42.5	CH_2	41.9	CH_2	28	23.2	CH_2	23.2	CH_2
14	56.9	CH	50.1	CH	29	12.1	CH_3	12.1	CH_3
15	24.5	CH_2	26.5	CH_2					

Comparison of all these physical and spectroscopic data with those described in the literature for β-sitosterol (stigmast-5-en-3β-ol), confirmed the identity of compound **2.5** (Ribeiro, Ferraz e Cruz, 2019).

2.1.2.2. 7-Oxo-β-sitosterol (**2.6**)

Compound **2.6** was isolated as white amorphous powder and further recognized as 7-oxo-β-sitosterol (**2.6**) or stigmast-5-en-3β-ol-7-one on the basis of its spectroscopic data (Ma, Lin and Zhang, 2009).

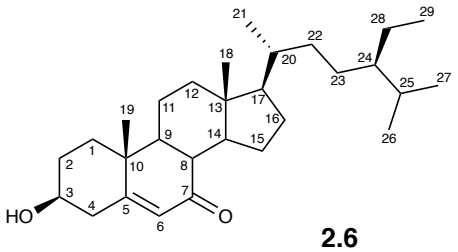

2.6

The ESI-MS, with a protonated molecular ion at m/z 429, and the ^{13}C NMR spectrum were consistent with the molecular formula $C_{29}H_{48}O$ corresponding to six degrees of unsaturation.

Comparing the NMR spectra of β-sitosterol (**2.5**), (Table 2.11 and 2.12), and compound **2.6**, it can be concluded that they are quite similar with some differences that stand out. Among these are the signals corresponding to the olefinic proton (δ_H 5.69 ppm, *d*, *J* = 1.7 Hz) and the methyl CH_3-19 (δ_H 1.19 ppm, *s*), which were shifted slightly downfield, having the former also a different multiplicity. Other main differences were verified in the ^{13}C NMR spectrum with the appearance of a carbonyl signal at δ_C 202.5 ppm and consequent changes at carbon signals of ring B namely C-5 (δ_C 140.9), C-6 (δ_C 126.1) and C-8 δ_C (45.4), thus indicating that the ketone was located at C-7 (Table 2.12).

The spectroscopic data of **2.6** were in agreement with those described in the literature for 7-oxo-β-sitosterol (Ma, Lin and Zhang, 2009).

2.1.3. Phenolic compounds

Two phenolic compounds were isolated in this study namely, p-hydroxybenzaldehyde and vanillin. Widely isolated in phytochemical studies, these compounds are the two main aromatic constituents of vanilla flavor (Remaud *et al.* 1997).

2.1.3.1. *p*-Hydroxybenzaldehyde (**2.7**)

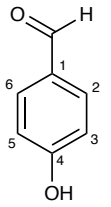

2.7

Compound **2.7** was isolated as a colorless oil. The ESI-MS, with a protonated molecular ion at m/z 123, and ^{13}C NMR data were consistent with the molecular formula $C_7H_6O_2$, corresponding to five degrees of unsaturation. The ^{1}H NMR spectrum exhibited two proton signals at δ_H 6,97 and 7.81 that indicated the presence of a *para*-substituted aromatic ring, and a singlet at δ_H 9.86 ppm that was consistent with the aldehyde group (Table 2.13).

The ^{13}C NMR and DEPT spectra exhibited five signals corresponding to two quaternary carbons, and three methines, one of them at δ_C 191.3 ppm corresponding to the carbonyl group.

Table 2.13 ^{1}H, ^{13}C and DEPT NMR data of *p*-hydroxybenzaldehyde (**2.7**), (300 MHz, $CDCl_3$; δ in ppm, *J* in Hz).

Position	^{1}H	^{13}C	DEPT
1	–	129.9	C
2	7.81 *m*	132.6 [a]	CH
3	6.97 *m*	116.1 [b]	CH
4	–	161.8	C
5	6.97 *m*	116.1 [b]	CH
6	7.81 *m*	132.6 [a]	CH
CHO	9.86 *s*	191.3	CH

[a, b] Overlapped signals

All mentioned spectroscopic data were in agreement with those reported in the literature for *p*-hydroxybenzaldehyde (Gui *et al.* 2015).

2.1.3.2. Vanillin (**2.8**)

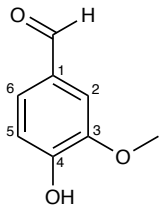

2.8

Compound **2.8** was isolated as white crystals of m.p. 81-82 ºC, with a very sweet and pleasant smell, and identified as vanillin on the basis of the comparison of its physical and spectroscopic data to those described on the literature (Kwon, Choi and Lee *et al.* 2001).

When comparing compound **2.8** with *p*-hydroxybenzaldehyde (**2.7**), it was clear that these compounds shared the same C6C1 phenolic structure. In fact, from the analysis of NMR spectra (Table 2.13 and Table 2.14), it was evident that the major differences between these two compounds were the presence of a methoxy group as a singlet at δ_H 3.97 ppm in the ^{1}H NMR spectrum and three signals for the aromatic protons at δ_H 7.04 ppm with an -*ortho* coupling (J = 8.5 Hz) and two overlapped signals at δ_H 7.43 ppm.

The ^{13}C NMR and DEPT spectra exhibited eight signals corresponding to three quaternary carbons, four methines, one of them at δ_C 191.1 ppm corresponding to the carbonyl group, and the carbon ressonance of the methoxy group at δ_C 56.3 ppm.

Table 2.14 ^{1}H, ^{13}C and DEPT NMR data of vanillin (**2.8**), (300 MHz, $CDCl_3$; δ in ppm, J in Hz).

Position	^{1}H	^{13}C	DEPT
1	–	129.9	C
2	7.43 *m* [a]	114.5	CH
3	–	151.8	C
4	–	147.2	C
5	7.04 *d* (8.5)	108.8	CH
6	7.43 *m* [a]	127.7	CH
CHO	9.83 *s*	191.1	CH
CH_3O	3.97 *s*	56.3	CH_3

[a] Overlapped signals

Comparison of the physical and spectroscopic data with those described in the literature for vanillin confirmed the identity of compound **2.8** (Kwon, Choi and Lee *et al.* 2001).

2.1.4. Lactones

2.1.4.1. S-(+)-Pantolactone (**2.9**)

Compound **2.9**, isolated from fraction E6 of the EtOAc extract, was obtained as one single crystal with m.p. 81-82 ºC and $[\alpha]_{\mathbf{D}}^{\mathbf{25}}$ + 28.5º.

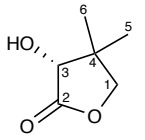

2.9

The ESI-MS with a protonated molecular ion at m/z 130 and the ^{13}C NMR data were consistent with the molecular formula $C_6H_{10}O_3$. The two degrees of unsaturation are in agreement with the presence of a ring and a carbonyl group. The ^{1}H NMR spectrum exhibited five proton signals, namely two doublets at δ_H 3.94 and δ_H 4.02 (J = 8.9 Hz), corresponding to the methylene protons, two singlets at δ_H 1.07 and 1.23, assignable to the tertiary methyl groups, and a singlet at δ_H 4.13 of H-3 (Table 2.15).

The ^{13}C NMR and DEPT spectra evidenced six carbon resonances, two quaternary carbons at δ_C 41.0 and δ_C 177.9 ppm, this last one corresponding to a carboxylic ester group, one methylene at δ_C 76.6, one methine at δ_C 75.8 and two methyls at δ_C 1.07 and 1.23 ppm (Table 2.15).

Table 2.15 ^{1}H, ^{13}C, DEPT, COSY and HMBC NMR data of pantolactone (**2.9**), (300 MHz, $CDCl_3$; δ in ppm, J in Hz).

Position	^{1}H	^{13}C	DEPT	COSY	HMBC
1	4.03 *d* (8.9) 3.94 *br d* (8.9)	76.6	CH_2	–	H-5, 6
2	–	177.9	C	–	H-1
3	4.13 *br s*	75.8	CH	–	H-5, 6
4	–	41.0	C	–	–
5	1.23 *s*	23.0	CH_3	–	H-3, 6
6	1.07 *s*	18.9	CH_3	–	H-3, 5

The 2D NMR HMBC spectrum confirmed the structure of compound **2.9** as a lactone by the cross-peaks observed between C-1 and H-5 and H-6, C-2 with H-1, C-3 with H-5 and H-6, C-5 with H-3 and H-6 and C-6 with H-3 and H-5 (Scheme 2.5).

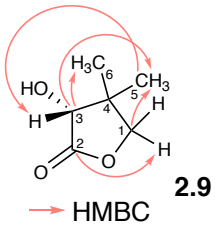

Scheme 2.5 Most relevant correlations observed in the HMBC spectrum of compound **2.9**.

Compound **2.9** was identified as S-(+)-pantolactone, also known as (S)-(+)-dihydro-3-hydroxy-4,4-dimethyl-2(3H)-furanone), on the basis of the comparison of its physical and spectroscopic data to those described on the literature (Upadhya, Gurunath and Sudalai 1999).

2.2. Antibacterial activity

The antibacterial activity of *G. hexamita* extracts/fractions, isolated compounds (**2.1**-**2.9**) and acyl derivatives (**2.10**-**2.13**) of lupeol (**2.1**) and betulin (**2.2**) was evaluated by determining their respective minimum inhibitory concentration (MIC), the lowest concentration of the sample that inhibits bacterial growth. MIC were determined by the microdilution method and the samples were assayed at a concentration range from 500-0.49 μg ml^{-1}.

For the evaluation of antibacterial activity, a selected panel of resistant and susceptible bacteria strains was used, which included Gram-positive bacteria, namely a sensitive strain of *Staphylococcus aureus* (MSSA, ATCC 6538) and resistant strains to reference antibiotics, specifically *Staphylococcus aureus* resistant to methicillin (MRSA, ATCC 43866) and a strain with intermediate sensitivity to vancomycin (VISA, CIP 106760). Also, within Gram-positive bacteria, two vancomycin-resistant *Enterococcus faecalis* strains (VRE) were tested (one wild type FFHB H164 and one ATCC 435628). Gram-negative bacterial strains (*Salmonella typhimurium*, ATCC 13311; *Pseudomonas aeruginosa*, ATCC 9027) were also included as representatives of Enterobactereaceae and non-Enterobactereaceae, respectively.

Combination assays were also performed to evaluate the type of interaction between the compounds isolated (**2.1**-**2.9**) and derivatives (**2.10**-**2.13**) with some reference antibiotics used in the treatment of *S. aureus* infections. It was intended to

determine the existence of synergistic effect between them and thus their ability to reverse bacterial resistance.

2.2.1. Preliminary screening of the antibacterial activity of the crude extracts

The evaluation of the antibacterial activity that accompanied the phytochemical study began with a preliminary screening of the various crude extracts of *G. hexamita* (*n*-hexane, DCM, EtOAc, MEOH and H_2O). The results are summarized in Table 2.16. As it can be observed, the methanol extract inhibited significantly the development of all *S. aureus* strains (MIC 8-62 $\mu g.mL^{-1}$), which are usually more resistant to conventional antibiotic therapy. Still against *S. aureus strains*, the ethyl acetate extract also presented a good inhibitory capacity with MIC values of 15-30 $\mu g.mL^{-1}$ and the *n*-hexane showed MIC values of 62 $\mu g.mL^{-1.}$

None of the extracts showed activity against the Gram-negative bacteria *E. faecalis*, *P. aeruginosa* and *S. typhimurium*.

2.2.2. Antibacterial activity of isolated compounds and derivatives

Considering the results of the preliminary screening, a bioassay-guided fractionation of the ethyl acetate and *n*-hexane soluble fractions of the methanol extract was performed. Regarding the evaluation of the antibacterial activity of the pure compounds, in addition to the mentioned Gram-positive and Gram-negative bacteria, *Escherichia coli* (ATCC 1228) was also tested. The results obtained are presented in Table 2.17.

As it can be observed, the best results were found for the pentacyclic triterpenes lupeol (**2.1**) and betulin (**2.2**), which showed MIC values of 30 and 15 $\mu g.mL^{-1}$, respectively, against both the sensitive and MRSA resistant strains and 62 $\mu g.mL^{-1}$ against resistant VISA strains. Betulinic aldehyde (**2.3**), with the same pentacyclic scaffold, showed a weaker bacterial growth inhibitory capacity with MIC values of 30 $\mu g.mL^{-1}$ against sensitive *S. aureus strain*, 62 $\mu g.mL^{-1}$ in resistant MRSA strain and no significant activity against VISA. When analyzing MIC values for the acyl derivatives (**2.10**-**2.13**)

of lupeol (**2.1**) and betulin (**2.2**), a decrease of the antibacterial activity was observed (Table 2.17).

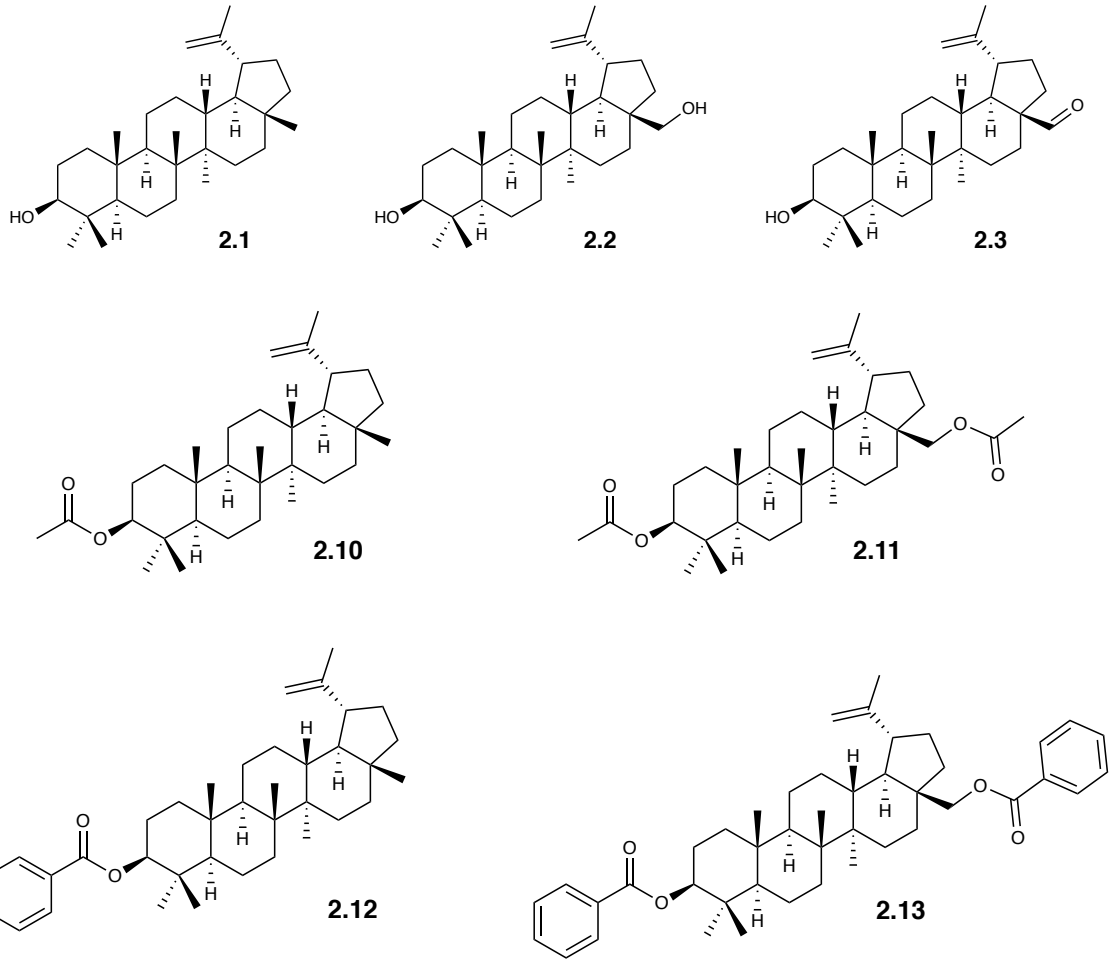

The only structural difference of compounds **2.1**, **2.2** and **2.3** is at C-28. Betulin (**2.2**), with a hydroxyl group at C-28, showed the highest activity. Thus, when analyzing the activity of the isolated and derivatized triterpenes it is hypothesized that the substituent at this position is directly linked to antibacterial activity of the molecule. The esterification of the hydroxyl group at C-3 in lupeol (**2.1**) derivatives (**2.10** and **2.12**) and the acylation at both positions, C-3 and C-28, in betulin (**2.2**) derivatives (**2.11** and **2.13**) did not have beneficial effects on their antibacterial activity.

The tetracyclic triterpene 3β-caffeoyl-cycloartane (**2.4**) exhibited a MIC value of 30 $\mu g.mL^{-1}$ against both sensitive and resistant MRSA strains and was inactive against the remaining strains.

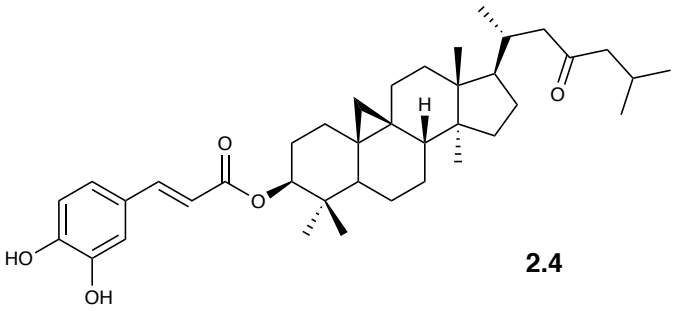

2.4

A good/moderate activity (MIC = 30/62 μg.mL^{-1}) was also found for β-sitosterol (**2.5**), 7-oxo-β-sitosterol (**2.6**), *p*-hydroxybenzaldehyde (**2.7**), vanillin (**2.8**) and pantolactone (**2.9**) against sensitive and sensitive *S. aureus* and MRSA strains.

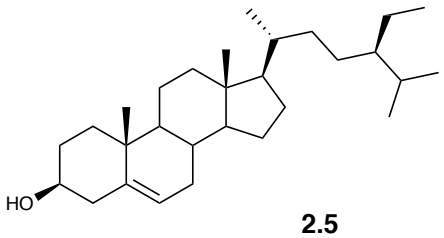

2.5

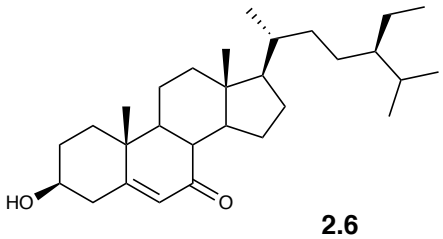

2.6

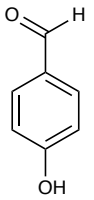

2.7

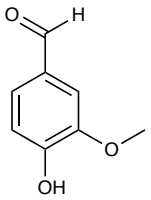

2.8

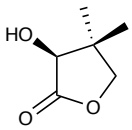

2.9

No inhibitory activities of bacterial growth were observed in Gram-positive *E. faecalis* VRE FFHB 164 nor in Gram-negative *P. aeruginosa* ATCC 9027, *S. typhymurium* ATCC 1311 and *E. coli* ATCC 8739 strains. The results in Gram-negative bacteria might be due to the presence of the outer membrane, which is an efficient barrier for compound entry, whereas Gram-positive bacteria lack the outer membrane structure.

Table 2.16 Preliminary screening of the antibacterial activity of *Grewia hexamita* crude fractions.

Bacterial strain		**MIC (µg.mL^{-1})**							
		Extract					**Antibiotic**		
		n-hexane	Dichloromethane	Ethyl acetate	Methanol	Water	Amoxicillin	Oxacillin	Vancomycin
S.aureus	MSSA ATCC 6538	62	62	15	8	30	0.2	0.2	0.2
	MRSA ATCC 43866	62	125	30	62	30	62	125	0.4
	VISA CIP 106760	62	250	15	8	30	250	250	4
E. faecalis	VRE FFHB H164	125	> 250	> 250	125	> 250	–	–	32
P. aeruginosa	ATCC 9027	> 250	> 250	> 250	> 250	> 250	> 250	> 250	> 250
S. typhimurium	ATCC 13311	> 250	> 250	> 250	> 250	> 250	> 250	> 250	> 250

All assays were performed in triplicate. No antibacterial activity (MIC > 250 mg/mL) was detected against Gram-negative strains (*P. aeruginosa* ATCC 9027 and *S. typhymurium* ATCC 13311) at the concentration tested.

Table 2.17 Antibacterial activity (MIC μg.mL^{-1}) of the MeOH extract and the *n*-hexane and EtOAc soluble fractions, compounds (**2.1**-**2.13**) and antibiotics.

	MIC (μg.mL^{-1})			
Bacteria	*S. aureus*			*E. faecalis*
	MSSA ATCC 6535	MRSA ATCC 43866	VISA CIP 106760	VRE FFHB H164
Sample				
MeOH	15	15	15	125
Ø Hex	62	62	62	125
Ø EtOAc	15	30	15	> 250
Natural				
2.1	30	30	62	> 250
2.2	15	15	62	> 250
2.3	30	62	250	> 250
2.4	30	30	125	> 250
2.5	30	62	125	> 250
2.6	30	62	250	> 250
2.7	62	62	125	> 250
2.8	30	62	250	> 250
2.9	30	30	250	> 250
Derivatives				
2.10	30	62	250	> 250
2.11	62	62	250	> 250
2.12	62	62	250	> 250
2.13	30	30	125	250
Antibiotics				
Amoxicillin	0.2	62	250	–
Oxacillin	0.2	125	250	–
Vancomycine	0.2	0.4	4	32

All assays were performed in triplicate. No antibacterial activity (MIC > 250 mg/mL) was detected against Gram-negative strains (*P. aeruginosa* ATCC 9027, *S. typhymurium* ATCC 13311 and *E. coli* ATCC 1228) at the concentration tested.

2.2.3. Combination between the compounds and antibiotics

In order to evaluate the effect between the compounds isolated from *G. hexamita* (**2.1**-**2.9**), as well as the prepared derivatives (**2.10**-**2.13**), amoxicillin and oxacillin, two reference antibiotics used to treat *Staphylococcus aureus* infections, a chemosensitization assay, using the checkerboard method, was performed in *S. aureus* strains (resistant MRSA ATCC 43866 and VISA CIP 106414). Vancomycin, a second line antibiotic used for the treatment of MRSA strains for which some strains began to show resistance (VISA), was also included. The objective was to determine if the compounds were able to modulate the activity of the antibiotic, and what type of interaction between them (synergism, antagonism or indifference), when tested against MRSA and VISA strains. The effects of combination, displayed in Table 2.18 for isolated compounds and Table 2.19 for the derivatives, were determined based on fractional inhibitory index (FICI) values. Thus, when the FICI values are equal to or less than 0.5, there is a synergistic interaction, whereas FICI values between 0.5 and 4.0 indicate that there is no interaction between the compound and the antibiotic. In turn, when FICI values are greater than 4 an antagonistic effect occurs (Al-Ani *et al.* 2015).

For the MRSA strain, the compounds that stood out were betulinic aldehyde (**2.3**) and 7-oxo-β-sitosterol (**2.6**) (Table 2.18). Betulinic aldehyde (**2.3**), which displayed a weak bacterial growth inhibitory capacity in resistant MRSA ATCC 43866 strain (MIC = 62 $\mu g.mL^{-1}$), restored synergistically the antibacterial activity of the two β-lactam antibiotics tested, amoxacillin from 62 to 3.8 $\mu g.mL^{-1}$, corresponding to a 16-fold reduction (FICI = 0.31) and oxacillin from 62 to 7.5 $\mu g.mL^{-1}$ (FICI = 0.37), corresponding to a 8-fold reduction. 7-oxo-β-Sitosterol (**2.6**) was also able to interact synergistically with amoxicillin against MRSA strain, lowering the antibiotic MIC from 250 $\mu g.mL^{-1}$ to 30 $\mu g.mL^{-1}$ (FICI = 0.48), corresponding to a 8-fold reduction. Compounds, **2.1**, **2.2**, **2.3**-**2.5** and **2.7**-**2.9** presented no interaction ($0.5 < FICI \leq 4$) with amoxicillin and oxacillin against MRSA strains.

For the VISA CIP 106760 strain, the compounds that stood out were β-sitosterol (**2.5**), vanillin (**2.8**) and pantolactone (**2.9**) (Table 2.18). The three compounds displayed no significant antibacterial activity alone but were able to restore synergistically the antibacterial activity of amoxacillin, from 250 $\mu g.mL^{-1}$ to 7.5 $\mu g.mL^{-1}$ (FICI = 0.18), 3.8 $\mu g.mL^{-1}$ (FICI = 0.05) and 1 $\mu g.mL^{-1}$ (FICI = 0.01), respectively, which represented a major decrease in their MIC values. For oxacillin, pantolactone (**2.9**) also decreased the

MIC values, from 250 to 30 μg.mL^{-1} (FICI = 0.37), reducing its MIC value eight times. Conversely, compounds, **2.1**-**2.4**, **2.6** and **2.7**, presented no interaction (0.5 < FICI ≤ 4) or antagonism (FICI > 4) with amoxicillin, oxacillin and vancomycin against VISA strains (Table 2.18).

Similarly, none of the prepared derivatives (**2.10**-**2.13**) of lupeol (**2.1**) and betulin (**2.2**) showed synergistic interactions against the resistant strains *S. aureus* ATCC 43866 and CIP 106760 when combined with the antibiotics (Table 2.19).

Table 2.18 Minimum inhibitory concentration (MIC) of antibiotics alone and combined with isolated compounds. Fractional inhibitory concentration index (FICI) values in the resistant *S. aureus* strains MRSA ATCC 43866 and VISA CIP 106760.

Strain *S. aureus*	**Compound**	**MIC** (μg.mL^{-1})		**FIC**	**FICI**	**Output**
		Alone	**Combined**			
MRSA ATCC 43866	**2.1**	30	7.5	0.25	0.75	Indifferent
	Amoxicillin	62	30	0.5		
	2.1	30	7.5	0.25	0.75	Indifferent
	Oxacillin	125	62	0.5		
	2.2	15	3.8	0.25	0.75	Indifferent
	Amoxicillin	62	30	0.5		
	2.2	15	3.8	0.25	0.75	Indifferent
	Oxacillin	125	62	0.5		
	2.3	62	3.8	0.06	0.31	**Synergism**
	Amoxicillin	62	15.5	0.25		
	2.3	62	7.5	0.12	0.37	**Synergism**
	Oxacillin	125	30	0.25		
	2.4	30	7.5	0.25	0.75	Indifferent
	Amoxicillin	62	30	0.5		
	2.4	30	7.5	0.25	0.75	Indifferent
	Oxacillin	125	62	0.5		
	2.5	62	15	0.25	0.75	Indifferent
	Amoxicillin	62	30	0.5		
	2.5	62	15	0.5	1	Indifferent
	Oxacillin	125	62	0.5		
	2.6	62	7.5	0.13	0.48	**Synergism**
	Amoxicillin	62	20.7	0.35		
	2.6	62	30	0.5	1.5	Indifferent
	Oxacillin	125	125	1		
	2.8	62	15	0.25	0.75	Indifferent
	Amoxicillin	62	30	0.5		
	2.8	62	7.5	0.13	0.63	Indifferent
	Oxacillin	125	30	0.5		
	2.9	30	7.5	0.25	0.75	Indifferent
	Amoxicillin	62	30	0.5		
	2.9	30	7.5	0.25	0.75	Indifferent
	Oxacillin	125	62	0.5		
	2.1	62	30	0.5	1.5	Indifferent
	Amoxicillin	250	250	1		

Continuation Table 2.18

	2.1	62	30	0.5	1.5	Indifferent
	Oxacillin	250	250	1		
	2.1	62	15	0.3	15.9	Antagonism
	Vancomycin	4	62	15.6		
	2.2	62	30	0.5	1.5	Indifferent
	Amoxicillin	250	250	1		
	2.2	62	30	0.5	1.5	Indifferent
	Oxacillin	250	250	1		
	2.2	62	15	0.3	15.9	Antagonism
	Vancomycin	4	62	15.6		
	2.3	250	125	0.5	1.5	Indifferent
	Amoxicillin	250	250	1		
	2.3	250	125	0.5	1.5	Indifferent
	Oxacillin	250	250	1		
	2.3	250	62	0.25	31.5	Antagonism
	Vancomycin	4	125	31.25		
	2.4	125	62	0.5	1.5	Indifferent
VISA	Amoxicillin	250	250	1		
	2.4	125	62	0.5	1.5	Indifferent
CIP	Oxacillin	250	250	1		
106760	**2.4**	125	62	0.5	8	Antagonism
	Vancomycin	4	30	7.5		
	2.5	125	7.5	0.06	0.18	**Synergism**
	Amoxicillin	250	30	0.12		
	2.5	125	62	0.5	1.5	Indifferent
	Oxacillin	250	250	1		
	2.5	125	30	0.25	31.5	Antagonism
	Vancomycin	4	125	31.25		
	2.6	250	125	0.5	1.5	Indifferent
	Amoxicillin	250	250	1		
	2.6	250	125	0.5	1.5	Indifferent
	Oxacillin	250	250	1		
	2.6	250	125	0.5	8	Antagonism
	Vancomycin	4	30	7.5		
	2.8	250	3.8	0.02	0.05	**Synergism**
	Amoxicillin	250	7.5	0.03		
	2.8	250	15	0.06	0.18	Indifferent
	Oxacillin	250	30	0.12		
	2.8	250	30	0.12	62.6	Antagonism
	Vancomycin	4	250	62.5		
	2.9	250	1	$4x10^{-3}$	0.01	**Synergism**
	Amoxicillin	250	2	$8x10^{-3}$		
	2.9	250	30	0.12	0.37	**Synergism**
	Oxacillin	250	62	0.25		
	2.9	250	62	0.25	31.5	Antagonism
	Vancomycin	4	125	31.25		

FICI = FIC(A) + FIC(B); FIC(A) = MIC (A in the presence of B)/MIC(A alone); FIC(B) = MIC(B in the presence of A)/MIC(B alone). Antagonism FICI > 4; Indifference 0.5 < FICI ≤ 4; Synergism FICI ≤ 0.5

Table 2.19 Minimum inhibitory concentration (MIC) of antibiotics alone and combined with lupeol (**2.1**) and betulin (**2.2**) acyl derivatives (**2.10**-**2.13**). Fractional inhibitory concentration index (FICI) values in the resistant strains *S. aureus* ATCC 43866 and CIP 1067

Strain *S. aureus*	**Extract/Compound**	**MIC** ($\mu g.mL^{-1}$)		**FIC**	**FICI**	**Interpretation**
		Alone	**Combined**			
MRSA ATCC 43866	**2.10**	62	15	0.25	0.75	Indifferent
	Amoxicillin	62	31	0.5		
	2.10	62	15	0.25	0.75	Indifferent
	Oxacillin	125	62	0.5		
	2.11	62	15	0.25	0.75	Indifferent
	Amoxicillin	62	30	0.5		
	2.11	62	30	0.5	1.5	Indifferent
	Oxacillin	125	125	1		
	2.12	62	30	0.5	1.5	Indifferent
	Amoxicillin	62	62	1		
	2.12	62	15	0.25	0.75	Indifferent
	Oxacillin	125	62	0.5		
	2.13	30	7.5	0.25	0.75	Indifferent
	Amoxicillin	62	30	0.5		
	2.13	30	15	0.5	1.5	Indifferent
	Oxacillin	125	125	1		
VISA CIP 106760	**2.10**	250	125	0.5	1.5	Indifferent
	Amoxicillin	250	250	1		
	2.10	250	125	0.5	1.5	Indifferent
	Oxacillin	250	250	1		
	2.10	250	125	0.5	8	Antagonism
	Vancomycin	4	30	7.5		
	2.11	250	62	0.25	0.75	Indifferent
	Amoxicillin	250	125	0.5		
	2.11	250	125	0.5	1.5	Indifferent
	Oxacillin	250	250	1		
	2.11	250	62	0.25	31.6	Antagonism
	Vancomycin	4	125	31.3		
	2.12	250	125	0.5	1.5	Indifferent
	Amoxicillin	250	250	1		
	2.12	250	125	0.5	1.5	Indifferent
	Oxacillin	250	250	1		
	2.12	250	125	0.5	8	Antagonism
	Vancomycin	4	30	7.5		
	2.13	125	62	0.5	1.5	Indifferent
	Amoxicillin	250	250	1		
	2.13	125	62	0.5	1.5	Indifferent
	Oxacillin	250	250	1		
	2.13	125	30	0.25	31.5	Antagonism
	Vancomycin	4	125	31.3		

FICI = FIC(A) + FIC(B); FIC(A) = MIC (A in the presence of B)/MIC(A alone); FIC(B) = MIC(B in the presence of A)/MIC(B alone). Antagonism FICI > 4; Indifference 0.5 < FICI ≤ 4; Synergism FICI ≤ 0.5

CHAPTER 3

Conclusions

3. Conclusions

The medicinal plant *Grewia hexamita* is used in traditional Mozambican medicine to treat infectious diseases. This dissertation had as main objective the isolation and characterization of the chemical constituents associated with the antibacterial activity attributed to this species. Thus, the bioassay-guided phytochemical study of the methanol extract of the roots of the plant was carried out. This study involved the evaluation of antibacterial activity against a selected panel of Gram-positive and Gram-negative bacteria.

Bioassay-guided fractionation of the methanol extract of the roots of *Grewia Hexamita* led to the isolation of four triterpenes, three pentacyclic, namely lupeol (**2.1**), betulin (**2.2**) and betulinic aldehyde (**2.3**) and a new tetracyclic triterpene named 3β-caffeoyl-cycloartane (**2.4**). Two steroids, β-sitosterol (**2.5**) and 7-oxo-β-sitosterol (**2.6**), two phenolic compounds, *p*-hydroxybenzaldehyde (**2.7**) and vanillin (**2.8**), as well as *S*-(+)-pantolactone (**2.9**), a γ-butyrolactone, were also isolated. Acylation of lupeol (**2.1**) and betulin (**2.2**), isolated in large amount, using acetic anhydride and benzoyl chloride, gave rise to four derivatives (**2.10**-**2.13**). The structures of the compounds were characterized by their spectroscopic data (IR, MS and one- and two-dimensional NMR).

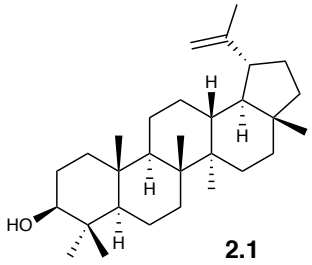

2.1

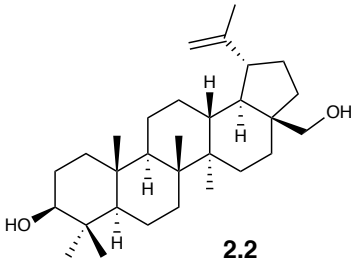

2.2

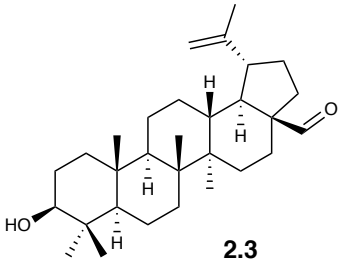

2.3

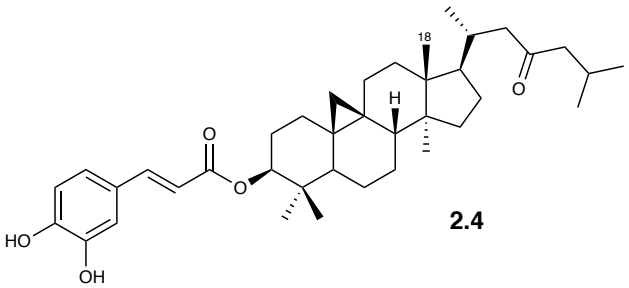

2.4

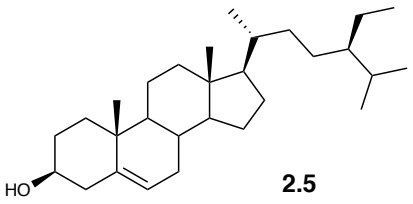

2.5

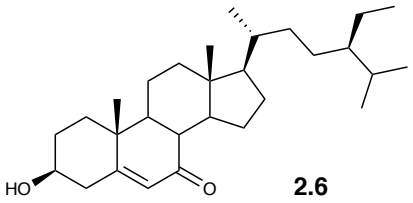

2.6

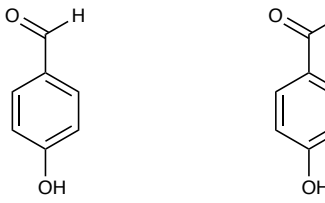

2.7

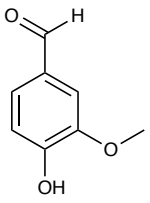

2.8

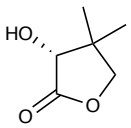

2.9

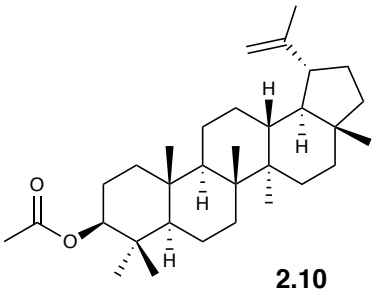

2.10

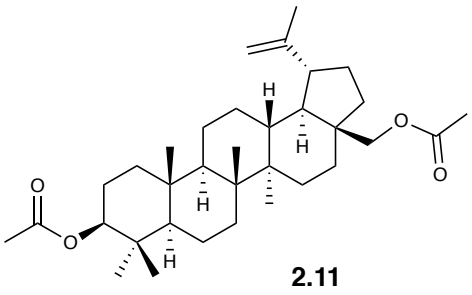

2.11

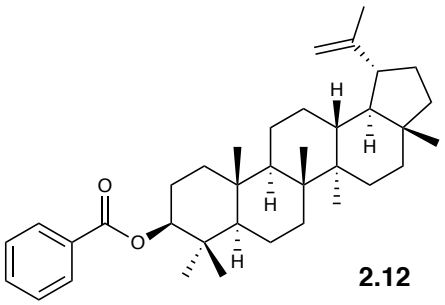

2.12

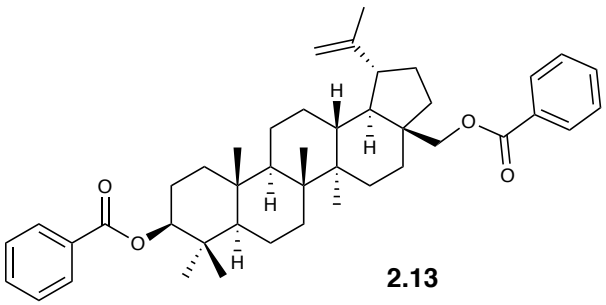

2.13

The evaluation of the antibacterial activity was performed by the microdilution method in sensitive *Staphylococcus aureus* (ATCC 6538) and resistant strains (MRSA ATCC 43866 and VISA CIP 106760) and in a vancomycin-resistant *Enterococcus faecalis* strain (VRE FFHB H164). Gram-negative strains, namely *Salmonella typhymurium* (ATCC 13311), *Pseudomonas aeruginosa* (ATCC 9027) and *Escherichia coli* were also used.

The best results were found for the pentacyclic triterpenes lupeol (**2.1**) and betulin (**2.2**), which showed significant antibacterial activity against both sensitive *S. aureus* and MRSA strains (MIC = 30 and 15 $\mu g.mL^{-1}$, respectively) and against resistant VISA strains (MIC 62 $\mu g.mL^{-1}$). In turn, betulinic aldehyde (**2.3**) exhibited MIC = 30 $\mu g.mL^{-1}$ and 62 $\mu g.mL^{-1}$, against sensitive and MRSA strains, respectively, and no significant activity against VISA. No inhibitory activities of bacterial growth were observed in Gram-positive *E. faecalis* VRE FFHB H164 nor in Gram-negative bacteria.

Combination assays, by the checkerboard method, were also performed to evaluate the type of interaction between the compounds and reference antibiotics. It was intended to determine the existence of synergistic effect between them and thus their

ability to reverse bacterial resistance. Betulinic aldehyde (**2.3**) restored synergistically the antibacterial activity of the two β-lactam antibiotics tested, amoxacillin from 62 to 3.8 $\mu g.mL^{-1}$, corresponding to a 16-fold reduction (FICI = 0.31) and oxacillin from 62 to 7.5 $\mu g.mL^{-1}$ (FICI = 0.37), corresponding to a 8-fold reduction. 7-oxo-β-Sitosterol (**2.6**) was also able to interact synergistically with amoxicillin, lowering the antibiotic MIC from 250 $\mu g.mL^{-1}$ to 30 $\mu g.mL^{-1}$ (FICI = 0.48), corresponding to a 8-fold reduction. Synergistic effects were also obtained against the VISA CIP 106760 strain, with β-sitosterol (**2.5**), vanillin (**2.8**) and pantolactone (**2.9**).

In summary, the data presented in this dissertation not only contribute to the phytochemical characterization of the species *Grewia hexamita*, but also represent an important validation of its use in traditional African medicine in the treatment of infectious diseases. According to the results obtained, the most active compounds may be promising prototypes for the development of new antibiotics against resistant strains.

CHAPTER 4

Experimental procedure

4. Experimental procedure

4.1. General instrumentations and techniques

Melting points were determined on a Köpffler apparatus and are uncorrected. Infrared IR spectra were plotted on Shimadzu IRAffinity-1 spectrophotometer. Nuclear magnetic resonance (NMR) spectra were recorded on a Brucker ARX-300 spectrometer (^{1}H 300 MHz; ^{13}C 75 MHz) using as solvent $CDCl_3$. The chemical shifts of ^{1}H and ^{13}C spectra are expressed as δ (ppm) and the coupling constants (*J*) in Hertz (Hz). Specific optical rotations were measured using a Jasco P-2000 polarimeter with a 1 dm long quartz cell and the samples were prepared in $CHCl_3$. ESI-MS analyzes were performed on a triple quadrupole (QT) electrospray ionization (ESI) mass spectrometer (Micromass Quattro Micro API), running in positive mode (Waters, Milford, USA). For column chromatography (CC) and Combiflash automatic system silica gel (Merck, ref. 9385) was used as adsorbent. Reverse phase chromatography was performed in Combiflash using as absorbent RP18 silica gel. The eluates were monitored by thin layer chromatography (TLC) using 0.2 mm thick silica plates (Merck, ref. 1.05554), with different eluents, depending on the characteristics of the samples applied. After its development, the plates were sprayed with a mixture of H_2SO_4/MeOH (1:1) and revealed by heat, having been visualized under UV light (λ 254 and λ 366 nm) before and after the action of the developing reagents. Silica plates 20 x 20 cm, 0.5 mm thick (Merck, ref. 1.05774) were used in preparative TLC, with different eluents, depending on the characteristics of the sample applied.

In the antibacterial assays, measurement of the optical density of the microtiter plates was performed on a Biotek ELX 808 microplate reader having recorded its absorbance at λ 630 nm.

4.2. Phytochemical study of *Grewia hexamita*

Grewia hexamita roots were collected in the Maputo region, Mozambique, in 2015. Its identification was carried out by Dr. Silva Mulhovo of Centro de Estudos Moçambicanos e de Etnociências (CEMEC), Faculty of Natural Sciences and Mathematics, Pedagogical University, Maputo, Mozambique.

4.3. Bioassay-guided fractionation: preliminary screening

Five crude plant extracts were prepared by submitting 100 g of air-dried powdered plant material to a sequential extraction procedure with 500 mL of *n*-hexane, dichloromethane (DCM), ethyl acetate (EtOAc), and methanol (MeOH) for 48 h, at room temperature. Then the extracts were filtrated through Whatman filter paper. After filtration, the extracts were fully dried, under reduced pressure at 40 ºC, by using a *Büchi* rotatory evaporator, and then stored at -22 ºC until their use in antibacterial assays. The last crude plant extract was prepared boiling 5 g of dried plant material in 150 mL of distilled water for 20 minutes, and then cooled down for 2 h at room temperature. The extract was filtrated, dried and stored as described above.

4.4. Extraction and Isolation

Grewia hexamita roots (4.1 kg) were dried, ground and exhaustively extracted with methanol, for three weeks with stirring and at room temperature. The extracts were decanted, filtered and combined and evaporated under *vacuum* to give a residue of 359.5 g. These crude extract was suspended in a mixture of MeOH/H_2O (1:1) and submitted to a sequentially liquid-liquid fractionation with *n*-hexane and ethyl acetate. The organic phases were combined, dried with anhydrous sodium sulfate, and evaporated, yielding 22.6 g of *n*-hexane and 45.6 g of ethyl acetate soluble fractions as shown in Scheme 3.1. Both fractions were chromatographed on a silica gel column (22.6 kg and 1.3 kg, respectively) where *n*-hexane/EtOAc and EtOAc/MeOH mixtures of increasing polarity were used as eluents.

In this work, *n*-hexane fractions C, D, G and HIJ were selected for phytochemical study, as well as ethyl acetate fractions B, D and E (Scheme 4.1).

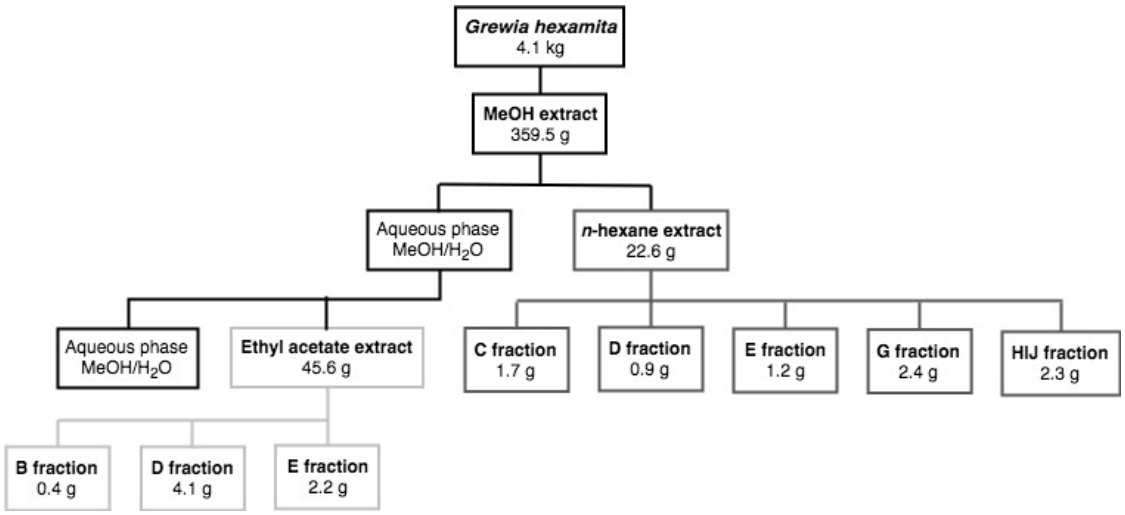

Scheme 4.1 Study of *Grewia hexamita*: extraction and fractionation procedures.

4.5. Bioassay-guided fractionation of the methanol extract: ethyl acetate soluble fraction

The ethyl acetate fraction (45.6 g) was chromatographed over silica (1.5 kg silica gel), using *n*-hexane/EtOAc and EtOAc/MeOH mixtures as eluents in a gradient of increasing polarity (*n*-hexane/EtOAc 1:0, 4L; 19:1, 2L; 9:1, 2L; 17:3, 2L; 4:1, 2L; 3:1, 2L; 7:3, 3L; 13:7, 2L; 3:2, 3L; 11:9, 3L; 5:5, 3L; 9:11, 3L; 2:3, 3L; 7:13, 3L; 3:7, 3L; 1:3, 3L; 1:4, 2L; 3:17, 1L; 1:9, 1L; 1:19, 1L; 0:1 1L; and EtOAc/MeOH 19:1, 1L; 9:1, 6L; 7:1, 1L; 17:3, 1L; 4:1, 1L; 7:3, 1L; 13:7, 1L; 3:2, 1L; 5:5, 2L; 1:3, 1L; 0:1, 1L), obtaining thirteen fractions, after association according to their chromatographic profile (Table 4.1).

According to the preliminary screening and their TLC profile several fractions were selected for study (B, D and E fractions, Fig. 4.1C).

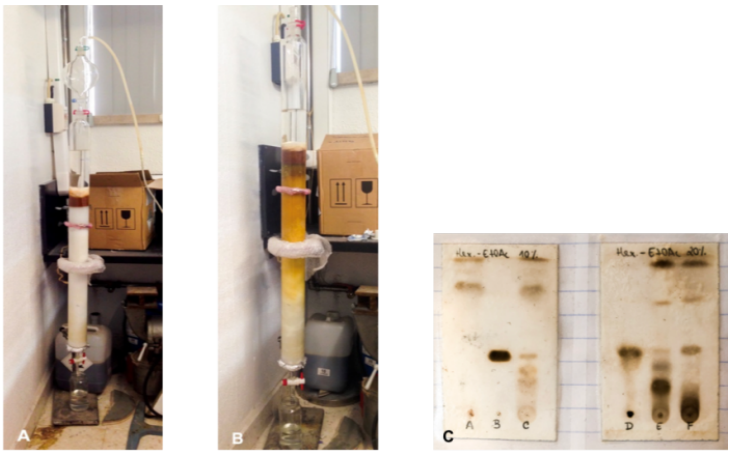

Figure 4.1 Phytochemical study of *G. hexamita*. A and B – fractionation of the EtOAc soluble fraction, C – TLC including the B, D and E fractions.

Table 4.1 Column chromatography of ethyl acetate soluble fraction.

Fraction	Mass (g)	Eluent (v/v)
A	0.43	*n*-hex/EtOAc (1:0 to 4:1)
B	0.44	*n*-hexane/EtOAc (4:1)
C	0.34	*n*-hexane/EtOAc (3:1 to 7:3)
D	4.10	*n*-hexane/EtOAc (7:3 to 13:7)
E	2.21	*n*-hexane/EtOAc (13:7 to 11:9)
F	0.80	*n*-hexane/EtOAc (5:5 to 9:11)
G	0.51	*n*-hexane/EtOAc (2:3 to 7:13)
H	0.77	*n*-hexane/EtOAc (7:13 to 1:3)
I	9.01	*n*-hexane/EtOAc (1:4 to EtOAc/MeOH 19:1)
J	9.71	EtOAc/MeOH (19:1 to 9:1)
L	9.75	EtOAc/MeOH (9:1 to 5:5)
M	0.47	EtOAc/MeOH (7:13)
N	0.75	MeOH (1:0)

Scheme 4.2 Fractionation of the EtOAc soluble fraction and isolated compounds.

4.5.1. Study of fractions B and D

Fractions B (443.3 mg) and D (4.104 g, *cf.* Table 4.1) were recrystallized with EtOAc/n-hexane to give 420 mg of lupeol (**2.1**) and 4.0 g of betulin (**2.2**), respectively.

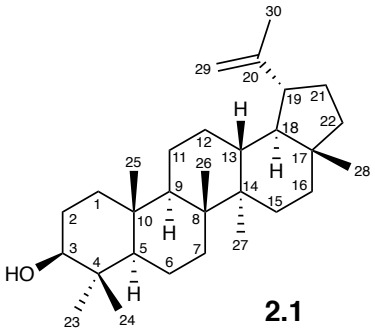

2.1

Lupeol (**2.1**)

White crystals

m.p. 205-207 ºC (EtOAc/*n*-hexane); Lit. 210 ºC (EtOAc/*n*-hexane), (Baek *et al.* 2010)

ESI-MS, *m/z*: 427 $[M+H]^+$, 409 $[M-H_2O+H]^+$

^{1}H NMR (300 MHz, $CDCl_3$): δ 0.76 (3 H, *s*, CH_3-24), 0.79 (3 H, *s*, CH_3-28), 0.83 (3 H, *s*, CH_3-25), 0.95 (3 H, *s*, CH_3-23), 0.97 (3 H, *s*, CH_3-27), 1.03 (3 H, *s*, CH_3-26), 1.68 (3 H, *s*, H-30), 2.38 (1 H, *td*, *J* = 11.0 and 5.6 Hz, H-19), 3.19 (1 H, *dd*, *J* = 11.0 and 5.3 Hz, H-3α), 4.57 (1 H, *dd*, *J* = 2.4 and 1.3 Hz, H-29'), 4.69 (1 H, *d*, *J* = 2.4 Hz, H-29).

^{13}C NMR (75 MHz, $CDCl_3$): δ 38.9 (C-1), 27.6 (C-2), 79.2 (C-3), 39.0 (C-4), 55.5 (C-5), 18.5 (C-6), 34.5 (C-7), 41.0 (C-8), 50.6 (C-9), 37.3 (C-10), 21.1 (C-11), 25.3 (C-12), 38.2 (C-13), 43.1 (C-14), 27.6 (C-15), 35.6 (C-16), 43.2 (C-17), 48.5 (C-18), 48.1 (C-19), 151.1 (C-20), 30.0 (C-21), 40.2 (C-22), 28.2 (C-23), 15.5 (C-24), 16.3 (C-25), 16.1 (C-26), 14.7 (C-27), 18.2 (C-28), 109.5 (C-29), 19.5 (C-30).

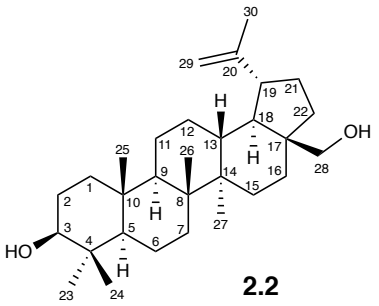

2.2

Betulin (**2.2**)

White crystals

m.p. 256-257 ºC (EtOAc/*n*-hexane); Lit. 256-257 ºC (EtOAc/*n*-hexane), (Tijjani, Ndukwe and Ayo 2012)

ESI-MS, *m/z*: 443 $[M+H]^+$, 425 $[M-H_2O+H]^+$, 407 $[M-2H_2O+H]^+$

^{1}H NMR (300 MHz, $CDCl_3$): δ 0.76 (3 H, *s*, CH_3-24), 0.83 (3 H, *s*, CH_3-25), 0.97 (3 H, *s*, CH_3-23), 0.98 (3 H, *s*, CH_3-27), 1.02 (3 H, *s*, CH_3-26), 1.68 (3 H, *s*, H-30), 2.38 (1 H, *td*, *J* = 11.0 and 5.6 Hz, H-19), 3.19 (1 H, *dd*, *J* = 10.8 and 5.3 Hz, H-3α), 3.33 (1 H, *d*, *J* = 10.8 Hz, H-28'), 3.80 (1 H, *dd*, *J* = 10.8 and 1.5 Hz, H-28), 4.58 (1 H, *dd*, *J* = 2.3 and 1.4 Hz, H-29'), 4.68 (1 H, *d*, *J* = 2.3, H-29).

^{13}C NMR (75 MHz, $CDCl_3$): δ 39.0 (C-1), 27.6 (C-2), 79.1 (C-3), 38.9 (C-4), 55.5 (C-5), 18.5 (C-6), 34.4 (C-7), 41.1 (C-8), 50.6 (C-9), 37.5 (C-10), 21.0 (C-11), 25.4 (C-12), 37.3 (C-13), 42.9 (C-14), 27.2 (C-15), 29.3 (C-16), 47.9 (C-17), 47.9 (C-18), 48.9 (C-19), 150.6 (C-20), 29.9 (C-21), 34.1 (C-22), 28.1 (C-23), 15.5 (C-24), 16.3 (C-25), 16.1 (C-26), 14.9 (C-27), 60.7 (C-28), 109.8 (C-29), 19.2 (C-30).

4.5.2. Study of fraction E

Fraction E (2.21 g) was chromatographed through a column with 192 g of silica gel, using *n*-hexane/EtOAc of increasing polarity (1:0, 375 mL; 19:1, 300 mL; 9:1, 300 mL; 17:3, 300 mL; 3:1, 300 mL; 7:3, 600 mL; 13:7, 600 mL; 3:2, 600 mL; 11:9, 300 mL; 5:5, 300 mL; 9:11, 300 mL; 2:3, 300 mL; 3:7, 300 mL; 1:4, 300 mL; 1:9, 300 mL; 0:1, 225 mL). After TLC monitoring, the eluates obtained were associated in several fractions, as indicated in Table 4.2 and Scheme 4.2.

Table 4.2 Column chromatography of fraction E1

Fraction	Mass (g)	Eluent (v/v)
E1.1	0.06	*n*-hexane/EtOAc (19:1 to 9:1)
E1.2	0.54	*n*-hexane/EtOAc (9:1 to 17:3)
E1.3	0.03	*n*-hexane/EtOAc (17:3)
E1.4	0.05	*n*-hexane/EtOAc (4:1 to 3:1)
E1.5	0.05	*n*-hexane/EtOAc (7:3)
E1.6	0.14	*n*-hexane/EtOAc (7:3 to 13:7)
E1.7	0.85	*n*-hexane/EtOAc (13:7 to 3:2)
E1.8	0.11	*n*-hexane/EtOAc (11:9 to 0:1)

Fraction E1.5 was a pure compound identified as betulin (**2.2**, 48.9 mg).

4.5.2.1. Study of fraction E1.6

The fraction E1.6 (0.14 g) was chromatographed through a column with 14 g of silica gel. The column was eluted using a *n*-hexane/EtOAc gradient (1:0, 40 mL; 19:1, 30 mL; 9:1, 30 mL; 17:3, 30 mL; 4:1, 30 mL; 3:1, 30 mL; 7:3, 90 mL; 13:7, 30 mL; 3:2, 30 mL; 11:9, 30 mL; 5:5, 30 mL; 2:3, 30 mL; 3:7, 30 mL; 1:4, 30 mL; 1:9, 30 mL; 0:1, 30 mL). After TLC analysis, similar chromatographic fractions were pooled, as indicated in Table 4.3.

Table 4.3 Column chromatography of fraction E1.6

Fraction	Mass (g)	Eluent (v/v)
E2.1	0.01	*n*-hexane/EtOAc (1:0 to 3:1)
E2.2	0.09	*n*-hexane/EtOAc (7:3)
E2.3	0.01	*n*-hexane/EtOAc (13:7 to 0:1)

4.5.2.2. Study of fraction E1.7

Fraction E1.7 (0.85 g) was chromatographed, using the Combiflash system equipped with a silica gel column (12g). The sample was eluted with *n*-hexane/EtOAc mixtures of increasing polarity at a flow rate of 17 mL/min and monitoring at 254 nm and

360 nm. After TLC analysis, the collected fractions were associated as described in Table 4.4.

Table 4.4 Column chromatography of fraction E1.7

Fraction	Mass (g)	Eluent (v/v)
E3.1	–	*n*-hexane/EtOAc (1:0 to 4:1)
E3.2	0.02	*n*-hexane/EtOAc (3:1 to 7:3)
E3.3	0.02	*n*-hexane/EtOAc (7:3)
E3.4	0.22	*n*-hexane/EtOAc (7:3 to 13:7)
E3.5	0.25	*n*-hexane/EtOAc (13:7)
E3.6	0.15	*n*-hexane/EtOAc (3:2 to 0:1)

4.5.2.3. Study of fraction E2.2

Fraction E2.2 (0.09 g) was chromatographed through a column with 8 g of silica gel. The column was eluted using a *n*-hexane/DCM gradient (5:5, 80 mL; 9:11, 80 mL; 2:3, 80 mL; 7:13, 70 mL; 3:7, 70 mL; 1:3, 70 mL; 1:4, 70 mL; 3:17, 70 mL; 1:9, 70 mL; 1:19, 70 mL; 0:1, 70 mL). After chromatographic analysis, the eluates obtained were associated in several fractions, as indicated in Table 4.5.

Table 4.5 Column chromatography of fraction E.2.2

Fraction	Mass (mg)	Eluent (v/v)
E4.1	2.2	*n*-hexane/DCM (5:5)
E4.2	1.5	*n*-hexane/ DCM (5:5)
E4.3	0.5	*n*-hexane/ DCM (11:9)
E4.4	17.4	*n*-hexane/ DCM (2:3)
E4.5	2.8	*n*-hexane/ DCM (2:3 to 7:13)
E4.6	7.7	*n*-hexane/ DCM (3:7)
E4.7	3.6	*n*-hexane/ DCM (3:7)
E4.8	11.5	*n*-hexane/ DCM (3:7 to 3:17)
E4.9	2.9	*n*-hexane/ DCM (1:9 to 0:1)

Fractions E4.4 and E4.7-E4.8 afforded the phenolic compounds vanillin (**2.8**, 17 mg) and 4-hydroxybenzaldehyde (**2.7**, 15 mg).

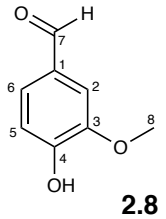

2.8

Vanillin (**2.8**)

White crystals

m.p. 81-82 ºC (EtOAc/*n*-hexane); Lit. 80 ºC (EtOAc/*n*-hexane), (Kwon, Choi and Lee 2001)

ESI-MS, *m/z***:** 153 $[M+H]^+$

^{1}H NMR (300 MHz, $CDCl_3$): δ 3.97 (3 H, *s*, CH_3O), 6.21 (1 H, *s*, OH) 7.04 (1 H, *d*, J = 8.5, H-5), 7.43 (1 H, *m*, H-2), 7.43 (1 H, *m*, H-6), 9.83 (1 H, *s*, H-7).

^{13}C NMR (75 MHz, $CDCl_3$): δ 129.9 (C-1), 114.5 (C-2), 151.8 (C-3), 147.2 (C-4), 108.8 (C-5), 127.7 (C-6), 191.1 (CHO), 56.3 (CH_3O).

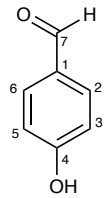

2.7

***p*-Hydroxybenzaldehyde** (**2.5**)

Colorless oil

ESI-MS, *m/z* **:** 123 $[M+H]^+$

^{1}H NMR (300 MHz, $CDCl_3$): δ 6.97 (2 H, *dd*, *J* = 8.4 and 1.6 Hz, H-3 and H-5), 7.81 (H, *dd*, *J* = 8.4 and 1.6 Hz, H-2 and H-6), 9.86 (1 H, *s*, CHO).

^{13}C NMR (75 MHz, $CDCl_3$): δ 129.9 (C-1), 132.6 (C-2 and C-6), 116.1 (C-3 and C-5), 161.9 (C-4), 191.3 (CHO).

4.5.2.4. Study of fractions E3.4 and E3.5

Fractions E3.4 and E3.5 (0.47 g) were associated due to their similar chromatographic profile and were chromatographed through a column with 26.0 g of silica gel. The column was eluted using a *n*-hexane/EtOAc gradient (1:0, 100 mL; 19:1, 100 mL; 9:1, 100 mL; 17:3, 100 mL; 4:1, 450 mL; 3:1, 200 mL; 7:3, 100 mL; 13:7, 100 mL; 3:2, 100 mL; 11:9, 100 mL; 5:5, 100 mL; 9:11, 100 mL; 0:1, 50 mL). After TLC analysis, the eluates obtained were gathered in several fractions, as indicated in Table 4.6.

Table 4.6 Column chromatography of fractions E3.4 and E3.5

Fraction	Mass (mg)	Eluent (v/v)
E5.1	6.0	*n*-hexane/EtOAc (1:0 to 4:1)
E5.2	324.8	*n*-hexane/EtOAc (4:1 to 3:1)
E5.3	38.6	*n*-hexane/EtOAc (3:1 to 9:11)
E5.4	–	*n*-hexane/EtOAc (9:11 to 0:1)

4.5.2.5. Study of fraction E5.2

Fraction E5.2 (0.32 g) was chromatographed through a column with 26 g of silica gel. The column was eluted using a DCM/MeOH gradient (100:0, 100 mL; 99.5:0.5, 100 mL; 99:1, 100 mL; 98.5:1.5, 300 mL; 49:1, 100 mL). After TLC analysis, chromatographic fractions were associated as indicated in Table 4.7.

Table 4.7 Column chromatography of fraction E5.2

Fraction	Mass (mg)	Eluent (v/v)
E6.1	9.6	DCM/MeOH (1:0 to 99:1)
E6.2	42.6	DCM/MeOH (98.5:1.5)
E6.3	92.2	DCM/MeOH (98.5:1.5)
E6.4	8.4	DCM/MEOH (49:1)

The fraction E6.2 (0.04 g) crystalized from DCM/MeOH and was identified as pantolactone (**2.6**, 14.7 mg).

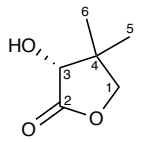

2.9

S-(+)-Pantolactone (**2.9**)

Colorless crystal

m.p. 88-89 ºC (EtOAc/*n*-hexane); Lit. m.p. 90 ºC (EtOAc/*n*-hexane), (Upadhya, Gurunath and Sudalai 1999).

$[\alpha]_D^{25}$ + 28.5º ($CHCl_3$, *c* = 0.2); Lit. $[\alpha]_D^{25}$ − 46.7º (H_2O, c = 2) for R-(−)-Pantolactone (Upadhya, Gurunath and Sudalai 1999).

ESI-MS, *m/z***:** 131 $[M+H]^+$, 130 $[M]^+$

^{1}H NMR (300 MHz, $CDCl_3$): δ 1.07 (3 H, s, CH_3-6), 1.23 (3 H, s, CH_3-5), 3.94 (1 H, *dd*, *J* = 8.9 and 0.8 Hz, H-1α), 4.02 (1 H, *d*, *J* = 9.0 Hz, H-1β), 4.13 (1 H, br s, H-3α).

^{13}C NMR (75 MHz, $CDCl_3$): δ 76.6 (C-1), 177.9 (C-2), 75.8 (C-3), 41.0 (C-4), 23.0 (C-5), 18.9 (C-6).

4.5.2.6. Study of fractions E5.3 and E6.4

Fractions E5.3 (0.04 g) and E6.4 (0.009 g) were gathered based on their similar TLC profile, and chromatographed through a column with 5.0 g of silica gel. The column was eluted using a DCM/acetone gradient (99.5:0.5, 100 mL; 99:1, 100 mL; 98.5:1.5, 150 mL; 49:1, 200 mL; 97.5:2.5; 100 mL; 97:3, 100 mL; 96.5:3.5; 70 mL; 24:1; 70 mL; 95.5;4.5; 100 mL; 19:1, 70 mL; 94.5:5.5, 70 mL; 47:3, 70 mL). After chromatographic analysis, the eluates obtained were associated in several fractions, as indicated in Table 4.8.

Table 4.8 Column chromatography of fractions E5.3 and E6.4

Fraction	Mass (mg)	Eluent (v/v)
E7.1	11	DCM/Acetone (99.5:0.5 to 99:1)
E7.2	2	DCM/Acetone (99:1)
E7.3	14	DCM/Acetone (98.5:1.5 to 49:1)
E7.4	14	DCM/Acetone (49:1 to 24:1)

Although these fractions were separated, their chromatographic profile looked very similar so they were all gathered together again.

4.5.2.7. Study of fraction E6.3

Fractions E6.3 (0.1 g) was chromatographed through a column with 8.0 g of silica gel. The column was eluted using *n*-hexane /DCM and DCM/MeOH mixtures in a gradient of increasing polarity (*n*-hexane /DCM 1:1, 50 mL; 2:3, 50 mL; 3:7, 50 mL; 1:4, 50 mL; 1:9, 50 mL; 0:1, 400 mL; DCM/MeOH 99.5:0.5, 100 mL; 99.3:0.7, 100 mL; 99:1, 400 mL; 98.5:1.5, 100 mL; 19:1, 100 mL). After chromatographic analysis, the eluates obtained were associated in several fractions, but in the end as it happened to the E7 fractions, they all seem to have the same chromatographic profile so they were also gathered together again.

4.5.2.8. Study of fraction E9

The final separation (E9) was carried out by preparative chromatography as the TLC of the two assembled fractions E7+E8 (0.14 g) had two distinct spots, one of them having strong U.V. absorption at 254 nm. The fraction was submitted to preparative chromatography ($CHCl_3$/MeOH, 97:3) yielding 42.2 mg of cycloartane-3β-caffeoyl-23-one (**2.4**)

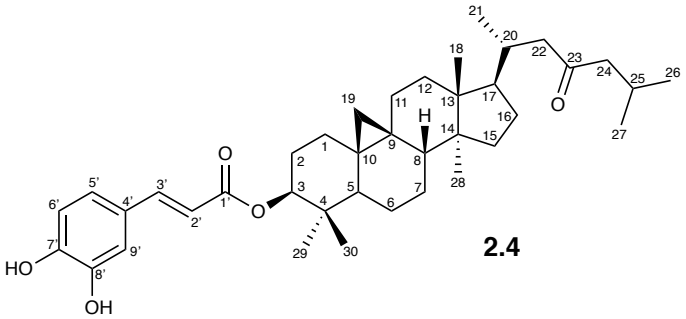

3β-caffeoyl-cycloartane (**2.4**)

Colorless crystals

m.p. 290 ºC (MeOH/$CHCl_3$)

$[\alpha]_D^{25}$ + 39.3º ($CHCl_3$, *c* = 0.2)

IR ν_{max} cm^{-1} (KBr): 3288, 1716, 1706, 1600, 1446, 1436, 1271, 1184, 1112, 1039.

ESI-MS, *m/z*: 605 $[M+H]^+$, 425 [M-caffeic acid+H]$^+$

^{1}H NMR (300 MHz, CDCl3): δ 0.36 (1 H, *d*, *J* = 4.2 Hz, H-19α), 0.60 (1 H, *d*, *J* = 4.2, H-19β), 0.88 (1 H, *s*, H-28), 0.88 (1 H, *s*, H-29), 0.89 (3 H, *d*, *J* = 6.0, CH_3-21), 0.91 (3H, *d*, *J* = 6.0, CH_3-27), 0.92 (3H, *d*, *J* = 6.3, CH_3-27), 0.96 (3 H, *s*, CH_3-30), 1.00 (3 H, *s*, CH_3-18), 2.15 (1 H, *m*, H-22α), 2.28 (2 H, *m*, CH_2-24), 2.46 (1 H, *dd*, *J* = 2.1 and 15.9, H-22β), 4.68 (1 H, *dd*, *J* = 4.5 and 10.8, H-3), 6.26 (1 H, *d*, *J* = 15.9, H-2'), 6.88 (1 H, *d*, *J* = 8.4, H-6'), 6.98 (1 H, *dd*, *J* = 1.8 and 8.4, H-5'), 7.13 (1 H, *d*, *J* = 1.8, H-9'), 7.56 (1 H, *d*, *J* =15.6, H-3').

^{13}C NMR (75 MHz, $CDCl_3$): δ 31.8 (C-1), 27.1 (C-2), 81.1 (C-3), 39.8 (C-4), 47.3 (C-5), 21.0 (C-6), 25.9 (C-7), 47.9 (C-8), 20.2 (C-9), 26.1 (C-10), 26.5 (C-11), 32.9 (C-12), 45.5 (C-13), 49.1 (C-14), 35.6 (C-15), 28.5 (C-16), 52.5 (C-17), 18.2 (C-18), 29.9 (C-19), 33.1 (C-20), 25.5 (C-21), 50.9 (C-22), 212.8 (C-23), 52.8 (C-24), 25.6 (C-25), 22.9 (C-26), 22.7 (C-27), 19.4 (C-28), 24.8 (C-29), 15.5 (C-30), 167.9 (C-1'), 116.1 (C-2'), 145.0 (C-3'), 127.5 (C-4'), 122.4 (C-5'), 115.5 (C-6'), 144.3 (C-7'), 146.8 (C-8'), 114.4 (C-9')

4.6. Bioassay-guided fractionation of methanol fraction: the *n*-hexane soluble fraction

The *n*-hexane soluble fraction (22.6 g) was chromatographed on a silica column (0.90 kg silica gel) using *n*-hexane/EtOAc and EtOAc/MeOH mixtures (*n*-hexane/EtOAc 1:0, 1.5L; 9:1, 1L; 4:1, 2L; 3:1, 1L; 7:3, 1.5L; 13:7, 1L; 11:9, 1.5L; 9:11, 1.5L; 1:3, 1L; and EtOAc/MeOH 9:1, 1L; 4:1, 1L; 7:3, 1L). According to differences in composition, as indicated by TLC, thirteen fractions were obtained (Table 4.9).

Several fractions of the *n*-hexane extract were selected for study (C, D E, G and HIJ). The C, E and G fractions precipitated during the chromatographic process (n-hexane/EtOAc, 4:1 to 3:1, and 3:1, 1.67 g, 1.16 and 2.36 g). (Figure 4.2C).

Table 4.9 Column chromatography of n-hexane soluble fraction.

Fraction	Mass (g)	Eluent (v/v)
A	–	*n*-hexane/EtOAc (1:0 to 9:1)
B	1.91	*n*-hexane/EtOAc (9:1 to 4:1)
C	1.66	*n*-hexane/EtOAc (4:1 to 3:1)
D	0.95	*n*-hexane/EtOAc (3:1)
E	1.16	*n*-hexane/EtOAc (3:1)
F	0.29	*n*-hexane/EtOAc (3:1)
G	2.36	*n*-hexane/EtOAc (3:1)
H	0.78	*n*-hexane/EtOAc (7:3)
I	1.08	*n*-hexane/EtOAc (7:3 to 13:7)
J	0.48	*n*-hexane/EtOAc (13:7 to 3:2)
L	0.44	*n*-hexane/EtOAc (11:9 to 9:11)
M	0.68	*n*-hexane/EtOAc (9:11 to 1:3)
N	0.60	*n*-hexane/EtOAc (1:3 to 0:1) EtOAc/MeOH (1:0 to 7:3)

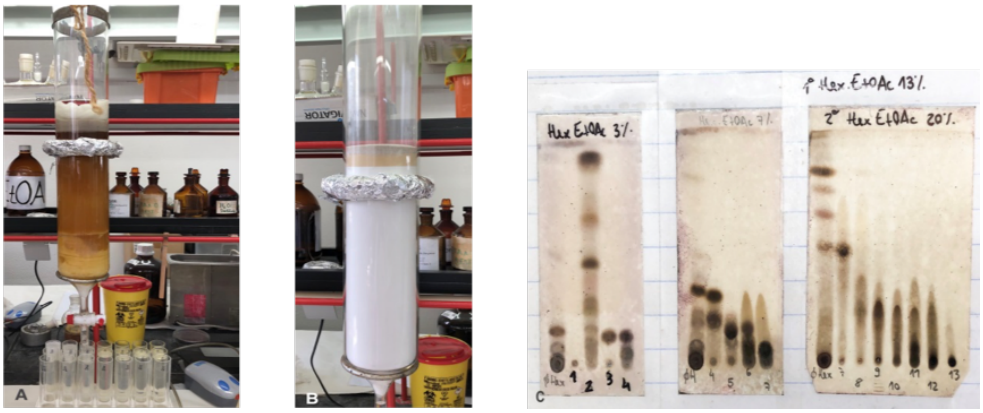

Figure 4.2 Phytochemical study of *G. hexamita*. A and B – fractionation of the *n*-hexane soluble fraction, B – TLC including all the *n*-hexane fractions.

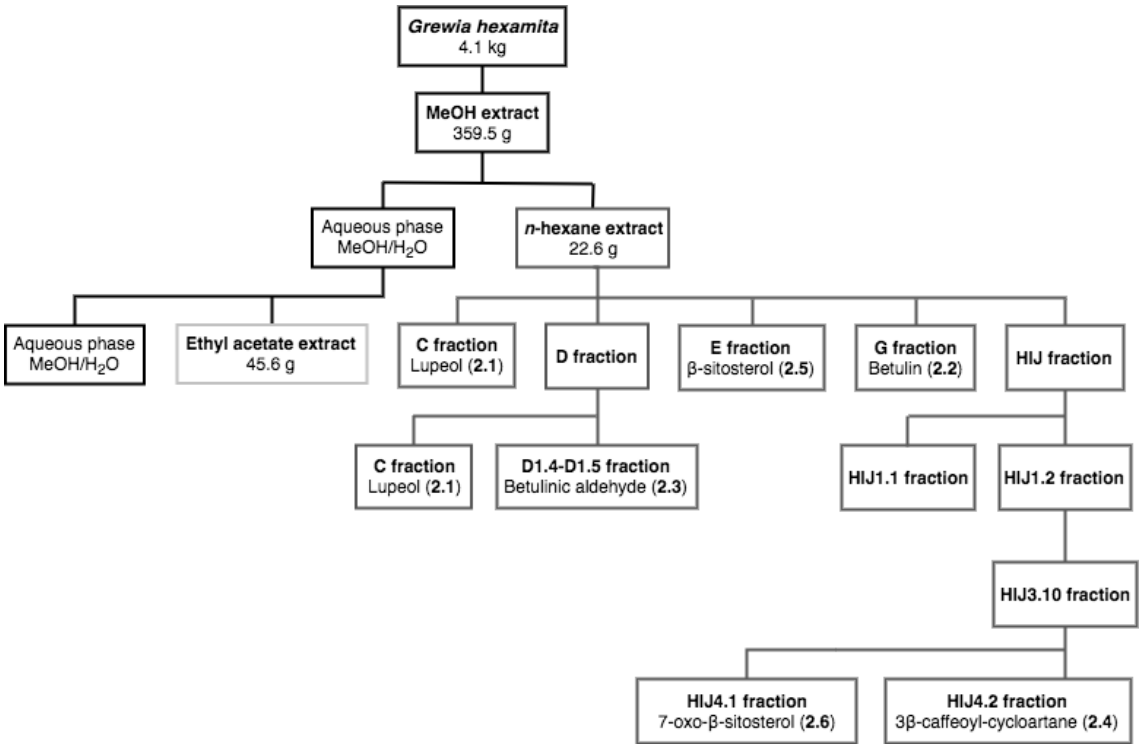

Scheme 4.3 Fractionation of the *n*-hexane soluble fraction and isolated compounds.

4.6.1. Study of the fractions C, E and G

Fractions C, E and G (1.66 g, 1.16 and 2.36 g, *cf.* Table 4.9) were recrystallized with EtOAc/n-hexane to give 1.32 g of lupeol (**2.1**) and 2.05 g of betulin (**2.2**) and 0.93 g of β-sitosterol (**2.5**).

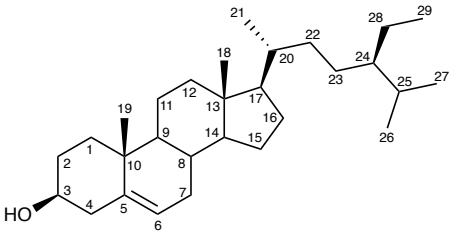

2.5

β-Sitosterol (**2.5**)

White crystals

m.p. 145-146 ºC (EtOAc/*n*-hexane); Lit. 147-148 ºC, (Manoharan *et al.* 2007)

ESI-MS, *m/z*: 415 $[M+H]^+$, 397 $[M-H_2O+H]^+$.

^{1}H NMR (300 MHz, CDCl3): δ 0.68 (3 H, *s*, CH_3-18), 0.80 (3 H, *s*, CH_3-26), 0.83 (3 H, *s*, CH_3-27), 0.84 (3 H, *s*, CH_3-29), 0.92 (3 H, *d*, *J* = 6.5 Hz, CH_3-21), 1.01 (3 H, *s*, CH_3-19), 3.52 (1 H, *m*, H-3α), 5.35 (1 H, *dd*, *J* = 4.2 and 2.5 Hz, H-6).

^{13}C NMR (75 MHz, $CDCl_3$): δ 37.4 (C-1), 31.8 (C-2), 71.9 (C-3), 42.4 (C-4), 140.9 (C-5), 121.9 (C-6), 32.1 (C-7), 32.1 (C-8), 50.3 (C-9), 36.7 (C-10), 21.2 (C-11), 39.9 (C-12), 42.5 (C-13), 56.9 (C-14), 24.5 (C-15), 28.4 (C-16), 56.2 (C-17), 12.0 (C-18), 19.6 (C-19), 36.3 (C-20), 18.9 (C-21), 34.1 (C-22), 26.3 (C-23), 46.0 (C-24), 29.3 (C-25), 19.9 (C-26), 19.5 (C-27), 23.2 (C-28), 12.1 (C-29).

4.6.2. Study of fraction D

Fraction D (0.95 g) was chromatographed through a column with 86 g of silica gel. The column was eluted using mixtures of *n*-hexane/EtOAc (1:0, 290 mL; 99:1, 400 mL; 98.5:1.5, 300 mL; 49:1, 200 mL; 97.5:2.5, 100 mL; 97:3, 1000 mL; 19:1, 100 mL; 9:1, 100 mL). After TLC analysis, the eluates obtained were associated in several fractions, as indicated in Table 4.10.

Table 4.10 Column chromatography of fraction D

Fraction	Mass (g)	Eluent (v/v)
D1.1	–	*n*-hexane/EtOAc (1:0 to 99:1)
D1.2	0.01	*n*-hexane/EtOAc (99:1 to 49:1)
D1.3	0.42	*n*-hexane/EtOAc (97.5:2.5 to 97:3)
D1.4	0.05	*n*-hexane/EtOAc (97:3)
D1.5	0.19	*n*-hexane/EtOAc (97:3)

Fractions D1.3, D1.4 and D1.5 were pure and compounds were identified as lupeol (**2.1**) and betulinic aldehyde (**2.9**).

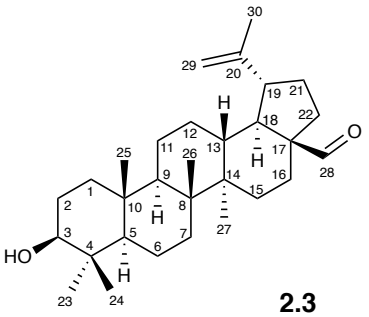

2.3

Betulinic aldehyde (**2.9**)

Colorless crystals

m.p. 190 ºC (EtOAc/*n*-hexane); Lit. 188-190 ºC (Haque *et al.* 2006).

IR ν_{max} cm^{-1} (KBr): 3275, 3070, 1716, 786.

ESI-MS, *m/z*: 441 $[M+H]^+$, 423 $[M-H_2O+H]^+$.

^{1}H NMR (300 MHz, $CDCl_3$): δ 0.74 (3 H, *s*, CH_3-24), 0.81 (3 H, *s*, CH_3-25), 0.96 (3 H, *s*, CH_3-23), 0.97 (3 H, *s*, CH_3-27), 1.03 (3 H, *s*, CH_3-26), 1.68 (3 H, *s*, CH_3-30), 2.38 (1 H, *td*, *J* = 11.0 and 5.6, H-19), 3.18 (1 H, *dd*, *J* = 10.9 and 5.1 Hz, H-3α), 4.62 (1 H, *dd*, *J* = 2.3 and 1.4 Hz, H-29α), 4.75 (1 H, *d*, *J* = 2.2, H-29β), 9.67 (1 H, *br s*, H-28).

^{13}C NMR (75 MHz, $CDCl_3$): δ 38.9 (C-1), 27.5 (C-2), 79.0 (C-3), 39.0 (C-4), 55.4 (C-5), 18.4 (C-6), 34.4 (C-7), 40.9 (C-8), 50.6 (C-9), 37.3 (C-10), 20.9 (C-11), 25.6 (C-12), 38.8 (C-13), 42.7 (C-14), 29.4 (C-15), 28.3 (C-16), 59.5 (C-17), 48.5 (C-18), 47.6 (C-19), 149.9 (C-20), 30.0 (C-21), 33.3 (C-22), 28.2 (C-23), 15.5 (C-24), 16.3 (C-25), 16.1 (C-26), 14.7 (C-27), 18.2 (C-28), 109.5 (C-29), 19.5 (C-30).

4.6.3. Study of fraction HIJ

Fractions H, I and J (0.78, 1.08 and 0.48 g, respectively) were gathered due to their similar chromatographic profile.

This fraction (2.34 g) was chromatographed, using the Combiflash system equipped with a silica gel column (24 g). The sample was eluted with DCM/MeOH mixtures of increasing polarity at a flow rate of 8 mL/min and monitoring at 225 nm and 254 nm. After TLC chromatographic analysis of the collected fractions, they were associated as described in Table 4.11.

Table 4.11 Column chromatography of fraction HIJ

Fraction	Mass (g)	Eluent (v/v)
HIJ1.1	0.52	DCM/MeOH (1:0)
HIJ1.2	0.83	DCM/MeOH (1:0 to 99:1)
HIJ1.3	0.22	DCM/MeOH (99:1 to 98.5:1.5)
HIJ1.4	0.06	DCM/MeOH (98.5:1.5 to 97:3)
HIJ1.5	0.03	DCM/MeOH (19:1)

4.6.3.1. Study of fraction HIJ1.1

The fraction HIJ1.1 (0.52 g) was chromatographed through a column with 46.8 g of silica gel. The column was eluted using a *n*-hexane/DCM and DCM/MeOH gradient (1:1, 600 mL; 9:11, 250 mL; 2:3, 250 mL, 3:7, 250 mL, 4:1, 250 mL; 9:1, 350 mL; DCM/MeOH 1:0, 250 mL; 99:1, 250 mL; 19:1, 250 mL; 9:1, 250 mL; 17:3, 250 mL; 3:1, 250 mL). After TLC analysis, the eluates obtained were associated in three fractions, as indicated in Table 4.12.

Table 4.12 Column chromatography of fraction HIJ1

Fraction	Mass (g)	Eluent (v/v)
HIJ2.1	0.52	*n*-hexane/DCM (5:5)
HIJ2.2	0.83	*n*-hexane/DCM (11:9 to 4:1)
HIJ2.3	0.22	*n*-hexane/DCM (4:1 to DCM/MeOH 3:1)

4.6.3.2. Study of fraction HIJ1.3

The fraction HIJ1.3 (0.83 g) was chromatographed through a column with 75 g of silica gel. The column was eluted using a DCM/acetone gradient (1:0, 450 mL; 99.5:0.5, 450 mL; 99:1, 600 mL; 98.5:1.5, 600 mL; 49:1, 800 mL; 97.5:2.5, 400 mL; 97:3, 200 mL; 24:1, 400 mL; 19:1, 200 mL; 47:3, 200 mL; 23:2, 200 mL; 22:3, 200 mL; 17:3, 200 mL; 4:1, 200 mL). After chromatographic analysis, the eluates obtained were associated in several fractions, as indicated in Table 4.13.

Table 4.13 Column chromatography of fraction HIJ1.3

Fraction	Mass (g)	Eluent (v/v)
HIJ3.5*	0.02	DCM/Acetone (99:1 to 98.5:1.5)
HIJ3.6	0.02	DCM/Acetone (98.5:1.5)
HIJ3.7	0.02	DCM/Acetone (98.5:1.5)
HIJ3.8	0.03	DCM/Acetone (49:1)
HIJ3.10*	0.28	DCM/Acetone (24:1 to 19:1)

*Previous fractions were neglected

4.6.3.3. Study of fraction HIJ3.10

Fraction HIJ3.10 (0.28 g) was submitted to preparative chromatography ($CHCl_3$/MeOH 95.5:4.5) to afford two pure compounds, identified as 7-oxo-β-sitosterol (**2.6**) (25 mg) and once again 3β-caffeoyl-cyclartane (**2.4**) (23 mg).

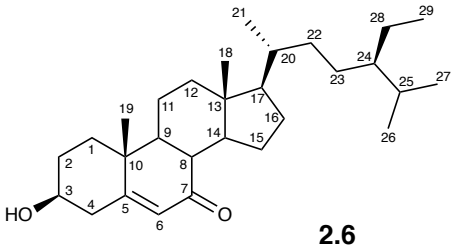

2.6

7-Oxo-β-sitosterol (**2.6**)

White amorphous powder

IR ν_{max} cm^{-1} (KBr): 3424, 2958, 2869, 1673, 1463, 1383, 1063.

ESI-MS, *m/z*: 429 $[M+H]^+$, 411 $[M-H_2O+H]^+$.

^{1}H NMR (300 MHz, $CDCl_3$): δ 0.68 (3 H, *s*, CH_3-18), 0.84 (3 H, *s*, CH_3-27), 0.80 (3 H, *s*, CH_3-26), 0.82 (3 H, *s*, CH_3-29), 0.92 (3 H, *m*, CH_3-21), 1.19 (3 H, *s*, CH_3-19), 3.67 (1 H, *m*, H-3α), 5.69 (1 H, *d*, *J* = 1.7 Hz, H-6).

^{13}C NMR (75 MHz, $CDCl_3$): δ 36.5 (C-1), 31.3 (C-2), 70.7 (C-3), 41.9 (C-4), 165.3 (C-5), 126.2 (C-6), 202.5 (C-7), 45.6 (C-8), 50.1 (C-9), 38.4 (C-10), 21.4 (C-11), 38.9 (C-12), 41.9 (C-13), 50.1 (C-14), 26.5 (C-15), 28.7 (C-16), 54.8 (C-17), 12.1 (C-18), 17.5 (C-19), 36.2 (C-20), 19.1 (C-21), 34.1 (C-22), 26.3 (C-23), 45.9 (C-24), 29.3 (C-25), 19.9

(C-26), 19.2 (C-27), 23.2 (C-28), 12.1 (C-29).

4.7. Molecular derivatization of lupeol (2.1) and betulin (2.2)

4.7.1. Acetylation

Lupeol (**2.1**, 50 mg) or betulin (**2.2,** 50 mg) were suspended in acetic anhydride (1.0 mL) and pyridine (1.0 mL) and both mixtures were stirred overnight at room temperature. The residues resulting from evaporation of the solvent were purified by CC, using mixtures of *n*-hexane and ethyl acetate to afford lupeol acetate (**2.10**) and betulin diacetate (**2.11**).

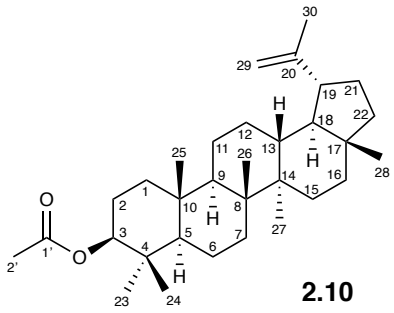

2.10

Lupeol acetate (**2.10**)

Colorless crystals

m.p. 220 ºC (EtOAc/*n*-hexane); Lit. 216-218 ºC (Muktar, Bello and Sallau 2018)

IR ν_{max} cm^{-1} (KBr): 3448, 3072, 2939, 2866, 1768, 1637, 1452, 1365, 1246, 1047, 1012, 875

ESI-MS, *m/z*: 469 $[M+H]^+$, 409 $[M\text{-}COOCH_3+H]^+$

^{1}H NMR (300 MHz, $CDCl_3$): δ 0.78 (3 H, *s*, CH_3-24), 0.83 (3 H, *s*, CH_3-25), 0.83 (3 H, *s*, CH_3-23), 0.84 (1 H, *s*, H-28), 0.93 (3 H, *s*, CH_3-27), 1.02 (3 H, *s*, CH_3-26), 1.66 (3 H, *s*, CH_3-30), 2.05 (3 H, s, CH_3-2'), 2.38 (1 H, *td*, *J* = 11.0 and 5.6, H-19), 4.47 (1 H, *m*, H-3α), 4.56 (1 H, *dd*, *J* = 2.8 and 1.4 Hz, H-29α), 4.69 (1 H, *d*, *J* = 2.5, H-29β).

^{13}C NMR (75 MHz, $CDCl_3$): δ 38.1 (C-1), 23.8 (C-2), 81.8 (C-3), 38.5 (C-4), 55.5 (C-5), 18.5 (C-6), 34.3 (C-7), 40.9 (C-8), 50.4 (C-9), 37.2 (C-10), 21.1 (C-11), 25.2 (C-12), 37.9 (C-13), 42.9 (C-14), 27.5 (C-15), 35.7 (C-16), 43.1 (C-17), 48.4 (C-18), 48.1 (C-19), 151.1 (C-20), 29.9 (C-21), 40.1 (C-22), 28.1 (C-23), 15.5 (C-24), 16.3 (C-25), 16.1 (C-

26), 14.6 (C-27), 18.2 (C-28), 109.5 (C-29), 19.4 (C-30), 171.2 (C-1'), 21.5 (C-2').

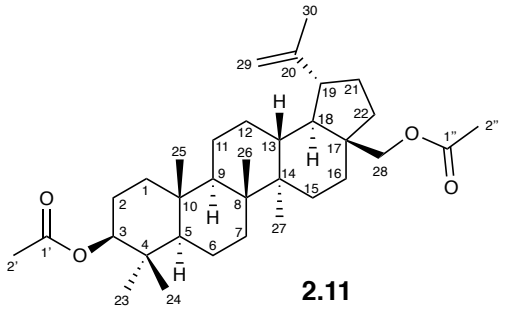

2.11

Betulin diacetate (**2.11**)

Colorless crystals

m.p. 219-221 ºC; Lit. 219-220 ºC (Salah and Bakibaev 2017)

IR ν_{max} cm^{-1} (KBr): 3462, 3408, 2934, 2897, 2870, 1712, 1637, 1448, 1379, 1311, 1280, 1176, 1111, 1097, 1066, 968, 885.

ESI-MS, *m/z*: 527 $[M+H]^+$

^{1}H NMR (300 MHz, CDCl^3): δ 0.82 (3 H, *s*, CH_3-25), 0.83 (3 H, *s*, CH_3-24), 0.83 (3 H, *s*, CH_3-23), 0.95 (3 H, *s*, CH_3-27), 1.01 (3 H, *s*, CH_3-26), 1.67 (3 H, *s*, CH_3-30), 2.03 (3 H, s, CH_3-2''), 2.06 (3 H, s, CH_3-2'), 2.43 (1 H, *td*, *J* = 10.9 and 5.7 Hz, H-19), 3.83 (1 H, *dd*, *J* = 11.0 and 1.2 Hz, H-28α), 4.23 (1 H, *dd*, *J* = 11.0 and 1.9 Hz, H-28β), 4.45 (1 H, *m*, H-3α), 4.57 (1 H, *dd*, *J* = 2.7 and 1.4 Hz, H-29α), 4.67 (1 H, *d*, *J* = 2.3 Hz, H-29β).

^{13}C NMR (75 MHz, $CDCl_3$): δ 38.1 (C-1), 23.8 (C-2), 81.8 (C-3), 38.5 (C-4), 55.5 (C-5), 18.5 (C-6), 34.3 (C-7), 40.9 (C-8), 50.4 (C-9), 37.2 (C-10), 21.1 (C-11), 25.2 (C-12), 37.9 (C-13), 42.9 (C-14), 27.5 (C-15), 35.7 (C-16), 43.1 (C-17), 48.4 (C-18), 48.1 (C-19), 151.1 (C-20), 29.9 (C-21), 40.1 (C-22), 28.1 (C-23), 15.5 (C-24), 16.3 (C-25), 16.1 (C-26), 14.6 (C-27), 62.9 (C-28), 109.5 (C-29), 19.4 (C-30), 171.8 (C-1'), 21.5 (C-2'), 171.2 (C-1''), 21.2 (C-2'').

4.7.2. Reaction with benzoyl chloride

To 50 mg of lupeol (**2.1**) or betulin (**2.2**), 1 ml of pyridine and 0.5 ml of benzoyl chloride were added, and both mixtures were stirred for one hour at room temperature. The reaction mixtures were diluted with EtOAc and washed successively with sodium

carbonate (5%) and hydrochloric acid (1%), dried over anhydrous sodium sulfate and filtered. The residues resulting from evaporation of the solvent were purified by CC using mixtures of *n*-hexane and ethyl acetate affording lupeol benzoate (**2.12,** 32 mg) and betulin dibenzoate (**2.13,** 28 mg).

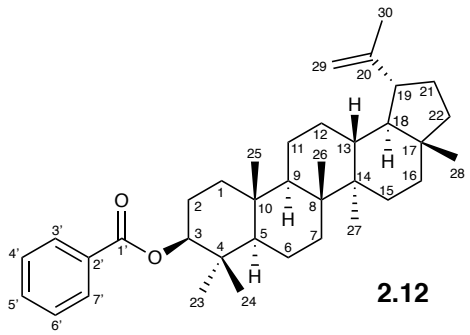

2.12

Lupeol benzoate (**2.12**)

Colorless crystals

m.p. 261 ºC; Lit. 259 ºC (Adotey *et al.* 2012)

IR ν_{max} cm^{-1} (KBr): 3068, 2956, 2920, 2872, 1718, 1448, 1363, 1228, 1149, 1035, 889.

ESI-MS, *m/z*: 531 $[M+H]^+$, 409 $[M-C_6H_5CO_2H+H]^+$

^{1}H NMR (300 MHz, $CDCl_3$): 0.79 (3 H, *s*, CH_3-24), 0.83 (3 H, *s*, CH_3-25), 0.84 (3 H, *s*, CH_3-28), 0.92 (1 H, *s*, H-23), 1.00 (3 H, *s*, CH_3-27), 1.05 (3 H, *s*, CH_3-26), 1.69 (3 H, *s*, CH_3-30), 2.05 (3 H, s, CH_3-2'), 2.39 (1 H, *td*, *J* = 11.0 and 5.6 Hz, H-19), 4.56 (1 H, *dd*, *J* = 2.6 and 1.4 Hz, H-29α), 4.69 (1 H, *d*, *J* = 2.5 Hz, H-29β), 7.44 (2 H, *m*, H-4' and H-6'), 7.54 (1 H, *m*, H-5'), 8.04 (2 H, *m,* H-3' and H-7')

^{13}C NMR (75 MHz, $CDCl_3$): δ 38.3 (C-1), 23.9 (C-2), 81.7 (C-3), 38.3 (C-4), 55.6 (C-5), 18.3 (C-6), 34.3 (C-7), 41.1 (C-8), 50.4 (C-9), 37.2 (C-10), 21.0 (C-11), 25.3 (C-12), 37.8 (C-13), 42.2 (C-14), 27.3 (C-15), 30.1 (C-16), 46.8 (C-17), 49.0 (C-18), 48.0 (C-19), 150.3 (C-20), 29.8 (C-21), 34.9 (C-22), 28.3 (C-23), 16.9 (C-24), 16.3 (C-25), 16.2 (C-26), 14.6 (C-27), 63.4 (C-28), 110.1 (C-29), 19.3 (C-30), 166.4 (C-1'), 131.1 (C-2'), 129.7 (C-3'), 128.4 (C-4'), 132.8 (C-5'), 128.4 (C-6'), 129.7 (C-7'), 167.1 (C-1''), 131.1 (C-2''), 129.7 (C-3''), 128.5 (C-4''), 133.0 (C-5''), 128.5 (C-6''), 129.7 (C-7'').

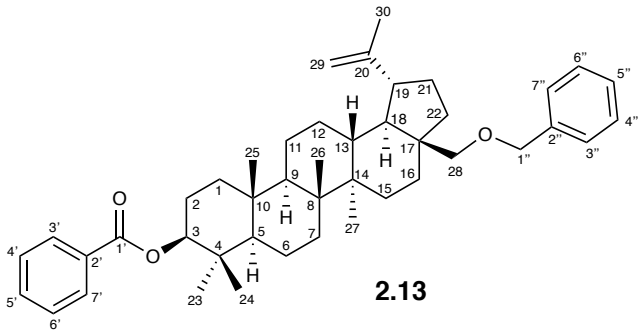

2.13

Betulin dibenzoate (**2.13**)

Colorless crystals

m.p. 142 ºC; 139-140 ºC (Levdanskii, Levdanskii and Kuznetsov 2017)

IR ν_{max} cm^{-1} (KBr): 3068, 2918, 2870, 2360, 1716, 1699, 1602, 1448, 1315, 1246, 1174, 1118, 1068, 1026, 885, 715

ESI-MS, *m/z* (int. rel.): 649 $[M-H]^+$.

^{1}H NMR (300 MHz, CDCl3): δ 0.91 (3 H, *s*, CH_3-25), 0.92 (3 H, *s*, CH_3-24), 1.00 (3 H, *s*, CH_3-23), 1.02 (3 H, *s*, CH_3-27), 1.09 (3 H, *s*, CH_3-26), 1.72 (3 H, *s*, CH_3-30), 2.54 (1 H, *td*, *J* = 10.8 and 5.7 Hz, H-19), 4.10 (1 H, *m*, H-28α), 4.54 (1 H, *dd*, *J* = 11.2 and 1.8 Hz, H-28β), 4.62 (1 H, *dd*, *J* = 2.3 and 1.4 Hz, H-29α), 4.70 (1 H, *m*, H-3α), 4.73 (1 H, *d*, *J* = 2.3 Hz, H-29β), 7.44 (4 H, *m*, H-4', H-4'', H-6' and H-6''), 7.55 (2 H, *m*, H-5' and H-5''), 8.05 (4 H, *m,* H-3', H-3'', H-7' and H-7'').

^{13}C NMR (75 MHz, $CDCl_3$): δ 38.3 (C-1), 23.9 (C-2), 79.2 (C-3), 38.5 (C-4), 55.5 (C-5), 18.4 (C-6), 34.3 (C-7), 40.9 (C-8), 50.5 (C-9), 37.2 (C-10), 21.1 (C-11), 25.2 (C-12), 38.1 (C-13), 42.9 (C-14), 27.6 (C-15), 35.7 (C-16), 43.1 (C-17), 47.9 (C-18), 48.4 (C-19), 151.1 (C-20), 29.9 (C-21), 40.1 (C-22), 28.3 (C-23), 16.1 (C-24), 16.9 (C-25), 16.4 (C-26), 14.6 (C-27), 63.4 (C-28), 109.5 (C-29), 19.4 (C-30), 166.4 (C-1'), 131.1 (C-2'), 129.7 (C-3'), 128.4 (C-4'), 132.8 (C-5'), 128.4 (C-6'), 129.7 (C-7').

4.8. Antibacterial activity evaluation

In order to evaluate the potential of the biological activity of the various extracts and fractions prepared from the roots of *Grewia hexamita*, as well as the isolated pure

compounds and synthetic derivatives, *in vitro* antibacterial activity evaluation studies were performed.

4.8.1. Determination of minimum inhibitory concentration (MIC)

4.8.1.1. Bacterial strains

Samples were tested on the following strains of *Staphylococcus aureus*: a sensitive strain *Staphylococcus aureus* ATCC 6538 (MSSA), a resistant to methicillin strain (MRSA) *Staphylococcus aureus* ATCC 43866, an intermediate vancomycin resistance strain (VISA) *Staphylococcus aureus* CIP 106706 and also in *Staphylococcus epidermis* ATCC 12228, *Salmonella typhymurium* ATCC 13311, *Pseudomonas aeruginosa* ATCC 9027, *Enterococcus faecalis* FFHB H164 and *Eschericia coli* strains ATCC 8739.

4.8.1.2. Determination of MIC values

For the antibacterial activity evaluation of the various extracts, fractions and isolated compounds, the minimum inhibitory concentration (MIC) was determined, which corresponds to the lowest sample concentration that inhibits bacterial growth. The liquid-micro-dilution technique was used, following the recommendations of the Clinical and Laboratory Standards Institute (CLSI, 2012).

The tested compounds [isolated (**2.1**-**2.2**, **2.4**, **2.5**-**2.10**) and synthetic derivatives (**2.11**-**2.14**)] were dissolved in a mixture of DMSO/Mueller-Hinton medium (1:9) to give a solution of 1 mg/ml and assayed in a concentrations range from 0.49-500 µg/mL. In a very brief manner, to the liquid Mueller-Hinton medium (100 μL) was added 100 μL of the sample solution to be tested. Successive dilution and subsequent addition to each well of a bacterium inoculum (10 µL, final concentration of 10^4 cfu/mL) were performed. A blank of solvent and bacteria was included on each plate. The plates were incubated for a period of 24 h at 37 °C, bacterial growth being evaluated by measuring the optical density of the wells at 630 nm on a Biotek ELX 808 spectrophotometer. This reading was always confirmed by the macroscopic observation of the plates. The antibiotics amoxicillin, oxacillin and vancomycin were used as positive controls.

4.8.1.3. Determination of fractional inhibitory concentration index (FICI) values

The effect of the combination between the compounds and the reference antibiotics was evaluated by the checkerboard method on *S. aureus* sensitive (MSSA) ATCC 6538, resistant ATCC 43866 (MRSA) strains and with intermediate resistance to vancomycin CIP 106414 (VISA) strains.

The samples were dissolved in DMSO and solutions were prepared with concentrations corresponding to 2-fold MIC. The antibiotic solutions were prepared in sterile distilled water at concentrations corresponding to four times the MIC of the antibiotic for each of the three strains studied. Thus to Muller-Hinton media (50 μL per cell in the microtiter plate) was added 50 μL of the reference antibiotic solution to be tested on the first horizontal line of the plate. Then, with a multi-channel pipette, successive dilutions were made in the respective vertical lines. Finally, 50 μl of the test sample and 10 μl of a bacteria inoculum were added to each well. A blank of solvent and bacteria was included on each plate. The plates were incubated for a period of 24 to 48 h at 37 °C. The interaction of the compounds with the antibiotics was evaluated using a range of compound concentrations between 1 to 1/64 of the MIC and the antibiotic between 1 to 1/1024 of the MIC.

The combinatorial effect was determined based on the fractional inhibitory concentration index (FICI) value which is calculated according to the following formula: FICI = FIC (compound) + FIC (antibiotic) where, FIC (compound) = compound MIC in the presence of the antibiotic / compound by itself MIC and FIC (antibiotic) = antibiotic MIC in the presence of the compound / antibiotic by itself MIC.

A synergistic effect occurs when the FICI value is equal to or less than 0.5. If the FICI value is between 0.5 and 4.0, there is no interaction between the compound and the antibiotic, and when the FICI value is greater than 4 an antagonistic effect occurs.

CHAPTER 5

Bibliography

5. Bibliography

Abou Zeid, A.H.S., Sleem, A.A. (2005). Anti-hyperlipidemic effect and lipoidal constituents of *Grewia asiatica* L. leaves. *Bulletin of the National Research Centre 30*, 557–573.

Adotey, J.P.K., Adukpo, G.E., Opoku Boahen, Y., and Armah, F.A. (2012). A Review of the Ethnobotany and Pharmacological Importance of *Alstonia boonei* De Wild (Apocynaceae) . *International Scholarly Research Notices Pharmacology 2012*, 1–9.

Ahamed, M.B.K., Krishna, V., and Dandin, C.J. (2010). In vitro antioxidant and in vivo prophylactic effects of two γ-lactones isolated from *Grewia tiliaefolia* against hepatotoxicity in carbon tetrachloride intoxicated rats. *European Journal of Pharmacology 631*, 42–52.

Ahamed, B.M.K., Krishna, V., and Malleshappa, K.H. (2009). In vivo wound healing activity of the methanolic extract and its isolated constituent, gulonic acid γ-lactone, obtained from *Grewia tiliaefolia*. *Planta Medica 75*, 478–482.

Al-Ani, I., Zimmermann, S., Reichling, J., and Wink, M. (2015). Pharmacological synergism of bee venom and melittin with antibiotics and plant secondary metabolites against multi-drug resistant microbial pathogens. *Phytomedicine 22*, 245–255.

Ali, Z., Khan, S.I., Pawar, R.S., Ferreira, D., and Khan, I.A. (2007). 9,19-Cyclolanostane derivatives from the roots of *Actaea pachypoda*. Journal of Natural Products *70*, 107–110.

Anjaneyulu, B., Rao, V.B., Ganguly, A.K., Govindachari, T.R., Joshi B.S., Kamat V.N. (1965). Chemical investigation of some plants. *Indian Journal of Chemistry 3*, 237.

Badami, S., Gupta, M.K., Ramaswamy, S., Rai, S.R., Nanjaian, M., Bendell, D.J., Subban, R., and Bhojaraj, S. (2004). Determination of betulin in *Grewia tiliaefolia* by HPTLC. *Journal of Separation Science 27*, 129–131.

Baek, M.Y., Cho, J.G., Lee, D.Y., Ahn, E.M., Jeong, T.S., and Baek, N.I. (2010). Isolation of triterpenoids from the stem bark of *Albizia julibrissin* and their

inhibition activity on ACAT-1 and ACAT-2. *Journal of Applied Biological Chemistry 53*, 310–315.

Barla, A., Birman, H., Kültür, Ş., and Öksüz, S. (2006). Secondary metabolites from *Euphorbia helioscopia* and their vasodepressor activity. *Turkish Journal of Chemistry 30*, 325–332.

Barnes, B.E., and Sampson, D.A. (2011). A literature review on community-acquired methicillin-resistant *Staphylococcus aureus* in the United States: Clinical information for primary care nurse practitioners. *Journal of the American Academy of Nurse Practitioners 23*, 23–32.

Bashir, A.K., Turner, T.D. and Rose, M.S. (1982). Phytochemical investigation of *Grewia villosa* roots, part-I. *Fitoterapia 53*, 68-70.

Bernardini, S., Tiezzi, A., Laghezza Masci, V., and Ovidi, E. (2018). Natural products for human health: an historical overview of the drug discovery approaches. *Natural Product Research 32*, 1926–1950.

Boon, R., and Pooley, E. (2010). Pooley's trees of Eastern South Africa. 2nd ed. Durban: *Flora and Fauna Publications Trust*.

Brown, D.G., Lister, T., and May-Dracka, T.L. (2014). New natural products as new leads for antibacterial drug discovery. *Bioorganic and Medicinal Chemistry Letters 24*, 413–418.

Brown, E.D., and Wright, G.D. (2016). Antibacterial drug discovery in the resistance era. *Nature 529*, 336–343.

Burrows, J., Burrows, S., Schmidt, E., Lotter, M., and Wilson, E. (2018). *Trees and shrubs Mozambique*. Cape Town: Print Matters History.

Chattopadhyay, S., and Pakrashi, S.C. (1975). Studies on Indian medicinal plants. Part XXXIV. Triterpenes from *Grewia asiatica*. *Journal of the Indian Chemical Society 52*, 553.

Cho, H., Uehara, T., and Bernhardt, T.G. (2014). Beta-lactam antibiotics induce a lethal malfunctioning of the bacterial cell wall synthesis machinery. Cell *159*, 1300–1311.

Chopra, R.N., Nayar, S.L. and Chopra, I.C. (1956). *Glossary of Indian medicinal plants.* New Delhi: Council of Scientific and Industrial Research.

Cragg, G.M., and Newman, D.J. (2013). Natural products: A continuing source of novel drug leads. *Biochimica et Biophysica Acta - General Subjects 1830*, 3670–3695.

Czaplewski, L., Bax, R., Clokie, M., Dawson, M., Fairhead, H., Fischetti, V.A., Foster, S., Gilmore, B.F., Hancock, R.E.W., Harper, D., *et al.* (2016). Alternatives to antibiotics-a pipeline portfolio review. The Lancet Infectious Diseases *16*, 239–251.

Gupta, P., Sharma, A., Verma, A.K. (2012). GC/MS profiling and antimicrobial effect of six Indian tropical fruit residues against clinically pathogenic bacterial strain. *International Journal of Pharmaceutical Research 3*, 1229–1235.

da Silva, U.P., Furlani, G.M., Demuner, A.J., da Silva, O.L.M., and Varejão, E.V.V. (2018). Allelopathic activity and chemical constituents of extracts from roots of *Euphorbia heterophylla* L. *Natural Product Research 1–4*.

Demain, A.L., and Fang, A. (2000). *The Natural Functions of Secondary Metabolites*. pp. 1–39.

Dewick, P.M. (2009). Medicinal Natural Products: A Biosynthetic Approach: Third Edition (John Wiley and Sons).

Dwyer, D.J., Collins, J.J., and Walker, G.C. (2015). Unraveling the Physiological Complexities of Antibiotic Lethality. *Annual Review of Pharmacology and Toxicology 55*, 313–332.

European Centre for Disease Prevention and Control (2018). Antimicrobial resistance surveillance in Europe 2017. Annual Report of the European Antimicrobial Resistance Surveillance Network (EARS-Net).

Fair, R.J., and Tor, Y. (2014). Antibiotics and bacterial resistance in the 21st century. *Perspectives in Medicinal Chemistry* 25–64.

Glen, H. (2005). *The meanings of the botanical names of trees*. Johannesburg: Jacana.

Grierson, D.S., and Afolayan, A.J. (1999). Antibacterial activity of some indigenous plants used for the treatment of wounds in the Eastern Cape, South Africa. *Journal of Ethnopharmacology 66*, 103–106.

Gui, R.Y., Lei, X., Yi, K., Ming, C., Qin, J.C., Li, L., Yang, S.X., and Zhao, L.C. (2015). Chaetominine, (+)-alantrypinone, questin, isorhodoptilometrin, and 4-hydroxybenzaldehyde produced by the endophytic fungus aspergillus sp. YL-6 inhibit wheat (*Triticum aestivum*) and radish (*Raphanus sativus*) germination. *Journal of Plant Interactions 10*, 87–92.

Hansra, N.K., and Shinkai, K. (2011). Cutaneous community-acquired and hospital-acquired methicillin-resistant *Staphylococcus aureus*. *Dermatologic Therapy 24*, 263–272.

Haque, M.E., Shekhar, H.U., Mohamad, A.U., Rahman, H., Islam, A.M., and Hossain, M.S. (2006). Triterpenoids from the Stem Bark of *Avicennia officinalis*. *Dhaka University Journal of Pharmaceutical Sciences 5*, 53–57.

Jackson, N., Czaplewski, L., and Piddock, L.J.V. (2018). Discovery and development of new antibacterial drugs: Learning from experience? *Journal of Antimicrobial Chemotherapy 73*, 1452–1459.

Jamshidi-Kia, F., Lorigooini, Z., and Amini-Khoei, H. (2018). Medicinal plants: Past history and future perspective. *Journal of HerbMed Pharmacology 7*, 1–7.

Jaspers, M.W.J.M., Bashir, A.K., Zwaving, J.H., and Malingre, T.M. (1986). Investigation of *Grewia bicolor* juss. *Journal of Ethnopharmacology 17*, 205–211.

Jayasinghe, U.L.B., Balasooriya, B.A.I.S., Bandara, A.G.D., and Fujimoto, Y. (2004). Glycosides from *Grewia damine* and *Filicium decipiens*. *Natural Product Research 18*, 499–502.

Johnston, C.W. and Magarvey, N.A. (2015). Natural products: untwisting the antibiotic'ome. *Nature Chemical Biology* 11, 94-111.

Kalan, L., and Wright, G.D. (2011). Antibiotic adjuvants: Multicomponent anti-infective strategies. *Expert Reviews in Molecular Medicine 13*.

Khadeer Ahamed, M.B., Krishna, V., and Dandin, C.J. (2010). In vitro antioxidant and in vivo prophylactic effects of two γ-lactones isolated from *Grewia tiliaefolia* against hepatotoxicity in carbon tetrachloride intoxicated rats. *European Journal of Pharmacology 631*, 42–52.

Kwaji, A., Adamu, H.M., Chindo, I.Y., and Atiko, R. (2018). Isolation, characterization and biological properties of betulin from *Entada africana* Guill. and Perr. (Mimosaceae). *Journal of Applied and Advanced Research 3*, 28.

Kwon, H.C., Choi, S.U., and Lee, K.R. (2001). Phytochemical constituents of *Artemisia stolonifera*. *Archives of Pharmacal Research 24*, 312–315.

Lakshmi, V., and Chauhan, J.S. (1976). Grewinol a keto-alcohol from the flowers of *Grewia asiatica*. Lloydia *39*.

Levdanskii, V.A., Levdanskii, A.V., and Kuznetsov, B.N. (2017). Synthesis of Betulin Dibenzoate and Diphthalate. *Chemistry of Natural Compounds 53*, 310–311.

Li, F., Wang, Y., Li, D., Chen, Y., and Dou, Q.P. (2019). Are we seeing a resurgence in the use of natural products for new drug discovery? Expert Opinion on *Drug Discovery 14*, 417–420.

Ma, C., Hong, J.Z., Ghee, T.T., Van Hung, N., Nguyen, M.C., Soejarto, D.D., and Fong, H.H.S. (2006). *Antimalarial compounds from Grewia bilamellata. Journal of Natural Products 69*, 346–350.

Ma XL, Lin WB, Zhang GL. (2009). Chemical constituents of *Osmanthus yunnanensis*. *Natural Product Research and Development 21*, 593–599.

Magiorakos, A.P., Srinivasan, A., Carey, R.B., Carmeli, Y., Falagas, M.E., Giske, C.G., Harbarth, S., Hindler, J.F., Kahlmeter, G., Olsson-Liljequist, B., et al. (2012). Multidrug-resistant, extensively drug-resistant and pandrug-resistant bacteria: An international expert proposal for interim standard definitions for acquired resistance. *Clinical Microbiology and Infection 18*, 268–281.

Manoharan, K.P., Fan, J.S., Benny, T.K.H., and Yang, D. (2007). Triterpenoids from *Eugenia grandis*: Structure elucidation by NMR spectroscopy. *Magnetic Resonance in Chemistry 45*, 279–281.

Muktar, B., Bello, I., and Sallau, M. (2018). Isolation, characterization and antimicrobial study of lupeol acetate from the root bark of Fig-Mulberry Sycamore (*Ficus sycomorus* LINN). *Journal of Applied Sciences and Environmental Management 22*, 1129.

Mugumbate, G., and Overington, J.P. (2015). The relationship between target-class and the physicochemical properties of antibacterial drugs. *Bioorganic and Medicinal Chemistry 23*, 5218–5224.

Neveu, V., Perez-Jiménez, J., Vos, F., Crespy, V., du Chaffaut, L., Mennen, L., Knox, C., Eisner, R., Cruz, J., Wishart, D., et al. (2010). Phenol-Explorer: an online comprehensive database on polyphenol contents in foods. *Database : The Journal of Biological Databases and Curation 2010*.

Newman, D.J., and Cragg, G.M. (2016). Natural Products as Sources of New Drugs from 1981 to 2014. *Journal of Natural Products 79*, 629–661.

Duarte, N. (2008). *Structural characterization and biological activities of terpenic and phenolic compounds isolated from euphorbia lagascae and euphorbia tuckeyana*. Ph.D. Faculdade de Farmácia da Universidade de Lisboa.

O'Neill, J. (2016). Antimicrobial Resistance : Tackling a crisis for the health and wealth of nations. Review on Antimicrobial Resistance 1–16.

Pereira, F., Madureira, A.M., Sancha, S., Mulhovo, S., Luo, X., Duarte, A., and Ferreira, M.J.U. (2016). *Cleistochlamys kirkii* chemical constituents: Antibacterial activity and synergistic effects against resistant *Staphylococcus aureus* strains. *Journal of Ethnopharmacology 178*, 180–187.

Remaud, G.S., Martin, Y.L., Martin, G.G., and Martin, G.J. (1997). Detection of Sophisticated Adulterations of Natural Vanilla Flavors and Extracts: Application of the SNIF-NMR Method to Vanillin and p-Hydroxybenzaldehyde. *Journal of Agricultural and Food Chemistry 45*, 859–866.

Ribeiro, P.R., Ferraz, C.G., and Cruz, F.G. (2019). New steroid and other compounds from non-polar extracts of Clusia burle-marxii and their chemotaxonomic significance. *Biochemical Systematics and Ecology 82*, 31–34.

Sai Prakash, C. V. and Prakash, I. (2012). Isolation and structural characterization of lupane triterpenes from *Polypodium vulgare*. *Research Journal of Pharmaceutical Sciences 1*, 23–27.

Salah, A., Bakibaev, A. (2017). Effective Method of Extraction of Betulin Diacetate from Birch Bark. *Journal of Natural Product and Plant Resources 1*, 90-93.

Tan, S. Y. and Tatsumura, Y. (2015). Alexander Fleming (1881–1955): Discoverer of penicillin. *Singapore Medical Journal 56*, 366-367.

Thimmappa, R., Geisler, K., Louveau, T., O'Maille, P., and Osbourn, A. (2014). Triterpene Biosynthesis in Plants. *Annual Review of Plant Biology 65*, 225–257.

Thirumurugan, D., Cholarajan, A., Raja, S.S.S., and Vijayakumar, R. (2018). An Introductory Chapter: Secondary Metabolites. In *Secondary Metabolites - Sources and Applications*, IntechOpen.

Tijjani, A., Ndukwe, I.G., and Ayo, R.G. (2012). Isolation and characterization of lup-20(29)-ene-3,28-diol (Betulin) from the stem-bark of *Adenium obesum* (Apocynaceae). *Tropical Journal of Pharmaceutical Research 11*, 259–262.

Tiwari, R., and Rana, C.S. (2015). Plant secondary metabolites: a review. *International Journal of Engineering Research and General Science 3*, 661–670.

Upadhya, T.T., Gurunath, S., and Sudalai, A. (1999). A new and short enantioselective synthesis of (R)-pantolactone. *Tetrahedron Asymmetry 10*, 2899–2904.

Vadivel, V., Sriram, S., and Brindha, P. (2016). Distribution of flavonoids among Malvaceae family members – A review. *International Journal of Green Pharmacy 10*, 33–45.

Yadav, A. (1999). Phalsa: A Potential New Small Fruit for Georgia. In: J. Janick, ed., *Perspectives on new crops and new uses*. Alexandria, VA: ASHS Press, 348–352.

Zia-Ul-Haq, M., Stanković, M.S., Rizwan, K., and De Feo, V. (2013). *Grewia asiatica* L., a food plant with multiple uses. *Molecules 18*, 2663–2682.